THESIS FOR THE DEGREE OF DOCTOR OF PHILOSOPHY

Metabolic Engineering of *Saccharomyces cerevisiae* for Polyhydroxybutyrate Production

KANOKARN KOCHARIN

Systems and Synthetic Biology
Department of Chemical and Biological Engineering

CHALMERS UNIVERSITY OF TECHNOLOGY
Göteborg, Sweden 2013

Metabolic Engineering of *Saccharomyces cerevisiae* for Polyhydroxybutyrate Production

KANOKARN KOCHARIN

ISBN 978-91-7385-819-9

Doktorsavhandlingar vid Chalmers tekniska högskola
Ny serie nr 3500
ISSN 0346-718X

Department of Chemical and Biological Engineering
Chalmers University of Technology
SE-412 96 Göteborg
Sweden
Telephone + 46 (0)31-772 1000

Cover:
Schematic illustration of metabolic engineering of the central carbon and redox metabolism aiming to increase cytosolic acetyl-CoA and NADPH supply for polyhydroxybutyrate (PHB) production in *Saccharomyces cerevisiae*.
Kocharin et al. (2013) Biotech Bioeng.

Printed by Chalmers Reproservice
Göteborg, Sweden 2013

PREFACE

This PhD dissertation serves as a partial fulfillment of the requirements for a PhD degree at Chalmers University of Technology, Sweden. The PhD project was carried out in the Systems and Synthetic Biology group, Department of Chemical and Biological Engineering under supervision of Professor Jens Nielsen as the main supervisor, Asst. Professor Keith Tyo (January 2009 - December 2010) and Verena Siewers (January 2011- April 2013) as co-supervisors.

When I first started my PhD in January 2009, my PhD research was initiated with a challenging project to establish the novel expression system in *Saccharomyces cerevisiae*. Later on in 2011, my research was entered the field of metabolic engineering in *S. cerevisiae*. I believe the knowledge and expertise gained throughout the years during my PhD research could potentially advance the research in metabolic engineering and serve as a powerful tool for research in Systems and Synthetic Biology.

This PhD research was funded by the Ministry of Science and Technology, Thailand and the Chalmers Foundation.

Kanokarn Kocharin

April 2013

Metabolic Engineering of *Saccharomyces cerevisiae* for Polyhydroxybutyrate Production

KANOKARN KOCHARIN

Systems and Synthetic Biology
Department of Chemical and Biological Engineering
Chalmers University of Technology

ABSTRACT

Establishing industrial biotechnology for the production of chemical compounds from the biosynthetic pathway has received a significant boost with the implementation of metabolic engineering. At present, metabolic engineering in *Saccharomyces cerevisiae* gains significant advantages of integration of knowledge acquired through a long history of use and data acquisition from novel –omics technologies hence enabling the development of a tailor-made *S. cerevisiae* with desired features for various industrial applications.

With regard to environmentally friendly (eco-friendly) materials, engineering of biodegradable polyhydroxybutyrate (PHB) producing microbes has been studied as a potential alternative to petroleum-based thermoplastics. Heterologous expression of the bacterial PHB biosynthesis pathway in *S. cerevisiae* involves the utilization of acetyl-CoA, an intermediate of the central carbon metabolism, as precursor and NADPH, a redox cofactor used during anabolic metabolism, as a required cofactor for the catalyzing enzymes in the PHB biosynthesis pathway. Provision of acetyl-CoA and NADPH by alteration of the endogenous pathways and/or implementation of a heterologous gene/pathway was investigated with the aim to improve PHB production in *S. cerevisiae*. Since the specific growth rate and the type of carbon source (fermentable/non-fermentable) influence cell physiology and affect the growth of *S. cerevisiae*, PHB production was examined at different specific growth rates on different carbon sources. Overexpression of genes in the native ethanol degradation pathway and heterologous expression of a phosphoketolase pathway from *Aspergillus nidulans* aiming to increase the production of cytosolic acetyl-coA and chromosomal integration of *gapN* from *Streptococcus mutans* to enhance the availability of NADPH were evaluated for their possibility to promote PHB production in *S. cerevisiae*. The enhancement of acetyl-CoA and NADPH either by the combined strategies of the ethanol degradation pathway and *gapN* or utilization of the phosphoketolase pathway resulted in the improved PHB content from 4 mg/gDW in the reference strain to approximately 28 mg/gDW. It is difficult for *S. cerevisiae* to compete with other natural PHB producers like *Ralstonia eutropha* which benefit from native enzymes for the biosynthesis or with the engineered *E. coli* since the metabolism in *S. cerevisiae* is more complex and involves compartmentalization and shuttle systems for precursor and redox balancing. However, the strategies employed in this study involve both engineering of the central carbon and redox metabolism and it demonstrated that it is possible to substantially improve PHB production. Furthermore, the applied strategies may well be suitable also for improving the production of other chemicals, derived from acetyl-CoA and requires NADPH for its biosynthesis.

Keywords: *S. cerevisiae*, Metabolic engineering, Polyhydroxybutyrate, Acetyl-CoA, NADPH

LIST OF PUBLICATIONS

This thesis is based on the work contained in the following publications:

I. Tyo KEJ, Kocharin K, Nielsen J. Toward design-based engineering of industrial microbes. Curr Opinion Microbiol 2010. 13(3):255-262.

II. Kocharin K, Tyo KEJ, Siewers V, Nielsen J. Chemical induced chromosomal evolution in *Saccharomyces cerevisiae*. (Manuscript in preparation)

III. Kocharin K, Chen Y, Siewers V, Nielsen J. Engineering of acetyl-CoA metabolism for the improved production of polyhydroxybutyrate in *Saccharomyces cerevisiae*. AMB Express. 2012. 2(1):52.

IV. Kocharin K, Nielsen J. Specific growth rate and substrate dependent polyhydroxybutyrate production in *Saccharomyces cerevisiae*. (Manuscript accepted for publication in AMB Express)

V. Kocharin K, Siewers V, Nielsen J. Improved polyhydroxybutyrate production by *Saccharomyces cerevisiae* through the use of the phosphoketolase pathway. Biotechnol Bioeng. 2013. [Epub ahead of print]

CONTRIBUTION SUMMARY

I. KK co-wrote some parts and created some of the figures in the review with KT and JN.

II. KT and JN conceived the study. KT and KK participated in the design of experiments. KK performed all the experiments, analyzed the data and wrote the manuscript. KT, VS and JN edited the manuscript.

III. KK and JN designed the study. JN and VS supervised the project and edited the manuscript. YC contributed with the plasmid, pIYC08, used in this study. KK performed the experimental work, analyzed the data and wrote the manuscript.

IV. KK and JN participated in the design of the experiment. KK performed all the experiments, analyzed the data and wrote the manuscript. JN edited the manuscript.

V. KK, VS and JN participated in the design of the experiment. KK performed all the experiments, analyzed the data and wrote the manuscript. JN and VS edited manuscript.

ABBREVIATIONS AND NOMENCLATURES COMMONLY USED

S. cerevisiae:	*Saccharomyces cerevisiae*
E. coli:	*Escherichia coli*
R. eutropha:	*Ralstonia eutropha*
S. mutans:	*Streptococcus mutans*
S. enterica:	*Salmonella enterica*
A. nidulan:	*Aspergillus nidulan*
CIChE:	Chemical induced chromosomal evolution
qPCR:	Quantitative real-time polymerase chain reaction
PHB	Polyhydroxybutyrate
NADPH:	Nicotinamide adenine dinucleotide phosphate hydrogen
PP pathway:	Pentose phosphate pathway
phaA:	Acetyl-CoA acetyltransferase
phaB:	NADPH-linked acetoacetyl coenzyme A (acetyl-CoA) reductase
phaC:	Poly-3-hydroxybutyrate polymerase
ADH2:	Alcohol dehydrogenase
ALD6:	Aldehyde dehydrogenase
ERG10:	Acetyl-CoA acetyltransferase
acs $^{L641P:}$	Acetyl-CoA synthetase variant
xpk:	Phosphoketolase
ack:	Acetate kinase
gapN:	$NADP^+$-dependent glyceraldehyde-3-phosphate dehydrogenase
CIT2:	Citrate synthase
MLS1:	Malate synthase

TABLE OF CONTENTS

Lists of Figures

Lists of Tables

CHAPTER 1. Introduction

1.1. Engineering of industrial microbes

Microbial production of chemical compounds offers several advantages over conventional chemical synthesis. Much improvement of microbial and cellular processes using industrial microbes has been achieved by improving the cell factory through an iterative cycle of modeling, implementation and data analysis (Figure 1a), often referred to as the metabolic engineering cycle. Genome-scale metabolic models (GEMs) have been used to predict changes in enzyme reaction rates (fluxes) in response to nutrient or genetic perturbations thus allowing the prediction of cellular alteration that will increase the production of a desired product. Stoichiometric models have been created through curating enzyme biochemistry literature and using comparative genomics approaches for organisms that have little biochemical evidence. The addition of regulatory information to the stoichiometric models as well as identifying the reversibility/irreversibility of enzymatic reactions by calculating the thermodynamic feasibility can improve the predictive capabilities of the models (Feist et al. 2007; Henry et al. 2007; Herrgard et al. 2006). The next step in the iterative metabolic engineering cycle is the implementation of strategies offered by the predictive model to construct the engineered microbe with the desired characteristics. Implementation generally consists of using strong plasmid-based overexpression, knockout and/or introduction of one or more heterologous gene(s). Instead of using a binary option of strong overexpression and deletion which can cause a metabolic burden in the cell (Gorgens et al. 2001), a well fine-tuned alteration of constitutive expression levels such as by engineering of a constitutive strong promoter (Nevoigt et al. 2006) and chemical induced chromosomal evolution (CIChE) is more attractive for strain improvements (Tyo et al. 2009). As models are not 100% predictive and molecular implementations may therefore not perform as expected, the engineered cells must be analyzed after construction. Technological advancements have enabled –omics measurements and hence generated a massive amount of –omics data of engineered microbes. Due to the availability of databases, a great number of mathematical models and integrative strategies have been developed and established as systems biology tools to integrate and visualize multidimensional data. Model reconstruction benefits from the integrative analysis of –omics data. Therefore, many models are significantly revised after

incorporating new biological information from the integrative –omics data analysis (Österlund et al. 2012). As much more information is gathered from each iterative cycle of modeling, implementation and analysis as well as the advancement in systems biology enable the transition from iterative engineering of industrial microbe to the design-oriented paradigm (Figure 1b).

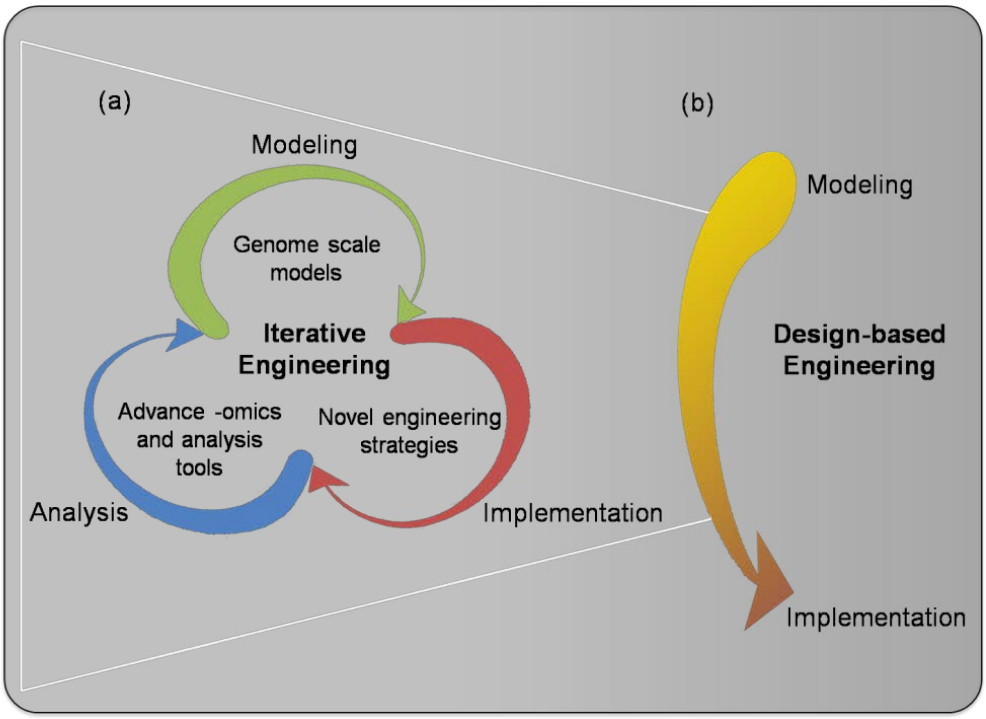

Figure 1 Transitioning from iterative to linear design-based engineering of industrial microbes. (a) Iterative engineering – genome-scale models describe the cellular processes under desired conditions. These models guide implementation of engineering strategies. These implementations are characterized by –omics and integrated analysis tools, which are used to revise the model and improve the predictive capability. (b) Design-based engineering – models and implementation tools are reliable enough that the expected outcome is usually achieved, as in civil and electrical engineering. The transition from an iterative cycle to a linear design-based engineering will be accomplished by better modeling and implementation aided by enhanced analysis (Tyo et al. 2010b).

1.2. CIChE as a molecular tool for implementation of desired features

Traditionally, improvement of microbial and cellular processes were achieved mainly by evolutionary (classical) breeding methods or repeated rounds of mutagenesis and selection of a desired phenotype (Kern et al. 2007). Until now, evolution engineering is still very useful for engineering of industrial microbes, since the implementation of constructive engineering from models may be hampered by the difficulty of predicting secondary responses or side effects of inter-related regulatory and metabolic processes in a cell (Conrad et al. 2011; Sauer 2001; Steen et al. 2008). In order to troubleshoot this difficulty, novel expression systems which allow fine-tuning of the expression system rather than a strong expression system without the scalability (either by overexpression or by deletion) have been developed (Alper et al. 2005; Nevoigt et al. 2006).

A novel fine-tuned expression system based on chemical induced chromosomal evolution (CIChE) has been successfully developed and implemented in *Escherichia coli* (Tyo et al. 2009). The CIChE in *E. coli* is a stabilized plasmid-free expression system which allows ~40 copies of a recombinant pathway to be implemented on the chromosome. This strategy uses an inducible promoter, antibiotic resistant marker, in combination with the *E. coli recA* homologous recombination system to introduce the genes of interest into the chromosome and evolve the strain with chromosomal integration in the increased antibiotic concentration thus resulting in an increased copy number of the integrated genes. This expression system is stabilized by the deletion of *E. coli recA* to prevent furthers change of the evolutionary recombinant pathway through homologous recombination. The resulting strain therefore requires no selection pressures and is unaffected by genetic instabilities. In case of *Saccharomyces cerevisiae*, most of the studies on chromosomal integration were carried out in order to implement a stable expression system for heterologous genes. However, when using the common integrative plasmids, in most cases only one copy of foreign DNA is integrated into the chromosome resulting in generally low expression levels (Plessis and Dujon 1993). Therefore, this expression system has been improved by using the long terminal repeats (LTRs) of Ty retrotransposons (e.g. delta or sigma elements) sequence and ribosomal DNA sequences to introduce multiple integrations and increased expression levels (Boeke et al. 1991; Fujii et al. 1990; Sakai et al. 1990).

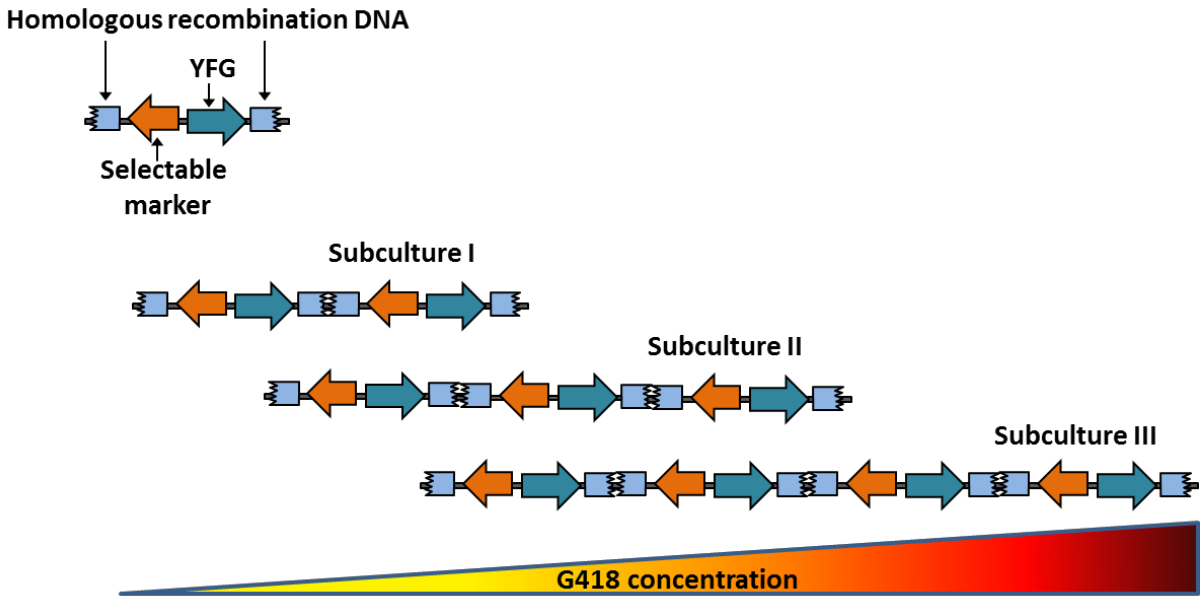

Figure 2 Chemical Induced Chromosomal Evolution (CIChE) strategy: The expression level of the genes of interest is controlled by the copy number of tandem repeats on the chromosome which corresponds to the concentration of antibiotic used as a selection pressure during the chromosomal evolution. YFG = Your Favorite Gene (Paper 2)

In order to develop a stable fine-tuned expression system in *S. cerevisiae*, the CIChE strategy was applied and investigated for heterologous expression. The CIChE strategy was implemented in *S. cerevisiae* by using a bacterial neo^r as a selectable marker. Neo^r, an aminoglycoside-3'-phosphotransferase, inactivates G418, aminoglycoside antibiotic which block protein synthesis by inhibit at the polypeptide elongation phase (Eustice and Wilhelm 1984). Since the bacterial neo^r used in this strategy is derived from a transposon Tn5, and no eukaryotic promoter is used in the construct, therefore the expression level is relatively low. Moreover, the increased copies of neo^r are direct proportional to the concentration of G418 it inactivates, therefore using neo^r as a selectable marker enables the CIChE integrative construct to be evolved when increasing antibiotic concentration. Two different types of integration sequences for homologous recombination were investigated for their integrative capability. The delta element of the Ty1 retrotransposon was selected as site for random integration of the insulin precursor while *his3Δ1* was selected for targeted integration of *gapN* into the yeast chromosome. The CIChE constructs used for either random integration or

targeted integration share the common design where the gene of interest and the selective marker are in the middle of the construct flanked by the homologous sites used for the chromosomal integration. After the whole construct was integrated into the chromosome, the evolutionary process was performed by repeated subculturing in medium containing a stepwise increase of antibiotic concentration as illustrated in Figure 2. The results of CIChE implementation in *S. cerevisiae* will be described in chapter 2.1.

1.3. Metabolic engineering and the industrial biotechnology process

During the past decades, metabolic engineering has been used extensively to improve the cellular processes in industrial microbes with the purpose of improving the product yield, broaden the range of substrate utilization, reduction of by-product formation and introduction of novel pathways leading to new products. By the definition of metabolic engineering given (Bailey et al. 1996; Nielsen 1998; Stephanopoulos and Sinskey 1993), metabolic engineering comprises the analysis of metabolic pathways using metabolic flux analysis to identify targets for manipulation and directed genetic modification in order to achieve the desirable phenotype. With the introduction of recombinant DNA technology, specifically to modify the targeted gene(s) or metabolic pathways, strain improvement has gradually shifted from classical breeding or random mutagenesis to a more rational approach. At present, through the advance in systems biology and the emerging of synthetic biology, metabolic engineering has gradually evolved and becomes more successful in designing tailor-made cell factories (Keasling 2012; Nielsen and Keasling 2011; Yadav et al. 2012).

1.3.1. *S. cerevisiae* as a host for heterologouse expression

S. cerevisiae has been used as a cell factory for the production of a wide range of industrial products due to the available knowledge obtained from a long history of its use and the ease of growth and its genetic manipulation. Several examples of industrial applications such as biofuels, biorefinery compounds and pharmaceutical proteins are reviewed (de Jong et al. 2012; Hong and Nielsen 2012; Hou et al. 2012; Martinez et al. 2012). Since the original sequence of the reference *S. cerevisiae* strain was released in 1996 (Goffeau et al. 1996) and

the Saccharomyces Genome Database became available (Cherry et al. 2012; Dwight et al. 2004), the genotype-phenotype relation of *S. cerevisiae* has been characterized in more detail. Furthermore, due to the extensive conservation of genes and pathways to higher eukaryotic cells, *S. cereivisiae* has also shown potential of being used as a model organism for pharmaceutical and medical application (Hou et al. 2012; Martinez et al. 2012; Munoz et al. 2012).

1.3.2. Polyhydroxybutyrate (PHB) as a target product

Polyhydroxyalkanoates (PHAs) are linear polyesters composed of several units of hydroxyalkanoate and produced by many microorganisms (Akaraonye et al. 2010; Green 2010; Khanna and Srivastava 2005) such as *Alcaligenes eutrophus* (Doi et al. 1992), *Pseudomonas aeruginosa* (Pham et al. 2004) and *Bacillus subtilis* (Singh et al. 2009). The chemical structure of the major PHAs is illustrated in Figure 3, where 'n' is the number of monomer units in each polymer chain, which varies between 100 and 30,000 and R is the side chain that includes alkyl groups which varies from methyl (C1) to tridecyl (C13) (Green 2010; Panchal et al.). Since the chemical properties of these biopolymers are very similar to the chemically produced conventional plastics and they are biodegradable, PHAs has become attractive targets for the production of alternative plastics.

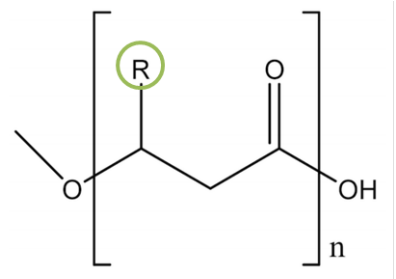

R-Group	PHA Name	Short Name
-H	Polyhydroxypropionate	PHP
$-CH_3$	Polyhydroxybutyrate	PHB
$-CH_2CH_3$	Polyhydroxyvalerate	PHV
$-CH_2CH_2CH_3$	Polyhydroxyhexanoate	PHH

Robin Green, 2010

Figure 3 General structure of PHAs. Structure and chemical properties can vary based on the composition of the attached R-group listed in the Table (Green 2010).

PHB is the most common type of polyhydroxyalkanoate (PHAs) synthesized and accumulated by microorganisms like *Ralstonia eutropha* (also known as *Cupriavidus necator*, *Wautersia eutropha*, *A. eutrophus*), *Bacillus megaterium* or *Pseudomonas sp*. as carbon and energy storage material in response to conditions of physiological stress (Steinbuchel et al. 1993). Biodegradable PHB is a linear polyester consisting solely of the stereospecific monomer, (R)-3-hydroxybutyric acid. It belongs to the group of short chain length PHAs consisting of C3-C5 hydroxyacid monomers. (Hankermeyer and Tjeerdema 1999; Melchiors et al. 1994).

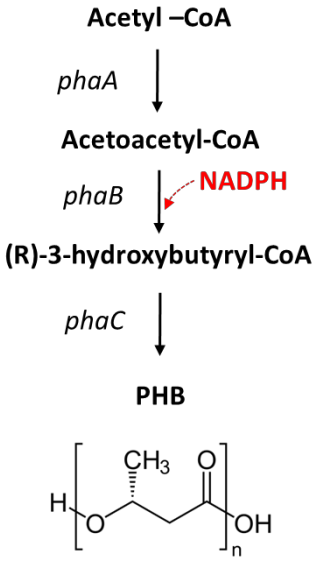

Figure 4 Polyhydroxybutyrate biosynthesis pathway: *phaA* encodes acetyl-CoA aetyltransferase, *phaB* encodes NADPH dependent acetoacetyl-CoA reductase, *phaC* encodes polyhydroxyalkanoate synthase

The biosynthesis pathway of PHB illustrated in Figure 4 involves three enzymes and their sequential reactions (Carlson et al. 2002; Steinbüchel 2001; Steinbüchel and Hein 2001). The first enzyme of the pathway is acetyl-CoA-acetyltransferase [EC 2.3.1.9], encoded by *phaA*, which catalyzes the condensation of two acetyl-CoA molecules to form acetoacetyl-CoA. The next step is the reduction of acetoacetyl-CoA to (R)-3-hydroxybutyryl-CoA, which is catalyzed by NADPH-dependent acetoacetyl-CoA reductase [EC 1.1.1.36] encoded by *phaB*. Finally, PHA synthase [EC 2.3.1.-] encoded by *phaC*, catalyzes the polymerization of (R)-3-hydroxybutyryl-CoA monomers to PHB (Peoples and Sinskey 1989). Several attempts have been made to evaluate *S. cerevisiae* as a cell factory for PHB production (Breuer et al. 2002;

Dimster-Denk and Rine 1996; Leaf et al. 1996; Marchesini et al. 2003; Zhang et al. 2006). Synthesis of PHB in *S. cerevisiae* has initially been demonstrated by expressing only the bacterial polyhydroxybutyrate synthase (Leaf et al. 1996). This PHB synthesis approach is successful because of the activity of native thiolase and reductase enzymes involved in the synthesis of D-3-hydroxybutyryl-CoA in *S. cerevisiae*. However, the yield obtained from employing only the polymerase activity was very low when compared with the expression of all three genes of the PHB biosynthesis pathway (Breuer et al. 2002; Carlson et al. 2002; Carlson and Srienc 2006). PHB synthesized in *S. cerevisiae* occurs and accumulates as small granules in the cytosol as revealed in Figure 5.

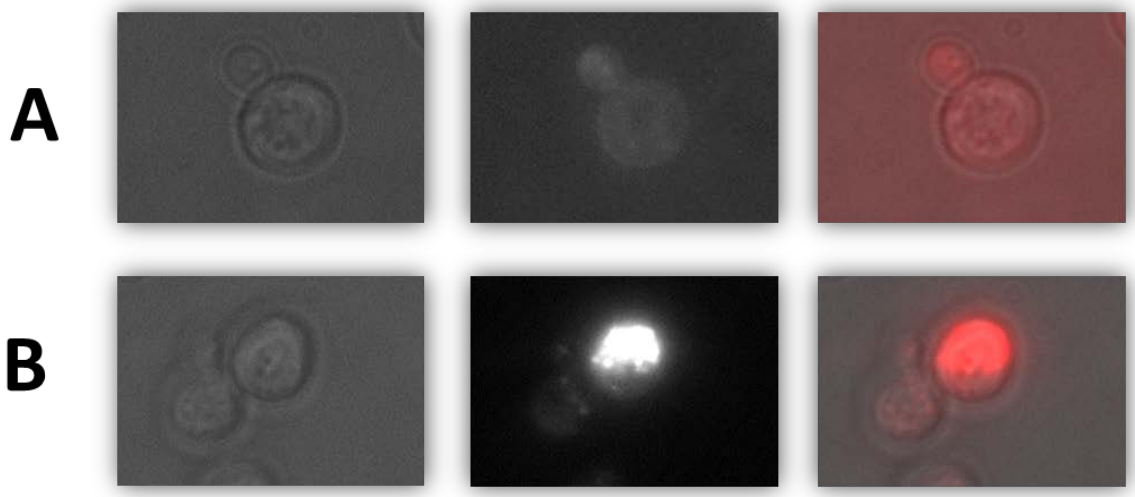

Figure 5 Nile red staining of PHB granules accumulated in the cytosol of *S. cerevisiae.* (A) Wild type and (B) PHB producing *S. cerevisiae* under a fluorescence microscope

In this study, PHB was selected as the model product for metabolic engineering in *S. cerevisiae* since its biosynthesis pathway utilizes acetyl-CoA, the intermediate in the central carbon metabolism, as a precursor. Moreover, the reaction in the pathway involves the consumption of NADPH as a required cofactor. Since many of the microbial-derived industrial products are directly and non-directly acetyl-CoA-derived products and associated with the redox balance in the metabolism, the platform developed for PHB biosynthesis in *S. cerevisiae* could be an advantage and applied for other industrially relevant products.

1.3.3. Acetyl-CoA and central carbon metabolism

Acetyl-CoA is a crucial intermediate metabolite that links anabolism and catabolism. Hence, it is involved in many central metabolic pathways, including the tricarboxylic acid cycle (TCA cycle), the glyoxylate cycle, fatty acid synthesis and β-oxidation, amino acid synthesis and sugar metabolism. Therefore, the availability of acetyl-CoA in the cell relies on the rate of its biosynthesis and its utilization in various metabolic pathways. The summary of acetyl-CoA metabolism is exemplified in Figure 6.

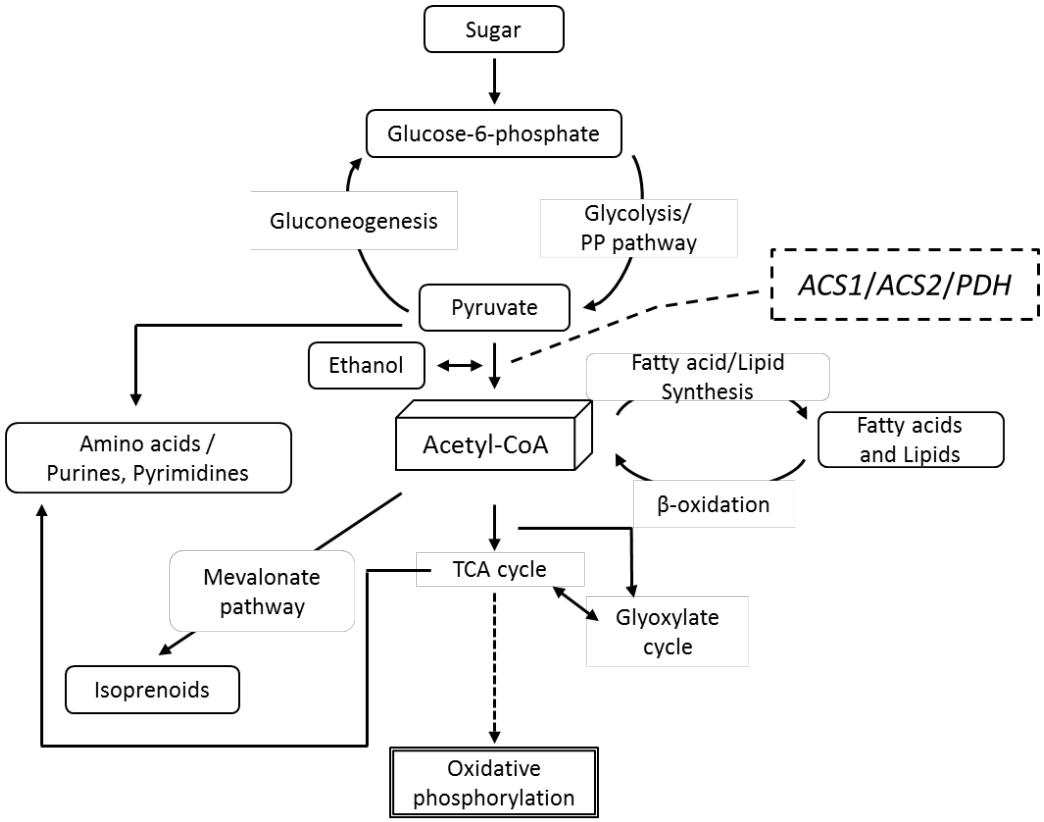

Figure 6 Summary of acetyl-CoA metabolism. *ACS1* and *ACS2* encode the isozymes of cytosolic acetyl-CoA synthetase and *PDH* represents the mitochondrial pyruvate dehydrogenase complex.

In *S. cerevisiae*, acetyl-CoA is synthesized by cytosolic acetyl-CoA synthetase, Acs1p or Acs2p, however these two acetyl-CoA synthetase differ in their kinetic properties and the transcriptional regulation (van den Berg et al. 1996). Since the expression of *ACS1* is

transcriptionally repressed at high concentrations of glucose or other fermentable sugars, *ACS1* contributes to acetyl-CoA synthesis only when cells undergo gluconeogenesis or in the presence of a non-fermentable carbon source (Kratzer and Schuller 1995). *ACS2* is likely to be (in)directly involved in the transcriptional regulation of *ACS1* since the absence of *ACS2* prevented the complete glucose repression of *ACS1* (van den Berg et al. 1996). Moreover, *ACS2* appears to be co-regulated with genes in the fatty acid biosynthesis pathway (Hiesinger et al. 1997). Acetyl-CoA can also be synthesized by the mitochondrial pyruvate dehydrogenase complex via oxidative decarboxylation (Pronk et al. 1996) and generated as the end-product from β-oxidation (Hiltunen et al. 1992). Acs1p is localized in mitochondria, nucleus, cytoplasm and peroxisome (Chen et al. 2012; Devirgilio et al. 1992) whereas Acs2p is localized in cytoplasm, nucleus and possibly endoplasmic reticulum (Chen et al. 2012; Huh et al. 2003) and is primarily responsible for extra-mitochondrial acetyl-CoA production (Takahashi et al. 2006). Therefore, the availability of acetyl-CoA is corresponding to the cellular processes in each compartment and depends on nutrient and growth conditions (Wellen and Thompson 2012).

Besides being important as an intermediate in cellular metabolism, acetyl-CoA is known for its potential as a building block for biosynthesis of industrially relevant products such as isoprenoids (Scalcinati et al. 2012), biofuels like butanol (Steen et al. 2008) and biodiesel (Shi et al. 2012). When acetyl-CoA is used as a precursor for producing these bioproducts, considering the localization of acetyl-CoA is important due to its impermeability through the membrane of the organelles. Acetyl-CoA is localized in at least four subcellular compartments: nucleus, mitochondria, cytosol and peroxisomes. The nuclear acetyl-CoA serves mainly as acetyl donor for histone acetylation (Takahashi et al. 2006), whereas acetyl-CoA localized in other compartments is influenced by the carbon source/sugar utilization and serves as a link between different metabolic pathways. The mitochondrial acetyl-CoA is generated by the pyruvate dehydrogenase complex and served as fuel for the TCA cycle. The peroxisomal acetyl-CoA is generated as the end product of β-oxidation and subsequently used by the glyoxylate cycle which seems to be the only possible route for carbon and energy source when *S. cerevisiae* is grown on oleate (Kunau et al. 1995) or as the endogenous turnover of intermediates leaking out of the fatty acid biosynthetic pathway (Hiltunen et al. 1992). Acetyl-CoA generated in peroxisome is supposed to be used in the same compartment since *S. cerevisiae* does not have the transport system for acetyl-CoA (van Roermund et al. 1995; van Roermund et al. 1999). However, the enzymes participating in the glyoxylate cycle

are located on both sides of the peroxisomal membrane, thus enable some of the intermediate metabolites to be transported across the peroxisomal membrane to the cytosol in the form of C4 dicarboxylic acids and hence be able to pass through the mitochondrial membrane and thus enter the TCA cycle (Kunze et al. 2006). Therefore, the partitioning of acetyl-CoA into each compartments influence the utilization of acetyl-CoA in various metabolic pathways. Citrate synthase (*CIT2*) and malate synthase (*MLS1*) are responsible for shunting acetyl-CoA into the glyoxylate cycle and supplying the C4 dicarboxylic acids to the TCA cycle, where they are subsequently used for growth and energy generation. When *S. cerevisiae* utilize ethanol as sole carbon source (Kunze et al. 2006) or grown on acetate rich medium, the glyoxylate cycle takes place in cytosol (Lee et al. 2011). The deletion of *CIT2* and *MLS1* was proposed to test their effect on the availability of cytosolic acetyl-CoA, which may influence the biosynthesis of PHB in *S. cerevisiae*. The results and discussion of the gene deletions and strategy used to improve the availability of cytosolic acetyl-CoA will be discussed in the next chapter 2.2.

1.3.4. NADPH and Redox balance

The productivity of numerous bioproducts including primary and secondary metabolites or heterologous expression of recombinant proteins and biopolymers produced by microbial fermentation are often limited by NADPH, precursors or other intermediate metabolites. There are several investigations focusing on the strategies to alter the redox balance and study the redox regulation in *S. cerevisiae* (Bro et al. 2006; Minard and McAlister-Henn 2005; Miyagi et al. 2009; Moreira dos Santos et al. 2003; Murray et al. 2011; Shi et al. 2005).

The sources of NADPH in *S. cerevisiae* vary with the carbon source and the availability of oxygen during cultivation since the energy and carbon metabolism are highly interconnected (Madsen et al. 2011; Minard and McAlister-Henn 2005). While NADH is a reducing equivalent produced and consumed mainly in the catabolic reactions, NADPH is regarded as an anabolic reductant. These cofactor pairs, $NADPH/NADP^+$ and $NADH/NAD^+$ play a central role as electron donor/acceptors thus influencing all oxidation-reduction metabolic pathways in the cell (Murray et al. 2011). In *S. cerevisiae*, NADH cannot directly be converted to $NADP^+$, or vice versa, due to the lack of transhydrogenase activity (Bruinenberg 1986). Moreover the compartmentalization of $NADPH/NADP^+$ and $NADH/NAD^+$ is also important

since it is believed that the mitochondrial membrane is impermeable to these cofactors (Outten and Culotta 2003; van Roermund et al. 1995). Figure 7 illustrated the proposed model for generation of cytosolic NADPH and mitochondrial NADPH. The major source of cytosolic NADPH production in *S. cerevisiae* grown on glucose has been attributed to glucose-6-phosphate dehydrogenase (Zwf1p) and 6-phosphogluconate dehydrogenase (Gnd1p/Gnd2p) in the pentose phosphate pathway (PP pathway), with the cytosolic aldehyde dehydrogenase (Ald6p) as a secondary source and isocitrate dehydrogenase (Idp2p) as a third source (Grabowska and Chelstowska 2003; Minard and McAlister-Henn 2005). A different system for generating cytosolic and mitochondrial NADPH in *S. cerevisiae* is illustrated in Figure 7 (Miyagi et al. 2009; Outten and Culotta 2003; Shi et al. 2005). In the cytosol, $NADP^+$ is converted to NADPH by the reactions mentioned above whereas in the mitochondria, NADH serves as the substrate for NADPH generation through the NADH kinase activity of Pos5p, a mitochondrial protein required for the response to oxidative stress (Outten and Culotta 2003). The activity of mitochondrial $NADP^+$ phosphatase (Bernofsky and Utter 1968) allows the recycling of $NADP^+$ to NAD^+ and its further use in the TCA cycle. Although there is evidence of the NADP(H) shuttle system in *S. cerevisiae* due to the viability of the mutant strain lacking ATP-NADH kinase, *utr1Δyef1Δ* and the lethality in the triple mutant, *utr1Δyef1Δ pos5Δ* which implies that cytosolic $NADP^+$ can be supplied by Pos5p from the mitochondrial $NADP^+$ pool (Bieganowski et al. 2006; Murray et al. 2011; Shi et al. 2005), *S. cerevisiae* must carefully regulate a balance between the production and consumption of NADH and NADPH to maintain the redox balance in the cell.

In *S. cerevisiae*, glucose is metabolized via the Embden Meyerhof Parnas (EMP) pathway or the pentose phosphate (PP) pathway depending on the cellular state and culture condition, which split at the glucose-6-phosphate point (Bruinenberg et al. 1983; Gombert et al. 2001; van Winden et al. 2005). Since most NADPH-consuming processes are located in the cytoplasm, the production of cytosolic NADPH and the redox balance are crucial for the energy metabolism and the formation of NADPH-dependent products (Bruinenberg et al. 1983; Vandijken and Scheffers 1986). Several systems have been investigated with the purpose of increasing NADPH availability including the introduction of the transhydrogenase system, alteration of the ammonium assimilation pathway and the heterologous expression of *gapN*, encodes NADP-dependent glyceraldehyde-3-phosphate dehydrogenase, to substitute the production of glycerol with the production of ethanol (Bro et al. 2006; Hou et al. 2009; Moreira dos Santos et al. 2003; Nissen et al. 2001).

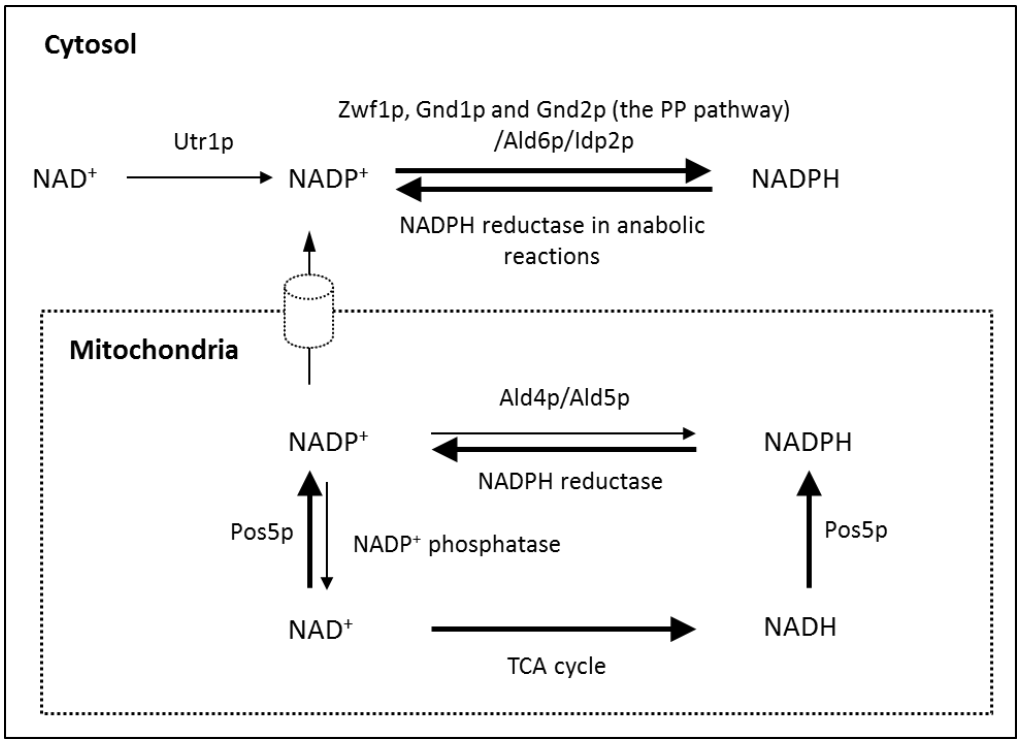

Figure 7 The proposed model for the generation of cytosolic and mitochondrial NADPH. ATP-NADH kinase phosphorylates both NAD and NADH while NAD kinase phosphorylates only NAD^+. The thick arrows represent the favored direction of the reaction.

Zwf1p = glucose-6-phosphate dehydrogenase, Gnd1p/Gnd2p = 6-phosphogluconate dehydrogenase, Ald4p/Ald5p/Ald6p = acetaldehyde dehydrogenase, Idp2p = isocitrate dehydrogenase, Utr1p = ATP-NAD kinase, Pos5p = ATP-NADH kinase

Introducing the *E. coli* membrane bound transhydrogenase (Anderlund et al. 1999) and the cytoplasmic transhydrogenase from *Azotobacter vinelandii* (Nissen et al. 2001) into *S. cerevisiae* were carried out in order to analyze the intracellular redox and the influence on product formation during anaerobic cultivation. The introduction of *A. vinelandii* transhydrogenase resulted in an increased formation of glycerol and 2-oxoglutarate since glycerol is produced when excess NADH is formed while NADPH used to convert 2-oxoglutarate to glutamate is depleted (Nissen et al. 2001). Moreover, the increased formation of 2-oxoglutarate was accompanied with a decrease in the specific growth rate, biomass and ethanol formation (Nissen et al. 2001). Therefore, the results imply the flavored direction toward NADH formation when the transhydrogenase is expressed in *S. cerevisiae*.

In *S. cerevisiae* utilizing ammonium as nitrogen source, the NADPH-dependent glutamate dehydrogenase encoded by *GDH1* accounts for the major fraction of NADPH consumption. Switching the cofactor requirement from NADPH to NADH was carried out by deletion of *GDH1* accompanied with the overexpression of *GDH2* (NADH-dependent glutamate dehydrogenase) or the GS-GOGAT system including the ATP-dependent glutamine synthetase (*GLN1*) and the NADH-dependent glutamate synthase (*GLT1*). Overexpression of *GDH2* or the GS-GOGAT system as an alternative pathway for ammonium assimilation partially restores the growth of *gdh1Δ*. The decreased flux through the PP pathway indicates a decrease in NADPH requirement when employing this redox alteration system (Moreira dos Santos et al. 2003).

Overexpression of *gapN* from *Streptococcus mutans* in *S. cerevisiae* was investigated for its capability to decrease the flux from glucose to glycerol and improve the ethanol yield during anaerobic cultivation. Although this strategy cannot completely eliminate glycerol formation, a 40% lower glycerol yield without affecting the maximum specific growth rate was observed (Bro et al. 2006). Since NADPH is produced during the reaction catalyzed by GapN, we employ the *gapN* strategy in this study for enhancing the availability of NADPH as a required cofactor used during the biosynthesis of PHB. Besides that, establishing the phosphoketolase pathway from *Aspergillus nidulans* was also investigated for its capability to shunt carbon from glucose to the PP pathway and hence enhance NADPH availability. The result and discussion of employing GapN and the phosphoketolase pathway to increase NADPH will be discussed in chapter 2.2.3.

CHAPTER 2. Results and Discussion

2.1. Case study I: CIChE implementation

For industrial application of genetically engineered microbes, it is important that the expression systems in the engineered strains remain stable throughout the production process. Therefore, we were interested in applying the CIChE strategy to the *S. cerevisiae* in order to develop a stable and tunable expression system. The implementation of the CIChE strategy in *S. cerevisiae* was investigated by using two modified CIChE constructs. The linear CIChE construct used for random integration of the insulin precursor expression cassette and one for targeted chromosomal integration of *gapN*, both illustrated in Figure 8.

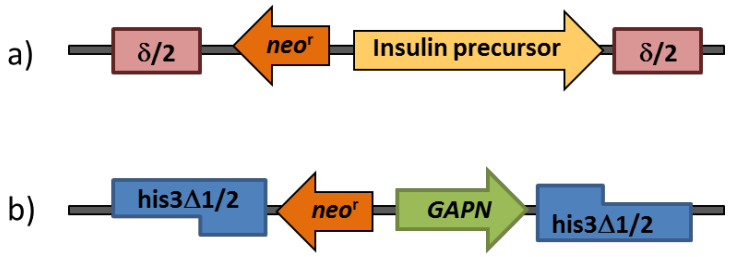

Figure 8 Schematic structure of linear CIChE constructs. a) Random CIChE integrative construct with the insulin precursor as the target product flanked by δ element sequences derived from the 3'end of the yeast Ty1 retrotransposon. b) Targeted CIChE integrative construct with GapN as a target product and his3Δ1 sequence for targeted homologous recombination

In both constructs, a bacterial *neo*^{r} gene was utilized as tunable and selectable marker, the copy number of which - due to its low expression level - should correlates with the concentration of G418 used during the evolutionary steps. Firstly, PHB was used as a target product to investigate the CIChE strategy in *S. cerevisiae* for both random and targeted integration. However, the PHB biosynthesis pathway contains three different genes hence resulting in a large integrative construct. Moreover, the heterologous PHB genes were controlled by the same promoter but in opposite direction when the genes are inserted into the

CIChE construct and this might have resulted in gene loses due to loop out events when the construct was integrated into the chromosome since no PHB was detected after the integration of CIChE-PHB. Moreover, this bulky construct (carrying 4 genes including the selectable marker) was prone to random integration rather than targeted integration. Therefore, in order to prove the concept of chemically inducible chromosomal evolution, we selected the insulin precursor as a target product for investigation of random integration and bacterial GapN for targeted integration due to their compactness, less than 1 kb, for each gene.

2.1.1. Random integration of CIChE construct

The evolution of strains carrying the randomly integrated CIChE-Insulin construct was accomplished by subculturing the strains in a medium containing a stepwise increasing concentration of the antibiotic, G418. Evaluation of the physiological properties of the evolved strain was carried out and the results are shown in Figure 9. When the evolved strains were grown at the respective G418 concentration, there was no significant difference in the specific growth rate, glucose consumption and insulin precursor production rate in the strains evolved from 0.2 $g \cdot L^{-1}$ G418 to 12.8 $g \cdot L^{-1}$ G418. However, the strains isolated from higher concentrations of G418 showed lower specific growth rates as well as lower biomass yield and insulin precursor production rate.

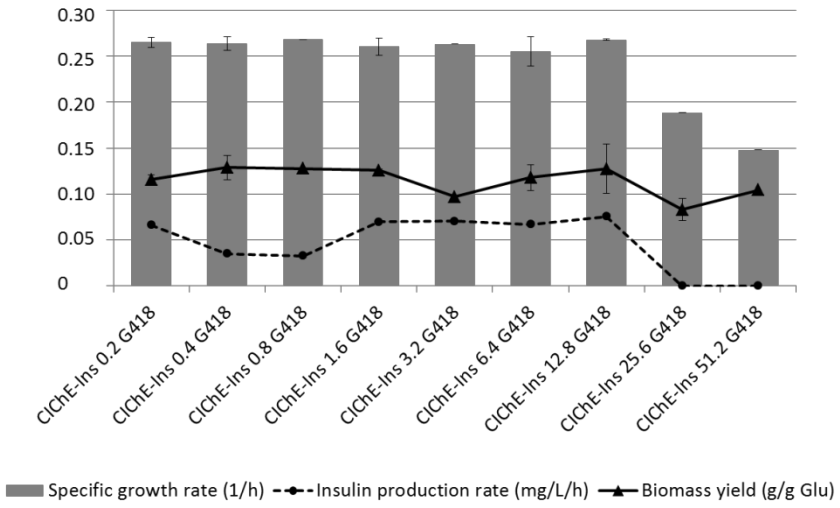

Figure 9: Specific growth rates, insulin precursor production rates and biomass yields of the CIChE-Ins strains isolated at different concentrations of G418.

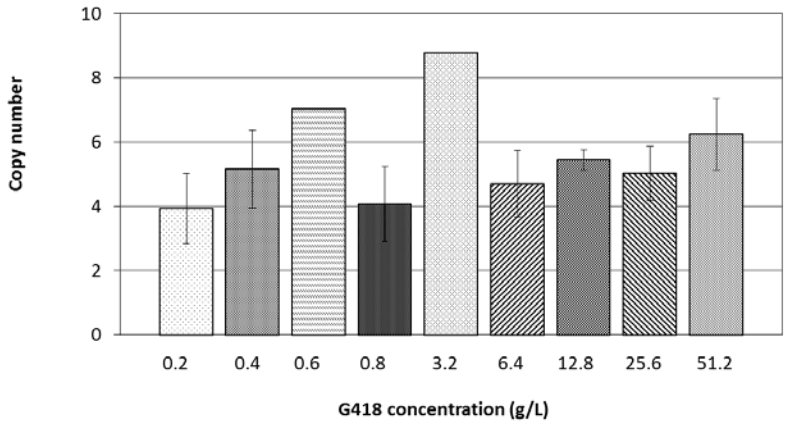

Figure 10: *Neo*^{r} copy number measurement. The copy number of *neo*^{r} in the genome of strains isolated from different concentration of G418 was determined by qPCR using single copy gene *TAF10* for normalization.

Evaluation of the *neo*^{r} copy number using quantitative PCR (qPCR) revealed that there was no correlation between the copy number and the G418 concentration applied during the evolution process as illustrated in Figure 10. Although a general trend of increasing copy number was observed up to a G418 concentration of 0.6 $g \cdot L^{-1}$, however this trend did not continue for higher concentrations of G418. The Ty1 delta element was employed in the CIChE construct with the intention to promote homologous recombination during the evolution process because it appears in many copies in the genome thus allow the dispersed integration of the CIChE construct to occur. However, the pattern of integrated CIChE constructs was found to be in a tandem repeat manner instead of random integration into different delta sequences as shown in Figure 11. This result is consistent with findings by Wang and coworkers (Wang et al. 1996) but different from what was observed by Boeke and coworkers (Boeke et al. 1988) who found integration of delta element at multiple sites in the genome, which may lead to further lack of correlation of gene expression and copy number due to varying expression levels at different chromosomal sites.

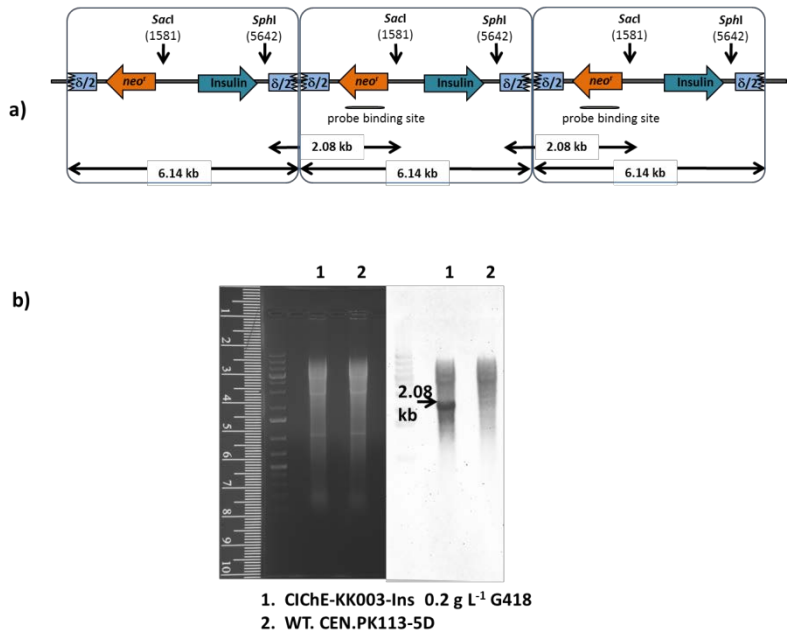

Figure 11: Southern blot analysis of CIChE strain. (a) Schematic presentation of tandem integrated CIChE construct (b) Genomic DNA of strains CIChE-KK003-Ins 0.2 g·L^{-1} G418 and CEN.PK113-5D was subjected to restriction enzyme digestion with *Sac*I and *Sph*I and separated by gel electrophoresis followed by hybridization with a probe containing a 1-kb *neo*^{r} fragment.

2.1.2. Targeted CIChE integration

His3Δ1 was selected as a homologous recombination site for targeted integration instead of the delta element, which leads to random integration into the chromosome. A non-phosphorylating NADP^{+} dependent glyceraldehyde-3-phosphate dehydrogenase encoded by *gapN* from *S. mutans* was selected as a target product instead of insulin precursor due to the ease of strain characterization and further use as a redox engineered strain. Besides that, the CIChE integrated construct was redesigned in order to reduce the size of the integrated cassette but still sharing the same concept of having 2 homologous sites flanking the CIChE integration cassette. It has been shown that expression of *gapN* reduces the amount of glycerol produced by *S. cerevisiae* when grown under anaerobic conditions (Bro et al. 2006). Therefore, characterization of the evolved strain with targeted CIChE-gapN integration was performed under anaerobic cultivation.

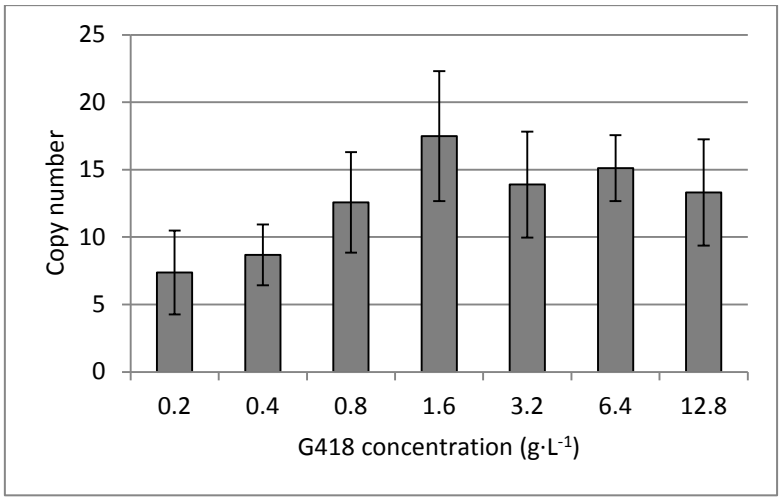

Figure 12 *Neo*^{r} copy number measurement. The copy number of *neo*^{r} in the genome of strains isolated from different concentration of G418 was determined by qPCR using single copy gene *TAF10* for normalization.

The copy number of CIChE-gapN construct tended to increase with the increasing G418 concentration (Figure 12). When the evolution was carried out in G418 concentration greater than 1.6 g·L^{-1} however, the copy number was not proportional with the increased concentration of G418 similar to what was observed in the random CIChE integration.

2.1.3. Chemical induced evolution and the tunability of *neo*^{r}

As the correlation between the increment of G418 resistance and the copy number of *neo*^{r} was not observed during the evolution process especially in the strain evolved at higher G418 concentrations, we suspected changes in the *neo*^{r} expression level. The transcriptional level of *neo*^{r} in the insulin precursor construct (Figure 13) showed that although the number of *neo*^{r} copies in the chromosome remained constant when the concentration of G418 was increased, the transcriptional level of the evolved strain increased three fold compared to the parental strain.

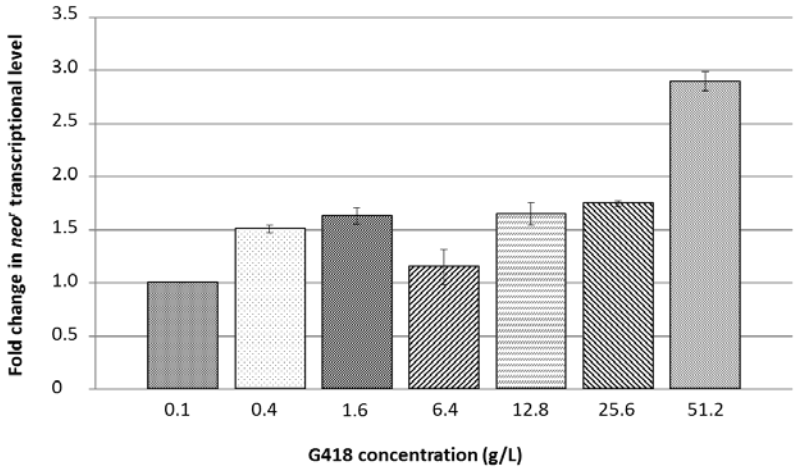

Figure 13 Comparison of *neo*^{r} transcription levels. RNA extracted from evolved strains at different concentrations of G418 was examined by qRT-PCR. *TAF10*, *ALG9* and *ACT1* were used as reference genes to normalize the transcript level of *neo*^{r}.

Although the CIChE approach is based on the assumption that the accretion in antibiotic resistance would result in an increased copy number of the CIChE construct, in this study such a correlation was only observed when the applied G418 concentration was low. This might be due to slower copy number evolution of the CIChE integrative construct in the genome compared to the acquisition of mutations leading either to higher expression of neoR or to G418 resistance. The dissociation between the occurrence of G418 resistance and the number of copies or integration sites of *neo*^{r} was also observed in another study (Quinto et al. 1992). RecA is the main homologous recombination protein in *E. coli* whereas the *RAD52* epistasis group (consisted of *RAD50*, *RAD51*, *RAD52*, *RAD54*, *RDH54/TID1*, *RAD55*, *RAD57*, *RAD59*, *MRE11*, and *XRS2*) in *S. cerevisiae* is responsible for the same recombination process (Symington 2002). Therefore, the more complex homologous recombination process in *S. cerevisiae* might also account for the different results in the evolution of the CIChE construct when integrated into the chromosome.

In order to reduce the technical difficulties when implementing the *E. coli* CIChE strategy to *S. cerevisiae*, two possibilities could be proposed, changing the selective marker and the homologous recombination sites. The changing of the resistance marker to another dominant marker such as metal ion resistance marker, CUP1^r from *S. cerevisiae*, the copy number of which regulates the level of copper resistance (Fogel and Welch 1982; Fogel et al. 1983),

might improve the evolution process of the integrated CIChE strain. Moreover, it will not leave an antibiotic resistance marker in the genome when applying the engineered strain in the industrial applications. Another possibility is to change the sites for chromosomal integration of the CIChE construct because different integration sites can influence the expression level of the heterologous genes (Bai Flagfeldt et al. 2009). Therefore, homologous recombination sites with low to intermediate expression level would be preferable. Overall, the investigated results presented here could serve as a basis guide for implementing the process of chemical induced chromosomal evolution that could be applied as a new tunable expression system in *S. cerevisiae*.

2.2. Case study II: PHB production

2.2.1. Precursor supplementation

Despite its benefits as a well-studied microorganism, elucidating *S. cerevisiae* as a model to develop a platform for producing acetyl-CoA derived molecules struggles with many constrains such as compartmentalization and transporters/shuttle systems for the heterologous target compounds. Apart from being an intermediate in several metabolic pathways, acetyl-CoA is localized in 4 subcellular compartments. In addition, acetyl-CoA cannot be transported through organelle membranes without the carnitine shuttle system, which is absent in *S. cerevisiae.* Nevertheless, acetyl-CoA can be indirectly relocated in form of acetyl-CoA derived organic acids such as succinic acid or malic acid, thus influencing the availability of acetyl-CoA and acetyl-CoA derived products formation in different compartments.

The availability of cytosolic acetyl-CoA is known to influence the production of certain compounds in *S. cerevisiae*. In this study, the biosynthesis of PHB in *S. cerevisiae* occurs in the cytoplasm and utilizes the cytosolic acetyl-CoA as a precursor, therefore the availability of cytosolic acetyl-CoA has been hypothesized to influence PHB production. Overexpression of genes from the ethanol degradation pathway including alcohol dehydrogenase (*ADH2*), acetaldehyde dehydrogenase (*ALD6*) and acetate synthetase variant (acs^{L641P}) was studied in order to increase the flux from ethanol to acetyl-CoA and further improve PHB production. Moreover, to maintain the availability of cytosolic acetyl-CoA, *CIT2* and *MLS1* as the routes shunting acetyl-CoA to the glyoxylate cycle were blocked and evaluated for their effect on cytosolic PHB production. The pathway used in this strategy is presented in Figure 14 and the strains used in Case study II are listed in Table1

Co-expression of beta-ketothiolase (PhaA), acetoaetyl-CoA reductase (PhaB) and PHA synthase (PhaC) results in PHB accumulation in *S. cerevisiae* as observed in previous studies (Breuer et al. 2002; Carlson et al. 2002; Carlson and Srienc 2006). Although thiolase enzymes already exist in *S. cerevisiae*, they function in three different compartments, in mitochondria and peroxisomes for fatty acid β-oxidation and in the cytoplasm for the mevalonate pathway (Hiser et al. 1994). Therefore, we believed that overexpression of native *ERG10* together with *PhaA* would facilitate PHB biosynthesis in the cytoplasm of *S. cerevisiae*.

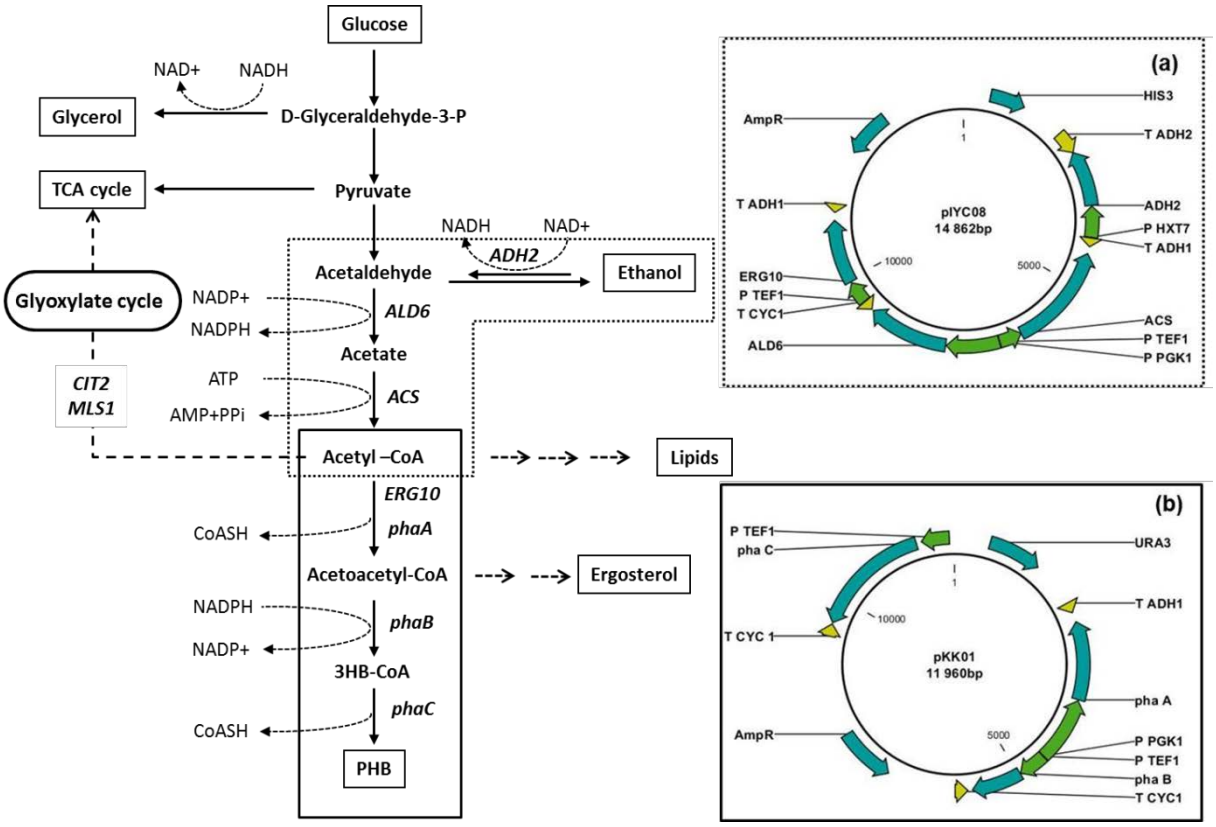

Figure 14 Schematic pathway and plasmid maps for polyhydroxybutyrate production in *S. cerevisiae*. (a) Acetyl-CoA boost plasmid (pIYC08) containing *ADH2*: alcohol dehydrogenase, *ALD6*: aldehyde dehydrogenase, *ACS*: acetyl-CoA synthetase variant (acs^{L641P}) and *ERG10*: acetyl-CoA acetyltransferase. (b) PHB plasmid (pKK01) containing PHB genes from *R. eutropha*, *phaA*: acetyl-CoA acetyltransferase, *phaB*: NADPH-linked acetoacetyl coenzyme A (acetyl-CoA) reductase and *phaC*: poly(3-hydroxybutyrate) polymerase. P and T in the plasmid map represent promoter and terminator, respectively.

Table 1 Yeast strains and plasmids used in Case study II.

Strain	Genotype or relevant feature(s)	Plasmid	Source
CEN.PK 113-11C	*MAT*a *SUC2 MAL2-8*^{c} *ura3-52 his3-Δ1*	-	P. Kötter[a]-
SCKK005	*MAT*a *SUC2 MAL2-8*^{c} *ura3-52 his3-Δ1*	pIYC04/pKK01	Paper 3-5
SCKK006	*MAT*a *SUC2 MAL2-8*^{c} *ura3-52 his3-Δ1*	pIYC08/pKK01	Paper 3-5
SCIYC32	*MAT*a *SUC2 MAL2-8*^{c} *ura3-52 his3-Δ1 cit2Δ*	-	(Chen et al. 2012)
SCIYC33	*MAT*a *SUC2 MAL2-8*^{c} *ura3-52 his3-Δ1 mls1Δ*	-	(Chen et al. 2012)
SCKK009	*MAT*a *SUC2 MAL2-8*^{c} *ura3-52 his3-Δ1 cit2Δ*	pIYC08/pKK01	Paper 3
SCKK010	*MAT*a *SUC2 MAL2-8*^{c} *ura3-52 his3-Δ1 mls1Δ*	pIYC08/pKK01	Paper 3
SCKK032	*MATa SUC2 MAL2-8*^{c} *ura3-52 his3-Δ1*	pJC7/pKK01	Paper 5
SCKK033	*MATa SUC2 MAL2-8*^{c} *ura3-52 his3-Δ1::gapN*[b]	pIYC04/pKK01	Paper 5
SCKK034	*MATa SUC2 MAL2-8*^{c} *ura3-52 his3-Δ1::gapN*	pIYC08/pKK01	Paper 5
SCKK035	*MATa SUC2 MAL2-8*^{c} *ura3-52 his3-Δ1::gapN*	pJC7/pKK01	Paper 5
SCKK036	*MATa SUC2 MAL2-8*^{c} *ura3-52 his3-Δ1::gapN*		Paper 5

[a] Institute of Microbiology, J.W. Goethe Universität, Frankfurt, Germany

[b] *gapN* here represents the integration cassette including *neo*^{r} and *gapN* under control of the *PGK1* promoter and *ADH1* terminator.

The acetyl-CoA boost plasmid contains 4 genes, *ADH2*, *ALD6*, *acs*^{L641P} and *ERG10*, involved in channeling carbon from ethanol to acetyl-CoA. *ADH2* encodes a cytosolic acetyl-CoA dehydrogenase responsible for the initial step in the utilization of ethanol as carbon source. *ALD6* encodes aldehyde dehydrogenase involved in the conversion of acetaldehyde to acetate. Although, there are two acetyl-CoA synthetases present in *S. cerevisiae*, the regulation of both enzymes is complex and therefore overexpression of acetyl-CoA synthetase is believed to increase the flux towards acetyl-CoA production. Acetyl-CoA synthetase with the mutation at Leu-641 from *S. enterica* was selected in the acetyl-CoA boost plasmid to catalyze the conversion of acetate to acetyl-CoA. Mutation of acetyl-CoA synthetase at Leu-641 prevent the acetylation by acetyltransferase bypassing the need for deacetylases and thus maintaining the enzyme in an active state (Starai et al. 2005). In the acetyl-CoA boost plasmid, *ALD6*, *acs*^{L641P} and *ERG10* are controlled by constitutive promoters, P_{TEF1} and P_{PGK1}, respectively, while *ADH2* is under control of the P_{HXT7} promoter which is strongly de-repressed under glucose depletion (Partow et al. 2010; Reifenberger et al. 1995; Sedlak and Ho 2004) hence ensuring the conversion of ethanol to acetaldehyde after glucose consumption phase. Co-transformation of acetyl-CoA boost plasmid and PHB plasmid improved the PHB production in SCKK006 to ~250 mg·L^{-1}, 18 times higher compared to the reference strain (SCKK005) as shown in Figure 15 b. Although the deletion of *CIT2* and *MLS1* was supposed to enhance the availability of cytosolic acetyl-CoA by reducing the drain of acetyl-CoA to the glyoxylate shunt, co-transformation of the acetyl-CoA boost plasmid and the PHB plasmid into the *cit2Δ* (SCKK009) and *mls1Δ* (SCKK010) strain resulted in lower biomass and PHB production compared to the non-deletion strains (Figure 15). Since the deletion of *CIT2* and *MLS1* cause an impaired metabolism due to the incapability to utilize C_2 carbon via the glyoxylate shunt, the accumulation of acetate, as high as 6 g·L^{-1},was observed in SCKK009 (*cit2Δ*).

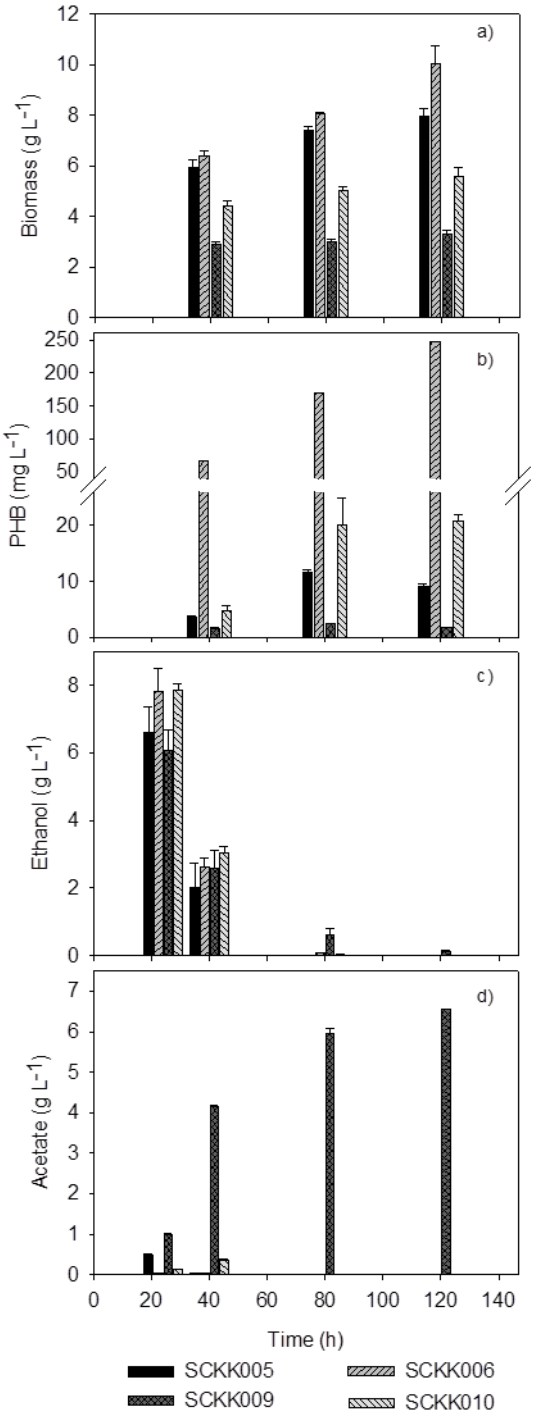

Figure 15 Measurements of biomass and PHB from shake flask cultivations in a modified minimal medium with 20 g L^{-1} glucose as carbon source. Strain SCKK005 harbors an empty plasmid (pIYC04) and the PHB plasmid (pKK01), strain SCKK006 harbors an acetyl-CoA boost plasmid (pIYC08) and the PHB plasmid (pKK01), SCKK009 and SCKK010 harbor pIYC08 and pKK01 and carry a *CIT2* and *MLS1* deletion, respectively.

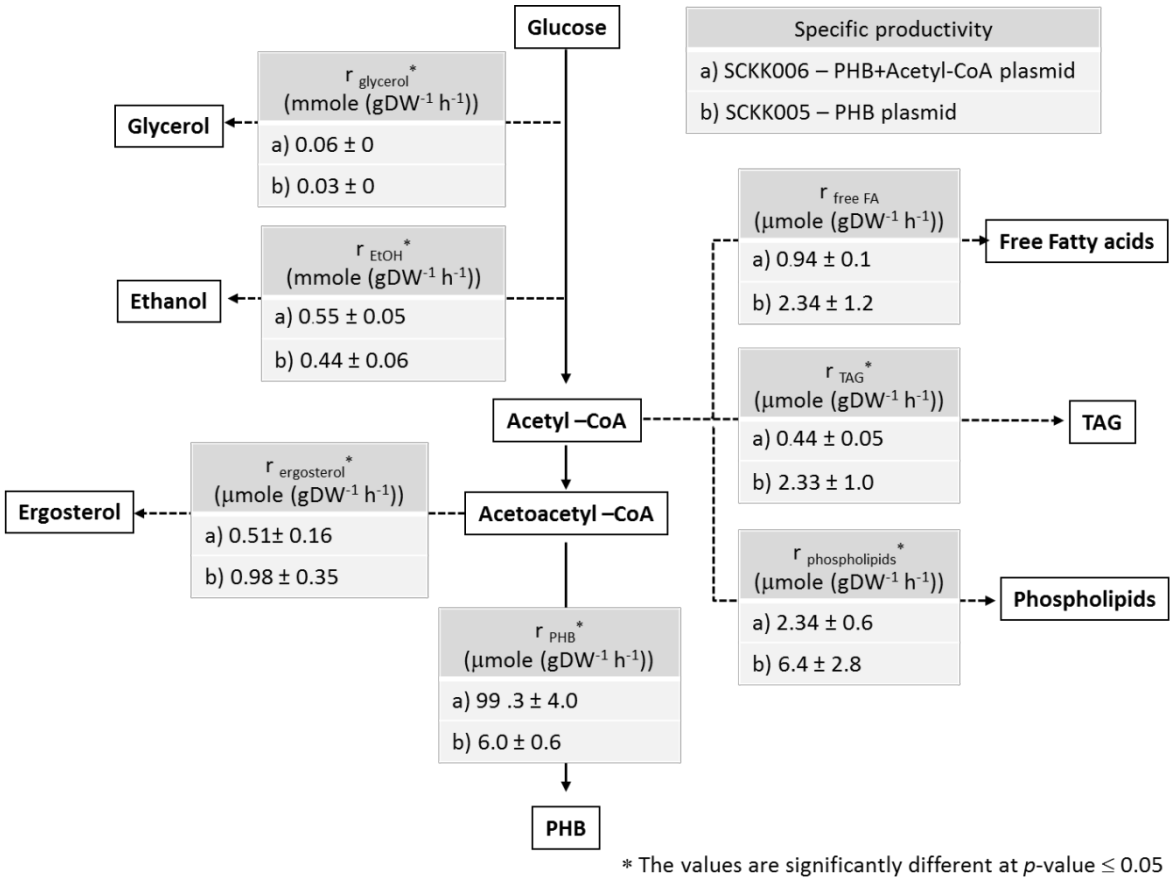

Figure 16 Comparison of specific fluxes in SCKK006 and SCKK005 during growth on glucose in aerobic batch bioreactor cultivation with 20 g L^{-1} glucose as carbon source. SCKK006 is *S. cerevisiae* harboring an acetyl-CoA boost plasmid (pIYC08) and the PHB plasmid (pKK01). SCKK005 is *S. cerevisiae* harboring an empty plasmid (pIYC04) and the PHB plasmid (pKK01). The fluxes towards the different lipids were calculated from measurement of the lipid composition of the biomass and the maximum specific growth rate. The mean value ± SD from at least triplicate fermentations are reported.

The specific product formation rate (flux) was calculated by using the equation: $r_p = \mu_{max} \cdot Y_{sp}/Y_{sx}$ and the specific glucose consumption rate was calculated by using the equation: $r_s = \mu_{max} /Y_{sx}$.

Considering acetyl-CoA as the intermediate which can be utilized as a precursor for other metabolites in the central carbon metabolism, the specific productivities of PHB including the directly and non-directly acetyl-CoA derived products were determined. The specific fluxes are reported in Figure 16. Employing the acetyl-CoA boost plasmid helped channeling the

carbon flow from ethanol to acetyl-CoA and increased the specific productivity of PHB from 6 µmol·gDW^{-1}·h^{-1} to 99 µmol·gDW^{-1}·h^{-1}. In addition, the specific productivities of free fatty acids, triacylglycol (TAG), phospholipids and ergosterol which utilized acetyl-CoA in the biosynthesis pathway were decreased in strain with the co-expression of acetyl-CoA boost plasmid and PHB plasmid. The higher specific productivity of glycerol in SCKK006 indicates the influence of *ADH2* overexpression and the insufficient capacity of the ethanol-acetaldehyde redox shuttle to reoxidize the cytosolic NADH (Overkamp et al. 2000) generated by the conversion reaction of ethanol to acetaldehyde thus triggering the formation of glycerol for redox balancing in the cytosol (Bakker et al. 2001). In addition, a three times higher maximum acetate concentration, 0.42 g·L^{-1}, was detected in SCKK005 (Figure 4 in Paper 3). Therefore, the different concentrations of glycerol and acetate are most likely a consequence of introducing the acetyl-CoA boost plasmid in the PHB producing strain.

By comparison of the specific productivities of PHB, we can conclude that enhancement of acetyl-CoA production by overexpression of genes from the ethanol degradation pathway improved the productivity of PHB during growth on glucose and further enhanced the productivity of PHB approximately 16.5 times in bioreactor cultivations and reduce the flux from acetyl-CoA to lipids (Paper 3).

2.2.2. Specific growth rate and substrate dependent PHB production

PHB production in *S. cerevisiae* is mainly produced during growth in the ethanol phase as presented in Figure 17, where the specific growth rate is substantially lower compared to the exponential phase when cells grow on glucose. In addition, it was observed that the growth of PHB producing strains in aerobic shake flasks was always lower with (maximum specific growth rate of 0.18 h^{-1}-0.20 h^{-1}) than growth in a fully aerobic bioreactor (0.27 h^{-1}-0.28 h^{-1}), although it resulted in higher PHB production. It is known that the specific growth rate influences the physiology of *S. cerevisiae* hence affected the fermentative capacity, TCA cycle activity and other metabolic activities (Blank and Sauer 2004; Frick and Wittmann 2005; Van Hoek et al. 1998). For this reason, we investigated the effect of specific growth rate on the PHB production in *S. cerevisiae* harboring the plasmid with overexpression of the ethanol degradation pathway (acetyl-CoA boost plasmid) and the PHB plasmid by employing the chemostat cultivation system, where the dilution rate is proportional to the specific growth

rate during batch cultivation. Besides that, we assessed the PHB production on different carbon sources - glucose, ethanol and the mixture of glucose and ethanol - with regards to their potential as a substrate for PHB production in *S. cerevisiae.*

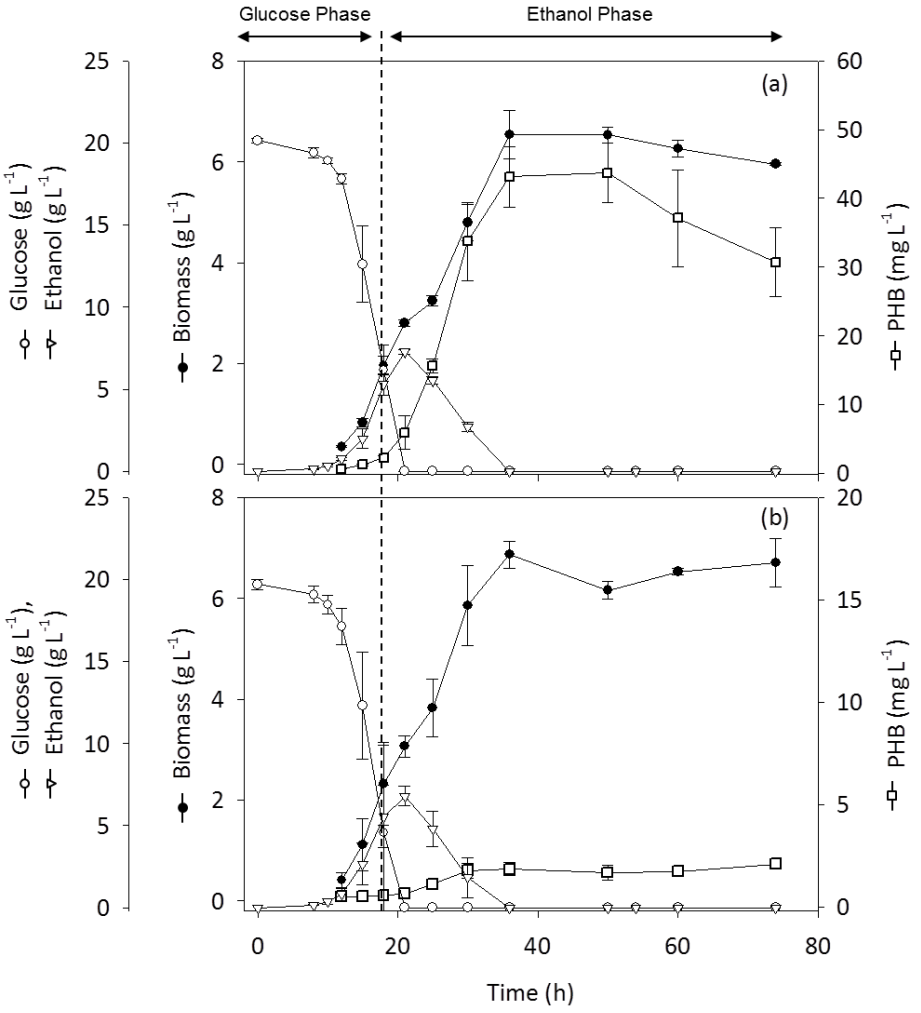

.

Figure 17: Fermentation profile of *S. cerevisiae* (SCKK006) producing PHB in aerobic batch bioreactor cultivation using a chemically defined medium with 20 g L^{-1} glucose as carbon source. (a) SCKK006: *S. cerevisiae* harboring an acetyl-CoA boost plasmid (pIYC08) and the PHB plasmid (pKK01). (b) SCKK005: *S. cerevisiae* harboring an empty plasmid (pIYC04) and the PHB plasmid (pKK01)

Table 2: Yields and kinetic parameters obtained during chemostat cultivations.

Feeding component	Dilution rate	Y_{sx}	Y_{sEtOH}	Y_{sPHB}	Ethanol accumulation	Y_{xPHB}
	h^{-1}	Cmol/ Cmol	Cmol/C mol	Cmmol/Cmol	Cmol/L	mg/gDW
Glucose	0.05	0.51 ± 0.01	-	2.51 ± 0.07	0	4.33 ± 0.19
	0.10	0.57 ± 0	-	3.67 ± 0	0	5.59 ± 0
	0.15	0.36 ± 0.02	0.02 ± 0	2.44 ± 0	-	5.94 ± 0.64
	0.20	0.29 ± 0	0.1 ± 0	1.92 ± 0	-	5.59 ± 0.23
Ethanol	0.05	0.45 ± 0.01	0	8.50 ± 0.23	0	16.55 ± 0.02
	0.10	0.37 ± 0	-	4.94 ± 0.58	0.0964 ± 0	13.49 ± 0
	0.15	0.12 ± 0.01	-	0.46 ± 0.05	0.2364 ± 0	5.30 ± 0.31
Glucose:Ethanol	0.05	0.48 ± 0.02	0	9.97 ± 0.07	0	18.34 ± 0.53
(1:2)	0.10	0.38 ± 0	-	7.41 ± 0	0.2012	12.41 ± 0
	0.15	0.30 ± 0	-	2.57 ± 0.1	0.1637	7.50 ± 0.19
	0.20	0.22 ± 0	-	1.13 ± 0	0.2769	4.56 ± 0

The values were calculated from duplicate fermentations and are represented as mean ± SD. The formula for biomass used in this calculation is $CH_{1.8}O_{0.5}N_{0.2}$. Y_{sx} = biomass yield on substrate, Y_{sEtOH} = ethanol yield on substrate, Y_{sPHB} = PHB yield on substrate, Y_{xPHB} = PHB yield per biomass

In this experiment, the chemostat cultivation was operated at different dilution rates ranging from 0.05 h^{-1} to 0.2 h^{-1} with the feeding medium being composed of different carbon sources. The biomass yields and PHB yields are reported in Table 2. Apart from growth on glucose, the biomass yield and PHB yield on substrate tended to decrease when increasing the dilution rates. The maximum PHB content, 18.34 mg/gDW, was obtained when the mixed substrate was used in the feed at a dilution rate of 0.05 h-1. Comparing either glucose or ethanol as sole carbon source, ethanol alone resulted in a ~3 times higher PHB yield when the chemostat was operated at D= 0.05 h-1although it led to a lower biomass yield on substrate. The high specific growth rate and sugar concentration trigger the production of ethanol according to the respirofermentative metabolism (Duntze et al. 1969; Hanegraaf et al. 2000; Maaheimo et al. 2001). Besides that, utilizing glucose as a carbon source in the feed medium at a high specific growth rate reduces the flux to the PP pathway, which might lower the supply of NADPH (Frick and Wittmann 2005) required as a cofactor in the PHB biosynthesis pathway. Therefore, when glucose is used as a carbon source, it substantially lowers the PHB production.

The simplified schemes in Figure 18 illustrate the possible directionality of the central carbon metabolism when glucose (a), ethanol (b) and the mixture of glucose and ethanol (c) are used as carbon sources for growth and PHB biosynthesis. When the feed is composed of ethanol, the PHB yield is higher than on glucose because ethanol could replace pyruvate and serve directly as a source for acetyl-CoA used for the synthesis of PHB particularly in the tested strain with overexpression of *ADH2*. However, *S. cerevisiae* grown on ethanol requires the activity of the glyoxylate and the gluconeogenesis pathway to accomplish the synthesis of biomass and the TCA cycle intermediates. Consequently, it resulted in the lower biomass yield compared to glucose. To compensate between growth and the biosynthesis of PHB, the mixed substrate was introduced to the system and showed its potential to be used for PHB production since glucose phosphorylation still occurs while malate synthase, which converts glyoxylate to malate in the glyoxylate cycle, replaces pyruvate in the synthesis of TCA intermediates and ethanol still serves as the main source for cytosolic acetyl-CoA production (de Jong-Gubbels et al. 1995).

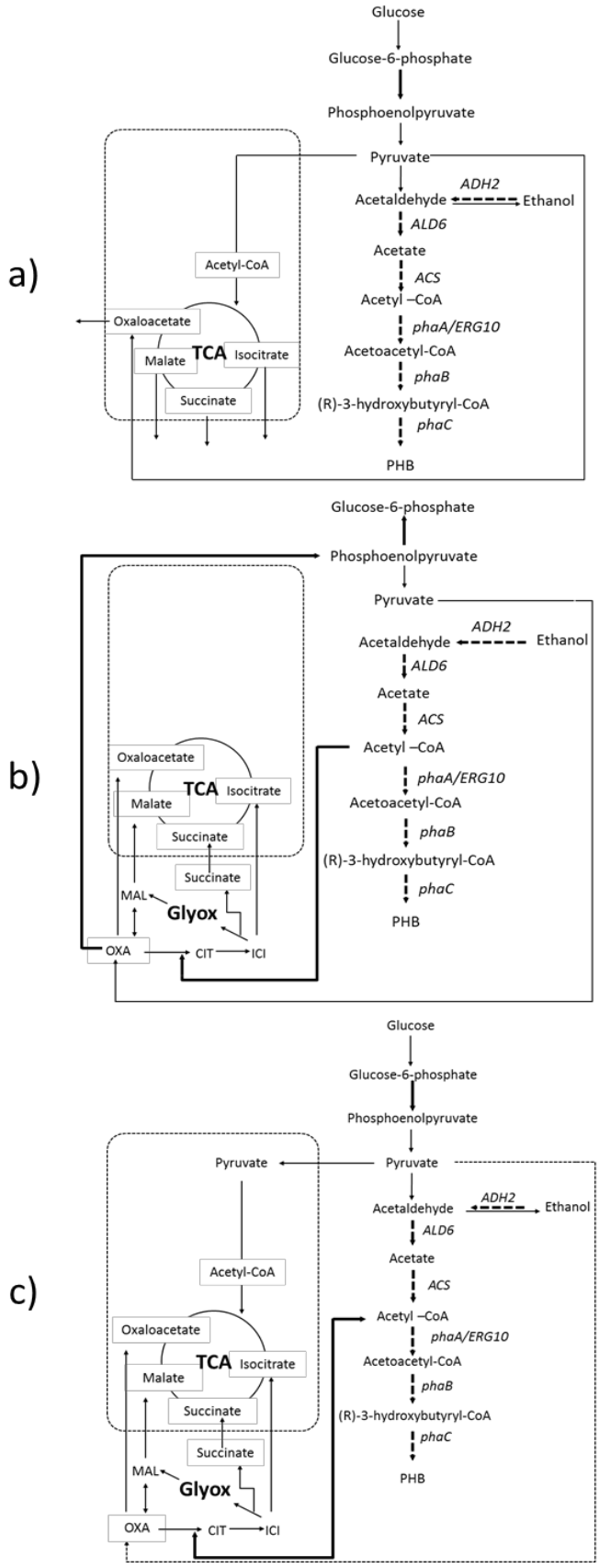

Figure 18: Central carbon metabolism of PHB producing *S. cerevisiae* grown on different substrates. a) Glucose, b) Ethanol and c) Mixed-substrate of glucose and ethanol.

ADH2 = alcohol dehydrogenase; *ALD6* = aldehyde dehydrogenase; *ACS* = acetyl-CoA synthetase (acs^{L641P}); *ERG10* = acetyl-CoA C-acetyltransferase; *PhaA* (β-ketothiolase); *PhaB* (acetoacetyl-CoA reductase); *PhaC* (polyhydroxyalkanoate synthase)

ICI = isocitrate; CIT = citrate: OXA = oxaloacetate; MAL = malate; Glyox = glyoxylate

From the industrial point of view, the overall volumetric productivity was best improved (refer to the conditions used in this study) when using the mixed substrate at the dilution rate of 0.1 h^{-1}. This operation led to a PHB productivity of 8.23 mg/gDW·h^{-1} (Figure 19). The assessment of volumetric productivity confirms the potential of using a mixed-substrate for PHB production. However when mixed substrate is used, the ratio between glucose and ethanol should be considered carefully since it reflects the pattern of central carbon metabolism.

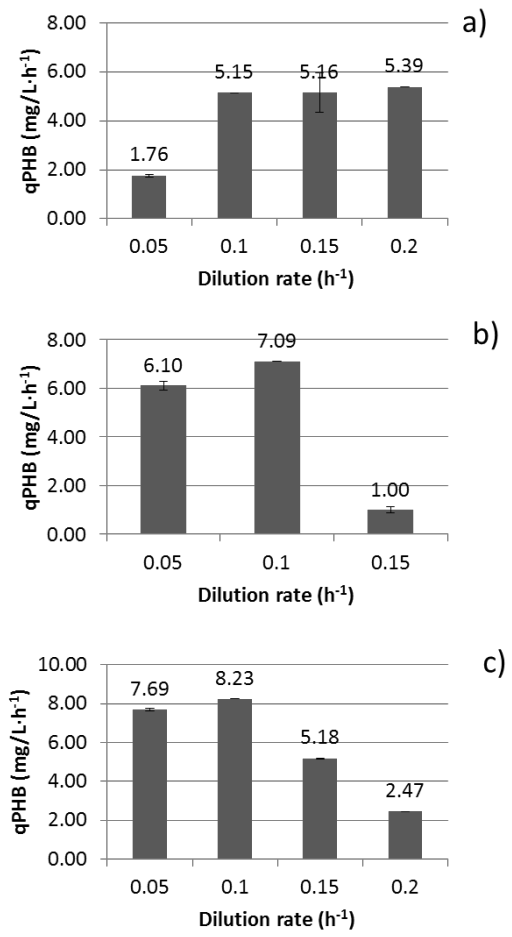

Figure 19: PHB productivities of recombinant *S. cerevisiae* grown on different substrates at different dilution rates from the chemostat cultivation. a) Glucose, b) Ethanol, c) Mixed-substrate

2.2.3. Cofactor supplementation

As the number of available databases and the reconstructed genome scale metabolic models increase, many approaches have been attempted to improve the efficiency of *S. cerevisiae* as a cell factory for the production of biocompounds. Simulations using the model of a natural PHB producer like *R. eutropha* revealed that the activities of all PHB pathway enzymes influence the overall PHB flux and that no single enzymatic step can easily be identified as rate limiting. The simulations also supported regulatory roles for both thiolase and reductase, mediated through acetyl-CoA/CoA and NADPH/$NADP^+$ ratios, respectively (Leaf and Srienc 1998). In engineered *E. coli* expressing the PHB biosynthesis pathway, instead of the availability of precursors, the expression level of acetoacetyl-CoA reductase (phaB) was suggested to be the factor controlling the flux to PHB, since the PHB flux was insensitive to the specific growth rate in a nitrogen-limited chemostat (Tyo et al. 2010a). In case of PHB producing yeast, the elementary mode analysis of recombinant *S. cerevisiae* expressing the PHB pathway was performed by Srienc and co-workers, which suggested that the introduction of the ATP citrate-lyase reaction and the transhydrogenase reaction can improve the theoretical PHB carbon yield by supplying metabolites, acetyl-CoA as precursor and NADPH as cofactor, used for PHB production (Carlson et al. 2002). .

Enhancing the availability of acetyl-CoA by overexpression of genes from the ethanol degradation pathway has been shown to improve PHB production (Paper 3). Apart from acetyl-CoA supply as mentioned earlier in Chapter 2.2.1, NADPH as a required cofactor for the activity of acetoacetyl-CoA reductase (PhaB) in the PHB biosynthesis pathway is also a factor that supposed to influence PHB production in *S. cerevisiae*. Therefore, GapN from *S. mutans* was introduced into the PHB producing yeast in order to supply NADPH required during the reduction of acetoacetyl-CoA in the PHB biosynthesis pathway.

Since the major source of cytosolic NADPH production in *S. cerevisiae* grown on glucose has been attributed to glucose-6-phosphate dehydrogenase in the PP pathway, implementation of the phosphoketolase pathway from *A. nidulans* which utilizes xylulose 5-phosphate, an intermediate from the PP pathway, was proposed for channeling the flux from the EMP to the PP pathway. Overexpression of the reconstructed phosphoketolase pathway together with acetyl-CoA synthetase in *S. cerevisiae* was settled as an alternative route for providing NADPH and simultaneously contributing to increased acetyl-CoA production.

Integration of bacterial GapN and implementation of the *Aspergillus* phosphoketolase pathway were investigated for their potential to improve the PHB production in *S. cerevisiae*. The schematic pathway representing the strategies for improving the availability of NADPH is illustrated in Figure 20.

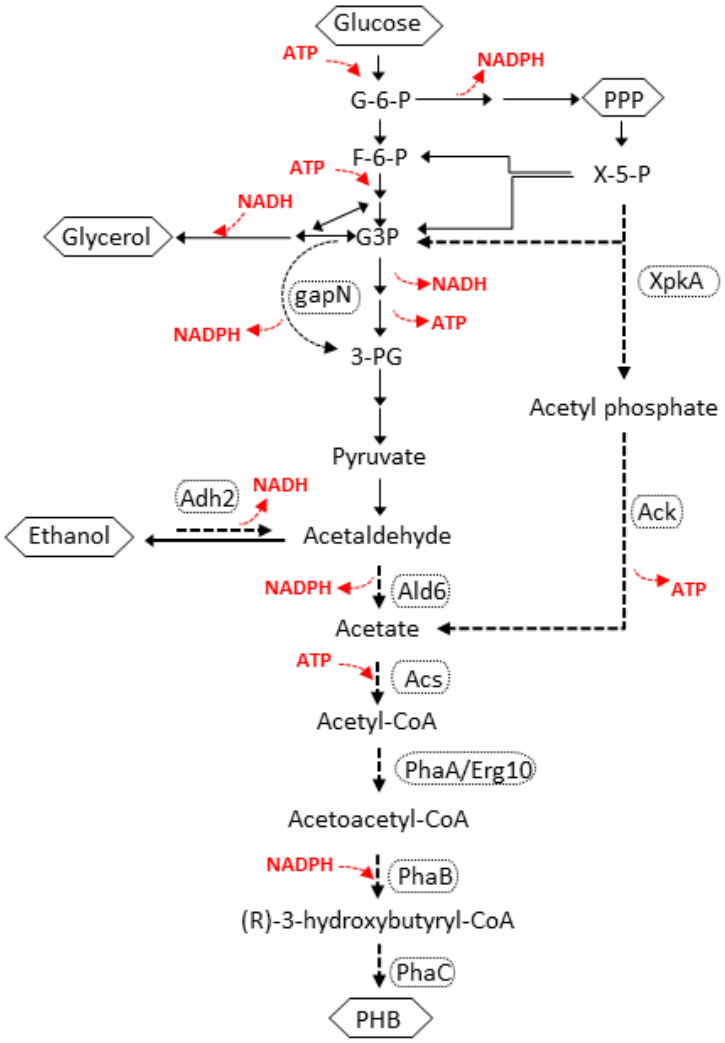

Figure 20: Schematic pathway representing metabolic engineering strategies for improving PHB production in *S. cerevisiae*. PPP = Pentose phosphate pathway, G-6-P = Glucose-6-phosphate, F-6-P = Fructose-6-phosphate, G3P = Glyceraldehyde-3-phosphate, 3-PG = 3-Phosphoglycerate, PHB = Polyhydroxybutyrate. Dashed arrows represent engineered pathway steps.

Besides influencing the redox metabolism by regenerating NADPH, integration of *gapN* may also result in an altered carbon flux resulting in an increased flux towards ethanol and a

reduced flux towards glycerol. When *gapN* is integrated into the chromosome of *S. cerevisiae*, a 45% decrease in glycerol formation was observed in this study (Paper.5). A comparison of PHB production in strains with and without *gapN* integration is illustrated in Figure 21. The effect of *gapN* on improving PHB production was clearly observed as the PHB yield on glucose and on ethanol of SCKK033 were substantially higher than for SCKK005 (Table 3) because GapN is expected to not only increase NADPH, but also reduce the split ratio from the glyceraldehyde-3-phosphate branch point towards glycerol. The maximum cellular PHB content obtained at 100 h in SCKK033, 14.87 mg/gDW, was 3.7 times higher than in the reference strain, SCKK005.

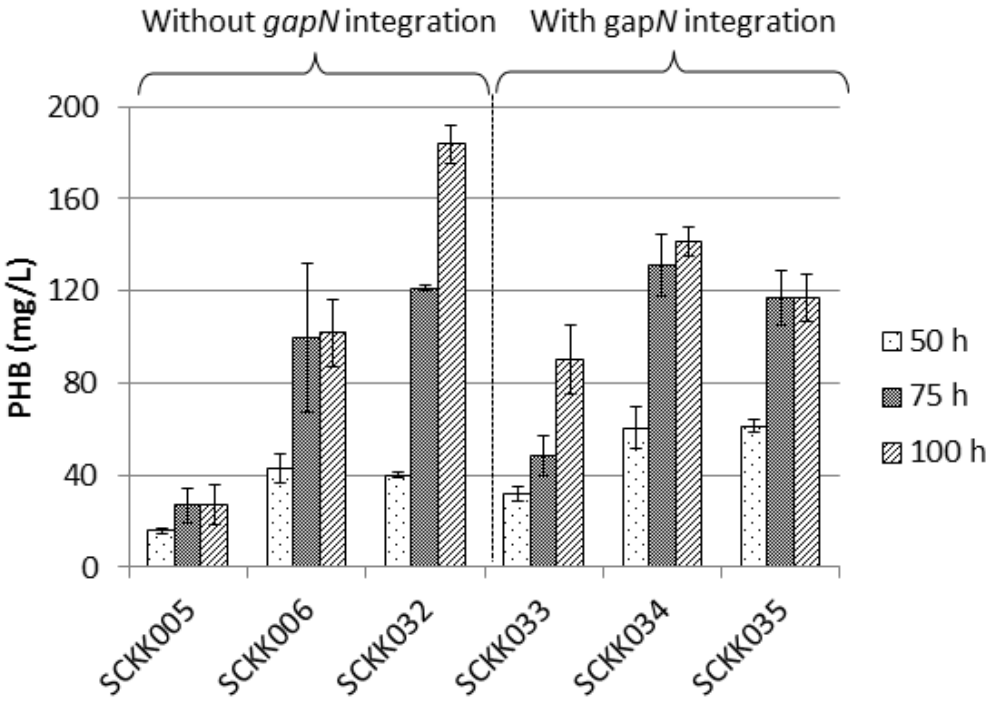

Figure 21 Polyhydroxybutyrate production in *S. cerevisiae* employing different strategies to improve PHB production. SCKK005 and SCKK033 harbor only the PHB plasmid (pKK01). SCKK032 and SCKK035 carry pJC7 (phosphoketolase pathway) whereas SCKK006 and SCKK034 carry pIYC08 (ethanol degradation pathway). Samples for PHB measurement were taken at 50 h (the glucose phase), 75 h (the ethanol phase) and 100 h (the end of fermentation where all the glucose and ethanol were depleted).

Table 3: Physiological parameters obtained during growth on minimal media with 20 $g \cdot L^{-1}$ glucose in shake flask cultivations

Strain	Strains without *gapN* integration			Strains with *gapN* integration		
	SCKK005	SCKK006	SCKK032	SCKK033	SCKK034	SCKK035
μ_{max} (h^{-1})	0.27 ± 0.02	0.28 ± 0	0.21 ± 0.01	0.22 ± 0	0.23 ± 0.02	0.22 ± 0.02
r_s (g/gDW/h)	1.80 ± 0.09	2.24 ± 0.33	2.00 ± 0	1.37 ± 0	1.31 ± 0.18	1.30 ± 0.12
Y_{SX} (g/g glc)	0.15 ± 0.01	0.13 ± 0.02	0.11 ± 0	0.16 ± 0	0.18 ± 0.02	0.17 ± 0.02
Y_{SEtOH} (g/ g glc)	0.35 ± 0.05	0.35 ± 0.07	0.39 ± 0.01	0.48 ± 0.01	0.35 ±0.01	0.43 ± 0
Y_{SGly} (g/g glc)	0.05 ± 0	0.07 ± 0	0.07 ± 0	0.04 ± 0.01	0.05 ± 0.01	0.04 ± 0
Y_{SPHB} (mg/ g glc)	0.02 ± 0.01	0.13 ± 0.02	0.03 ± 0	0.27 ± 0.01	0.12 ± 0	0.06 ± 0
$Y_{EtOH \cdot PHB}$ (mg/ g EtOH)	0.22 ± 0.04	6.09 ± 1.44	56.40 ± 0.77	16.11 ± 2.38	14.50 ± 2.90	12.48 ± 0.81
PHB content at 100 h (mg/gDW)	4.02 ± 0.16	15.89 ± 0	27.86 ± 0	14.87 ± 0.4	27.52 ± 4.82	21.41 ± 0.69

These values were calculated from at least triplicate shake flasks ($n \geq 3$) and are represented as mean ± SD.

All strains listed in Table 3 harbor the PHB plasmid (pKK01). SCKK005 and SCKK032 carry pKK001 and pIYC04. SCKK032 and SCKK035 express the phosphoketolase pathway, SCKK006 and SCKK034 overexpress the ethanol degradation pathway.

μ_{max} = maximum specific growth rate on glucose, r_s = specific glucose consumption, Y_{SX} = biomass yield on substrate (glucose), Y_{SEtOH} = ethanol yield on substrate (glucose), Y_{SGly} = glycerol yield on substrate (glucose) Y_{SPHB} = PHB yield on substrate (glucose), $Y_{EtOH \cdot PHB}$ = PHB yield on ethanol

Although integration of *gapN* involved both redox and carbon alteration, it helps increase the flux toward PHB biosynthesis pathway by supplying more NADPH rather than channeling the carbon since there was no significant difference in the specific productivity of glycerol and ethanol in SCKK005 and SCKK033 (Figure 22). Therefore, integration of *gapN* to supply NADPH supports our hypothesis that increase production of NADPH can improve PHB production in *S. cerevisiae*.

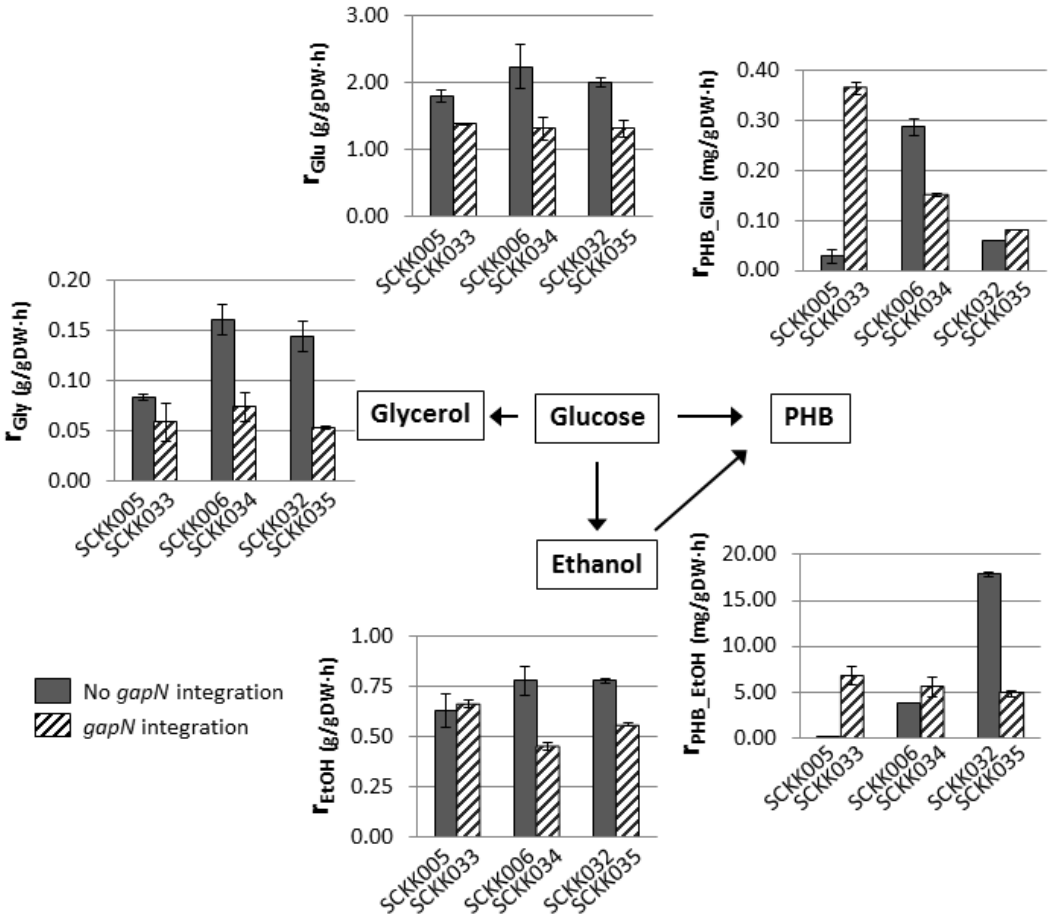

Figure 22 Specific productivity of ethanol, glycerol and PHB obtained from shake flask cultivations. The specific product formation rate was calculated by using the equation: $r_p = u_{max} Y_{sp}/Y_{sx}$

r_{EtOH} = specific productivity of ethanol, r_{Gly} = specific productivity of glycerol, r_{PHB_Glu} = specific productivity of PHB in the glucose consumption phase, r_{PHB_EtOH} = specific productivity of PHB in the ethanol consumption phase

The combined strategies to enhance the precursor, acetyl-CoA, and cofactor, NADPH, supply using *gapN* integration and over-expression of the ethanol degradation pathway is able to improve PHB production. However, there was no benefit from the provision of NADPH by GapN when combined with the reconstructed phosphoketolase pathway since no improvement on PHB production was observed. This might be due to the lack of a mitochondrial NADPH dehydrogenase in *S. cerevisiae* which otherwise couples the oxidation of cytosolic NADPH to the mitochondrial respiratory chain. Therefore, a direct oxidation of a surplus NADPH generated by the PP pathway in the respiration chain is not possible (Bruinenberg 1986; Siso et al. 1996). Furthermore, an increased production of NADPH by the EMP pathway may result in a reduced flux through the PP pathway as the glucose-6-phosphate dehydrogenase flux is very sensitive to the NADP/NADPH ratio (Vaseghi et al. 1999). When *S. cerevisiae* is grown on glucose, the PP pathway is the major source for NADPH production, specifically the dehydrogenase activity during the two first steps in the pathway (Grabowska and Chelstowska 2003; Minard and McAlister-Henn 2005). When the reconstructed phosphoketolase pathway is implemented in *S. cerevisiae*, it likely changed the split ratio of carbon from entering the lower EMP pathway to the PP pathway. The flux analysis in the strain expressing the reconstructed phosphoketolase pathway revealed a flux increase to the PP pathway (from G6P to P5P) from 32.44 to 44.55 and decreased flux to the lower EMP (from G6P to F6P) from 46.53 to 33.06 (Papini et al. 2012). Therefore, an increasing carbon flux through the PP pathway has a direct consequence for the supply of NADPH required in various anabolic reactions and of certain anabolic precursors (Frick and Wittmann 2005). For this reason, a noticeable high yield of PHB on ethanol was observed for the strain that can generate acetyl-CoA and NADPH simultaneously through the PP pathway, SCKK032. These results strongly support our hypothesis that the improved PHB production in *S. cerevisiae* required both sufficient precursor and cofactor supply.

CHAPTER 3. Conclusion

Throughout my thesis work I have focused on metabolic engineering of *S. cerevisiae* as a model organism and the concept of metabolic engineering has been investigated for its impact on establishing *S. cerevisiae* as a platform for production of industrially relevant chemical compounds. By adapting the stable and tunable expression system from *E. coli*, the implementation of CIChE was investigated for its practicability as a novel tunable expression system in *S. cerevisiae*. Pathway engineering was examined for the potential to enhance the production of acetyl-CoA and NADPH as required precursor and cofactor for the production of PHB, the model compound in this research.

To develop a stable expression system in *S. cerevisiae*, the CIChE strategy developed in *E. coli* has shown potential to be applied in *S. cerevisiae.* However, additional studies need to be carried out. An alternative selectable marker such as the metallothionein gene would be preferable over an antibiotic resistance marker since it might improve the evolution process and be more practical for industrial applications since no antibiotic resistance marker is present in the CIChE engineered strain. It has been seen in *E. coli* that deletion of *RecA* helped stabilizing the CIChE strain. However deletion or down-regulation of genes involved homologous recombination in *S. cerevisiae,* the *RAD52* epistasis group, must be done carefully since the regulation of homologous recombination in *E. coli* and *S. cerevisiae* is different and it might affect the growth ability of the evolved strain.

Metabolic engineering of eukaryote such as *S. cerevisiae* is different from prokaryotes like *E. coli* since the cell is more complex and compartmentalized. Some metabolites can be transported or diffuse across the membrane while intermediate metabolites that interlink with many metabolic pathways such as acetyl-CoA cannot be transported across the organelles without the shuttle system. Therefore, metabolic engineering of *S. cerevisiae* that involves utilization of acetyl-CoA and NADPH should take compartmentalization into consideration.

Employing PHB as the model product in this study showed that the availability of acetyl-CoA and NADPH influences PHB production. Two alternative routes to produce cytosolic acetyl-CoA have been investigated, 1) overexpression of the ethanol degradation pathway and 2) implementation of heterologous phosphoketolase pathway to increase the split ratio of carbon to the PP pathway and simultaneously generating NADPH as required cofactor. Deletion of genes that drain cytosolic acetyl-CoA and use it in the glyoxylate cycle was not able to

promote PHB production. Moreover, it resulted in a defective growth behavior. Introduction of bacterial GapN to increase NADPH resulted in an improved PHB production. However, combined strategies did not lead to any superior effect on improving PHB production.

Since the source of acetyl-CoA varied with the type of carbon sources, ethanol seems to be the best substrate for PHB production. However in terms of productivity, the mixture of glucose and ethanol at the appropriate ratio will improve the PHB production since it compensates between biomass and product formation.

In conclusion, the papers described in the thesis demonstrate proof-of-concepts of using metabolic engineering to develop *S. cerevisiae* as a cell factory for producing industrially relevant compounds. Although the PHB production in this study could not reach the ultimate productivity compared to the natural producer, I believe that the strategies employed here could be applied to develop a platform for any product that is derived from acetyl-CoA and requires NADPH in the biosynthesis pathway.

CHAPTER 4. Perspectives on developing *S. cerevisiae* as a cell factory for biocompounds production

There are many reasons supporting the utilization of *S. cerevisiae* as a model organism for expression of various heterologous pathways. Systems and synthetic biology also advance metabolic engineering in *S. cerevisiae* to meet the point where the engineered heterologous pathway can compromise with the native host metabolic pathway and ultimately be competitive with the traditional chemical synthesis pathway. Despite the success of metabolic engineering to improve PHB production in *S. cerevisiae*, there still exist areas for continued development by implementation of knowledge obtained from this study. For instance, in order to maximize the flux to product formation, pathway engineering is achieved either by removing the competitive enzyme(s) at the branch point of competing pathways or overexpressing the enzymes in the heterologous pathway, so that the substrate can be directed to the desired products instead of by-product formation. Unfortunately, a complete removal of enzymes from the competitive pathways, sometimes results in a defect in growth (as seen for the deletion of genes involved in the glyoxylate cycle- Paper 3). Therefore, implementation of CIChE, which enables the tunable control of the expression level of a specific gene in a particular pathway can be applied (1) to balance the expression level with other genes in the biosynthesis pathway, (2) to control the expression level of a gene encoding an enzyme that has been identified as a factor limiting the specific productivity or the flux toward product formation, and (3) to control the expression level of an essential gene encoding a by-product formation. When a non-native pathway is employed in *S. cerevisiae* that involves intermediates such as acetyl-CoA or the redox cofactor NADPH, compartmentalization should be taken into account since *S. cerevisiae* is not capable of de novo synthesis of carnitine involved in the shuttle system for acetyl-CoA and the evidence for NADPH transport across the mitochondrial membrane still needs to be provided. Altogether, to accomplish the development of *S. cerevisiae* as a universal platform for industrial applications requires the knowledge from molecular regulation to particular pathway engineering and the overall cell physiology and metabolism.

ACKNOWLEDGEMENTS

From 2009, my PhD journey started and it has been a challenging trip, with both ups and downs. Fortunately, with the great support from so many people, I can walk through these obstacles and accomplish a big step in my life.

First and foremost, I would like to thank my supervisor, Prof. Jens Nielsen. You gave me a great opportunity to pursue a PhD under your supervision. Your optimism and scientific enthusiasm always motivate and encourage me. I really appreciate your trust and unlimited support as well as all valuable guidance over the past four years. I would also like to thank Asst. Prof. Keith Tyo, my co-supervisor during the early stage of my PhD for sharing your expertise and teaching me good manners in the lab, I learned so much from you. I am also indebted to Dr. Verena Siewer, my co-supervisor for being patient and always kindly assist me whenever I asked for help.

I would also like to acknowledge the administrative staffs; Erica Dahlin, Martina Butorac and the Laboratory staffs; Marie Nordqvist, Malin Nordvall, Ximena Sevilla and Suwanee Jansa-Ard for your supports which make everything run smoothly.

A research work would be difficult without good colleagues. I would like to thank Dr. Yun Chen, Dr. António Roldão, Dr. Zihe Liu, Dr. Anastasia Krivoruchko, Dr. Eugenio Arturo Meza Mora, Yiming Zhang, Jichen Bao, Klaas Buijs, Juan Octavio Valle Rodriguez. Please forgive me if your name is not mentioned here but you know that I really appreciate working with you all. My sincere gratitude also goes to Asst. Prof. Wanwipa Vongsangnak, Dr. Intawat Nookaew, Dr. Pramote Chumnanpuen, Dr. Sakda Khoomrung, Dr. Jie Zhang, Dr. Siavash Partow, Dr. Marta Papini, Dr. Gionata Scalcinati, Dr. Kuk-ki Hong, Kwanjeera Wanichthanarak, Natapol Pornputtapong, Tobias Österlund, Christoph Knuf, Bouke de Jong, Stefan Tippmann, and Nina Johansson. Living far away from home, life would not be this wonderful without friends like you.

I would like to thank the Ministry of Science and Technology, Thailand and the Chalmers Foundation for financial support during my PhD study.

My deeply gratitude goes to my family, mom and dad for no questions of supporting me. A special thanks goes to my younger sister for taking care of everything when I am here.

Kanokarn Kocharin

April, 2013

REFERENCES

Akaraonye E, Keshavarz T, Roy I (2010) Production of polyhydroxyalkanoates: the future green materials of choice. J Chem Technol Biotechnol 85(6):732-743

Alper H, Fischer C, Nevoigt E, Stephanopoulos G (2005) Tuning genetic control through promoter engineering. PNAS 102(36):12678-12683

Anderlund M, Nissen TL, Nielsen J, Villadsen J, Rydstrom J, Hahn-Hagerdal B, Kielland-Brandt MC (1999) Expression of the *Escherichia coli pntA* and *pntB* genes, encoding nicotinamide nucleotide transhydrogenase, in *Saccharomyces cerevisiae* and its effect on product formation during anaerobic glucose fermentation. Appl Environ Microbiol 65(6):2333-40

Bai Flagfeldt D, Siewers V, Huang L, Nielsen J (2009) Characterization of chromosomal integration sites for heterologous gene expression in *Saccharomyces cerevisiae*. Yeast 26(10):545-551

Bailey JE, Sburlati A, Hatzimanikatis V, Lee K, Renner WA, Tsai PS (1996) Inverse metabolic engineering: A strategy for directed genetic engineering of useful phenotypes. Biotechnol Bioeng 52(1):109-21

Bakker B, Overkamp K, van Maris A, Kotter P, Luttik M, van Dijken J, Pronk J (2001) Stoichiometry and compartmentation of NADH metabolism in *Saccharomyces cerevisiae*. FEMS Microbiol Rev 25(1):15 - 37

Bernofsky C, Utter MF (1968) Interconversions of mitochondrial pyridine nucleotides. Science 159(3821):1362-3

Bieganowski P, Seidle HF, Wojcik M, Brenner C (2006) Synthetic lethal and biochemical analyses of NAD and NADH kinases in *Saccharomyces cerevisiae* establish separation of cellular functions. J Biol Chem 281(32):22439-45

Blank LM, Sauer U (2004) TCA cycle activity in *Saccharomyces cerevisiae* is a function of the environmentally determined specific growth and glucose uptake rates. Microbiol 150(Pt 4):1085-93

Boeke JD, Eichinger DJ, Natsoulis G (1991) Doubling Ty1 element copy number in *Saccharomyces cerevisiae*: host genome stability and phenotypic effects. Genetics 129(4):1043-52

Boeke JD, Xu H, Fink GR (1988) A general method for the chromosomal amplification of genes in yeast. Science 239(4837):280-2

Breuer U, Terentiev Y, Kunze G, Babel W (2002) Yeasts as producers of polyhydroxyalkanoates: Genetic engineering of *Saccharomyces cerevisiae*. Macromol Biosci 2(8):380-386

Bro C, Regenberg B, Forster J, Nielsen J (2006) In silico aided metabolic engineering of *Saccharomyces cerevisiae* for improved bioethanol production. Metab Eng 8(2):102-11

Bruinenberg PM (1986) The NADP(H) redox couple in yeast metabolism. Antonie Leeuwenhoek 52(5):411-29

Bruinenberg PM, Vandijken JP, Scheffers WA (1983) A theoretical-analysis of NADPH production and consumption in yeasts. J Gen Microbiol 129(Apr):953-964

Carlson R, Fell D, Srienc F (2002) Metabolic pathway analysis of a recombinant yeast for rational strain development. Biotechnol Bioeng 79(2):121-34

Carlson R, Srienc F (2006) Effects of recombinant precursor pathway variations on poly[(R)-3-hydroxybutyrate] synthesis in *Saccharomyces cerevisiae*. J Biotechnol 124(3):561-73

Chen Y, Siewers V, Nielsen J (2012) Profiling of cytosolic and peroxisomal acetyl-CoA metabolism in *Saccharomyces cerevisiae*. PloS one 7(8):e42475

Cherry JM, Hong EL, Amundsen C, Balakrishnan R, Binkley G, Chan ET, Christie KR, Costanzo MC, Dwight SS, Engel SR, Fisk DG, Hirschman JE, Hitz BC, Karra K, Krieger CJ, Miyasato SR, Nash RS, Park J, Skrzypek MS, Simison M, Weng S, Wong ED (2012) Saccharomyces Genome Database: the genomics resource of budding yeast. Nucleic Acids Res 40(D1):D700-D705

Conrad TM, Lewis NE, Palsson BO (2011) Microbial laboratory evolution in the era of genome-scale science. Mol Syst Biol 7:509

de Jong-Gubbels P, Vanrolleghem P, Heijnen S, van Dijken JP, Pronk JT (1995) Regulation of carbon metabolism in chemostat cultures of *Saccharomyces cerevisiae* grown on mixtures of glucose and ethanol. Yeast 11(5):407-18

de Jong B, Siewers V, Nielsen J (2012) Systems biology of yeast: Enabling technology for development of cell factories for production of advanced biofuels. Curr Opin Biotechnol 23(4):624-30

Devirgilio C, Burckert N, Barth G, Neuhaus JM, Boller T, Wiemken A (1992) Cloning and disruption of a gene required for growth on acetate but not on ethanol - the acetyl-coenzyme A synthetase gene of *Saccharomyces cerevisiae*. Yeast 8(12):1043-1051

Dimster-Denk D, Rine J (1996) Transcriptional regulation of a sterol-biosynthetic enzyme by sterol levels in *Saccharomyces cerevisiae*. Mol Cell Biol 16(8):3981-9

Doi Y, Kawaguchi Y, Koyama N, Nakamura S, Hiramitsu M, Yoshida Y, Kimura H (1992) Synthesis and degradation of polyhydroxyalkanoates in *Alcaligenes eutrophus*. FEMS Microbiol Lett 103(2–4):103-108

Duntze W, Neumann D, Gancedo JM, Atzpodien W, Holzer H (1969) Studies on the regulation and localization of the glyoxylate cycle enzymes in *Saccharomyces cerevisiae*. Eur J Biochem 10(1):83-9

Dwight SS, Balakrishnan R, Christie KR, Costanzo MC, Dolinski K, Engel SR, Feierbach B, Fisk DG, Hirschman J, Hong EL, Issel-Tarver L, Nash RS, Sethuraman A, Starr B, Theesfeld CL, Andrada R, Binkley G, Dong Q, Lane C, Schroeder M, Weng S, Botstein D, Cherry JM (2004) Saccharomyces genome database: underlying principles and organisation. Briefings Bioinf 5(1):9-22

Eustice DC, Wilhelm JM (1984) Mechanisms of action of aminoglycoside antibiotics in eucaryotic protein synthesis. Antimicrob Agents Chemother 26(1):53-60

Feist AM, Henry CS, Reed JL, Krummenacker M, Joyce AR, Karp PD, Broadbelt LJ, Hatzimanikatis V, Palsson BO (2007) A genome-scale metabolic reconstruction for *Escherichia coli* K-12 MG1655 that accounts for 1260 ORFs and thermodynamic information. Mol Syst Biol 3:121

Fogel S, Welch JW (1982) Tandem Gene amplification mediates copper resistance in yeast. P Natl Acad Sci-Biol 79(17):5342-5346

Fogel S, Welch JW, Cathala G, Karin M (1983) Gene amplification in yeast - Cup1 copy number regulates copper resistance. Curr Genet 7(5):347-355

Frick O, Wittmann C (2005) Characterization of the metabolic shift between oxidative and fermentative growth in *Saccharomyces cerevisiae* by comparative 13C flux analysis. Microb Cell Fact 4(1):30

Fujii T, Kondo K, Shimizu F, Sone H, Tanaka J, Inoue T (1990) Application of a ribosomal DNA integration vector in the construction of a brewer's yeast having α-acetolactate decarboxylase activity. Appl Environ Microbiol 56(4):997-1003

Goffeau A, Barrell BG, Bussey H, Davis RW, Dujon B, Feldmann H, Galibert F, Hoheisel JD, Jacq C, Johnston M, Louis EJ, Mewes HW, Murakami Y, Philippsen P, Tettelin H, Oliver SG (1996) Life with 6000 genes. Science 274(5287):546, 563-7

Gombert AK, Moreira dos Santos M, Christensen B, Nielsen J (2001) Network identification and flux quantification in the central metabolism of *Saccharomyces cerevisiae* under different conditions of glucose repression. J Bacteriol 183(4):1441-1451

Gorgens JF, van Zyl WH, Knoetze JH, Hahn-Hagerdal B (2001) The metabolic burden of the *PGK1* and *ADH2* promoter systems for heterologous xylanase production by *Saccharomyces cerevisiae* in defined medium. Biotechnol Bioeng 73(3):238-45

Grabowska D, Chelstowska A (2003) The *ALD6* gene product is indispensable for providing NADPH in yeast cells lacking glucose-6-phosphate dehydrogenase activity. J Biol Chem 278(16):13984-8

Green R (2010) Current strategies for optimizing polyhydroxyalkanoate production in bacteria systems. MMG 445 Basic Biotechnol 6(1)

Hanegraaf PP, Stouthamer AH, Kooijman SA (2000) A mathematical model for yeast respiro-fermentative physiology. Yeast 16(5):423-37

Hankermeyer CR, Tjeerdema RS (1999) Polyhydroxybutyrate: Plastic made and degraded by microorganisms. Reviews of Environmental Contamination and Toxicology. In: Ware GW (ed). vol 159. Springer New York, pp 1-24

Henry CS, Broadbelt LJ, Hatzimanikatis V (2007) Thermodynamics-based metabolic flux analysis. Biophys J 92(5):1792-805

Herrgard MJ, Lee BS, Portnoy V, Palsson BO (2006) Integrated analysis of regulatory and metabolic networks reveals novel regulatory mechanisms in *Saccharomyces cerevisiae*. Genome Res 16(5):627-35

Hiesinger M, Wagner C, Schuller HJ (1997) The acetyl-CoA synthetase gene *ACS2* of the yeast *Saccharomyces cerevisiae* is coregulated with structural genes of fatty acid biosynthesis by the transcriptional activators Ino2p and Ino4p. FEBS letters 415(1):16-20

Hiltunen JK, Wenzel B, Beyer A, Erdmann R, Fosså A, Kunau WH (1992) Peroxisomal multifunctional β-oxidation protein of *Saccharomyces cerevisiae*. Molecular analysis of the *fox2* gene and gene product. J Biol Chem 267(10):6646-6653

Hiser L, Basson ME, Rine J (1994) *ERG10* from *Saccharomyces cerevisiae* encodes acetoacetyl-CoA thiolase. J Biol Chem 269(50):31383-31389

Hong KK, Nielsen J (2012) Metabolic engineering of *Saccharomyces cerevisiae*: a key cell factory platform for future biorefineries. Cell Mol Life Sci 69(16):2671-90

Hou J, Lages NF, Oldiges M, Vemuri GN (2009) Metabolic impact of redox cofactor perturbations in *Saccharomyces cerevisiae*. Metab Eng 11(4-5):253-261

Hou J, Tyo KE, Liu Z, Petranovic D, Nielsen J (2012) Metabolic engineering of recombinant protein secretion by *Saccharomyces cerevisiae*. FEMS Yeast Res 12(5):491-510

Huh WK, Falvo JV, Gerke LC, Carroll AS, Howson RW, Weissman JS, O'Shea EK (2003) Global analysis of protein localization in budding yeast. Nature 425(6959):686-91

Keasling JD (2012) Synthetic biology and the development of tools for metabolic engineering. Metab Eng 14(3):189-195

Kern A, Tilley E, Hunter IS, Legiša M, Glieder A (2007) Engineering primary metabolic pathways of industrial micro-organisms. J Biotechnol 129(1):6-29

Khanna S, Srivastava AK (2005) Recent advances in microbial polyhydroxyalkanoates. Process Biochem 40(2):607-619

Kratzer S, Schuller HJ (1995) Carbon source-dependent regulation of the acetyl-coenzyme A synthetase-encoding gene *ACS1* from *Saccharomyces cerevisiae*. Gene 161(1):75-9

Kunau WH, Dommes V, Schulz H (1995) beta-oxidation of fatty acids in mitochondria, peroxisomes, and bacteria: a century of continued progress. Prog Lipid Res 34(4):267-342

Kunze M, Pracharoenwattana I, Smith S, Hartig A (2006) A central role for the peroxisomal membrane in glyoxylate cycle function. Biochim. Biophys. Acta 1763(12):1441 - 1452

Leaf TA, Peterson MS, Stoup SK, Somers D, Srienc F (1996) *Saccharomyces cerevisiae* expressing bacterial polyhydroxybutyrate synthase produces poly-3-hydroxybutyrate. Microbiol 142 (Pt 5):1169-80

Leaf TA, Srienc F (1998) Metabolic modeling of polyhydroxybutyrate biosynthesis. Biotechnol Bioeng 57(5):557-570

Lee Y, Jang J, Kim K, Maeng P (2011) TCA cycle-independent acetate metabolism via the glyoxylate cycle in *Saccharomyces cerevisiae*. Yeast 28(2):153 - 166

Maaheimo H, Fiaux J, Cakar ZP, Bailey JE, Sauer U, Szyperski T (2001) Central carbon metabolism of *Saccharomyces cerevisiae* explored by biosynthetic fractional ^{13}C labeling of common amino acids. Eur J Biochem 268(8):2464-79

Madsen KM, Udatha GD, Semba S, Otero JM, Koetter P, Nielsen J, Ebizuka Y, Kushiro T, Panagiotou G (2011) Linking genotype and phenotype of *Saccharomyces cerevisiae* strains reveals metabolic engineering targets and leads to triterpene hyper-producers. PloS one 6(3):e14763

Marchesini S, Erard N, Glumoff T, Hiltunen JK, Poirier Y (2003) Modification of the monomer composition of polyhydroxyalkanoate synthesized in *Saccharomyces cerevisiae* expressing variants of the beta-oxidation-associated multifunctional enzyme. Appl Environ Microbiol 69(11):6495-9

Martinez JL, Liu L, Petranovic D, Nielsen J (2012) Pharmaceutical protein production by yeast: towards production of human blood proteins by microbial fermentation. Curr Opin Biotechnol 23(6):965-71

Melchiors M, Keul H, Höcker H (1994) Synthesis of highly isotactic poly[(R)-3-hydroxybutyrate] by ring-opening polymerization of (R,R,R)-4,8,12-trimethyl-1,5,9-trioxacyclododeca-2,6,10-trione. Macromol Rapid Commun 15(6):497-506

Minard KI, McAlister-Henn L (2005) Sources of NADPH in yeast vary with carbon source. J Biol Chem 280(48):39890-6

Miyagi H, Kawai S, Murata K (2009) Two sources of mitochondrial NADPH in the yeast *Saccharomyces cerevisiae*. J Biol Chem 284(12):7553-60

Moreira dos Santos M, Thygesen G, Kotter P, Olsson L, Nielsen J (2003) Aerobic physiology of redox-engineered *Saccharomyces cerevisiae* strains modified in the ammonium assimilation for increased NADPH availability. FEMS Yeast Res 4(1):59-68

Munoz AJ, Wanichthanarak K, Meza E, Petranovic D (2012) Systems biology of yeast cell death. FEMS Yeast Research 12(2):249-265

Murray DB, Haynes K, Tomita M (2011) Redox regulation in respiring *Saccharomyces cerevisiae*. Biochim Biophys Acta, Gen Subj 1810(10):945-958

Nevoigt E, Kohnke J, Fischer CR, Alper H, Stahl U, Stephanopoulos G (2006) Engineering of promoter replacement cassettes for fine-tuning of gene expression in *Saccharomyces cerevisiae*. Appl Environ Microbiol 72(8):5266-5273

Nielsen J (1998) Metabolic engineering: Techniques for analysis of targets for genetic manipulations. Biotechnol Bioeng 58(2-3):125-132

Nielsen J, Keasling JD (2011) Synergies between synthetic biology and metabolic engineering. Nat Biotechnol 29(8):693-695

Nissen TL, Anderlund M, Nielsen J, Villadsen J, Kielland-Brandt MC (2001) Expression of a cytoplasmic transhydrogenase in *Saccharomyces cerevisiae* results in formation of 2-oxoglutarate due to depletion of the NADPH pool. Yeast 18(1):19-32

Outten CE, Culotta VC (2003) A novel NADH kinase is the mitochondrial source of NADPH in *Saccharomyces cerevisiae*. Embo J 22(9):2015-2024

Overkamp KM, Bakker BM, Kötter P, van Tuijl A, de Vries S, van Dijken JP, Pronk JT (2000) In vivo analysis of the mechanisms for oxidation of cytosolic NADH by *Saccharomyces cerevisiae* mitochondria. J Bacteriol 182(10):2823-2830

Panchal, B., A. Bagdadi and I. Roy, (2013) Polyhydroxyalkanoates: The natural polymers produced by bacterial fermentation. In: Advances in natural polymers. S. Thomas, P. M. Visakh & A. P. Mathew (eds). Springer Berlin Heidelberg, pp. 397-421.

Papini M, Nookaew I, Siewers V, Nielsen J (2012) Physiological characterization of recombinant *Saccharomyces cerevisiae* expressing the *Aspergillus nidulans* phosphoketolase pathway: validation of activity through ^{13}C-based metabolic flux analysis. Appl Microbiol Biotechnol 95(4):1001-10

Partow S, Siewers V, Bjorn S, Nielsen J, Maury J (2010) Characterization of different promoters for designing a new expression vector in *Saccharomyces cerevisiae*. Yeast 27(11):955-64

Peoples OP, Sinskey AJ (1989) Poly-β-hydroxybutyrate (PHB) biosynthesis in *Alcaligenes eutrophus* H16. Identification and characterization of the PHB polymerase gene (*phbC*). J Biol Chem 264(26):15298-303

Pham TH, Webb JS, Rehm BHA (2004) The role of polyhydroxyalkanoate biosynthesis by *Pseudomonas aeruginosa* in rhamnolipid and alginate production as well as stress tolerance and biofilm formation. Microbiol 150(10):3405-3413

Plessis A, Dujon B (1993) Multiple tandem integrations of transforming DNA sequences in yeast chromosomes suggest a mechanism for integrative transformation by homologous recombination. Gene 134(1):41-50

Pronk JT, Yde Steensma H, Van Dijken JP (1996) Pyruvate metabolism in *Saccharomyces cerevisiae*. Yeast 12(16):1607-33

Quinto I, Scala G, Mallardo M, Arcucci A, Ruocco MR, De Lorenzo F (1992) Spontaneous and mutagen-mediated amplification of a *neo* gene integrated at different genomic sites in rat 2 fibroblasts. Carcinog 13(3):439-45

Reifenberger E, Freidel K, Ciriacy M (1995) Identification of novel *HXT* genes in *Saccharomyces cerevisiae* reveals the impact of individual hexose transporters on glycolytic flux. Mol Microbiol 16(1):157-67

Sakai A, Shimizu Y, Hishinuma F (1990) Integration of heterologous genes into the chromosome of *Saccharomyces cerevisiae* using a delta sequence of yeast retrotransposon Ty. Appl Microbiol Biotechnol 33(3):302-306

Sauer U (2001) Evolutionary engineering of industrially important microbial phenotypes. Adv Biochem Eng/Biotechnol 73:129-69

Scalcinati G, Partow S, Siewers V, Schalk M, Daviet L, Nielsen J (2012) Combined metabolic engineering of precursor and co-factor supply to increase alpha-santalene production by *Saccharomyces cerevisiae*. Microb Cell Fact 11:117

Sedlak M, Ho NW (2004) Characterization of the effectiveness of hexose transporters for transporting xylose during glucose and xylose co-fermentation by a recombinant *Saccharomyces* yeast. Yeast 21(8):671-84

Shi F, Kawai S, Mori S, Kono E, Murata K (2005) Identification of ATP-NADH kinase isozymes and their contribution to supply of NADP(H) in *Saccharomyces cerevisiae*. FEBS J 272(13):3337-49

Shi S, Valle-Rodriguez JO, Khoomrung S, Siewers V, Nielsen J (2012) Functional expression and characterization of five wax ester synthases in *Saccharomyces cerevisiae* and their utility for biodiesel production. Biotechnol Biofuels 5:7

Singh M, Patel S, Kalia V (2009) *Bacillus subtilis* as potential producer for polyhydroxyalkanoates. Microb Cell Fact 8(1):38

Siso MIG, Picos MAF, Cerdan ME (1996) Reoxidation of the NADPH produced by the pentose phosphate pathway is necessary for the utilization of glucose by *Kluyveromyces lactis rag2* mutants. FEBS letters 387(1):7-10

Starai VJ, Gardner JG, Escalante-Semerena JC (2005) Residue Leu-641 of acetyl-CoA synthetase is critical for the acetylation of residue Lys-609 by the protein acetyltransferase enzyme of *Salmonella enterica*. J Biol Chem 280(28):26200-5

Steen E, Chan R, Prasad N, Myers S, Petzold C, Redding A, Ouellet M, Keasling J (2008) Metabolic engineering of *Saccharomyces cerevisiae* for the production of n-butanol. Microb Cell Fact 7(1):36

Steinbuchel A, Hustede E, Liebergesell M, Pieper U, Timm A, Valentin H (1993) Molecular basis for biosynthesis and accumulation of polyhydroxyalkanoic acids in bacteria. FEMS Microbiol Rev 10(3-4):347-50

Steinbüchel A (2001) Perspectives for biotechnological production and utilization of biopolymers: Metabolic engineering of polyhydroxyalkanoate biosynthesis pathways as a successful example. Macromol Biosci 1(1):1-24

Steinbüchel A, Hein S (2001) Biochemical and molecular basis of microbial synthesis of polyhydroxyalkanoates in microorganisms. biopolyesters. In: Babel W, Steinbüchel A (eds). Adv Biochem Eng/Biotechnol, vol 71. Springer Berlin / Heidelberg, pp 81-123

Stephanopoulos G, Sinskey AJ (1993) Metabolic engineering--methodologies and future prospects. Trends Biotechnol 11(9):392-6

Symington LS (2002) Role of *RAD52* epistasis group genes in homologous recombination and double-strand break repair. Microbiol Mol Biol Rev 66(4):630-70

Takahashi H, McCaffery JM, Irizarry RA, Boeke JD (2006) Nucleocytosolic acetyl-coenzyme a synthetase is required for histone acetylation and global transcription. Mol Cell 23(2):207-17

Tyo KE, Ajikumar PK, Stephanopoulos G (2009) Stabilized gene duplication enables long-term selection-free heterologous pathway expression. Nat Biotechnol 27(8):760-5

Tyo KEJ, Fischer CR, Simeon F, Stephanopoulos G (2010a) Analysis of polyhydroxybutyrate flux limitations by systematic genetic and metabolic perturbations. Metab Eng 12(3):187-195

Tyo KEJ, Kocharin K, Nielsen J (2010b) Toward design-based engineering of industrial microbes. Curr Opin Microbiol 13(3):255-262

van den Berg MA, de Jong-Gubbels P, Kortland CJ, van Dijken JP, Pronk JT, Steensma HY (1996) The two acetyl-coenzyme A synthetases of *Saccharomyces cerevisiae* differ with respect to kinetic properties and transcriptional regulation. J Biol Chem 271(46):28953-28959

Van Hoek P, Van Dijken JP, Pronk JT (1998) Effect of specific growth rate on fermentative capacity of baker's yeast. Appl Environ Microbiol 64(11):4226-33

van Roermund CW, Elgersma Y, Singh N, Wanders RJ, Tabak HF (1995) The membrane of peroxisomes in *Saccharomyces cerevisiae* is impermeable to NAD(H) and acetyl-CoA under in vivo conditions. Embo J 14(14):3480-6

van Roermund CW, Hettema EH, van den Berg M, Tabak HF, Wanders RJ (1999) Molecular characterization of carnitine-dependent transport of acetyl-CoA from peroxisomes to mitochondria in *Saccharomyces cerevisiae* and identification of a plasma membrane carnitine transporter, Agp2p. Embo J 18(21):5843-52

van Winden WA, van Dam JC, Ras C, Kleijn RJ, Vinke JL, van Gulik WM, Heijnen JJ (2005) Metabolic-flux analysis of *Saccharomyces cerevisiae* CEN.PK113-7D based on mass isotopomer measurements of ^{13}C-labeled primary metabolites. FEMS Yeast Res 5(6-7):559-68

Vandijken JP, Scheffers WA (1986) Redox balances in the metabolism of sugars by yeasts. FEMS Microbiol Rev 32(3-4):199-224

Wang X, Wang Z, Da Silva NA (1996) G418 Selection and stability of cloned genes integrated at chromosomal delta sequences of *Saccharomyces cerevisiae*. Biotechnol Bioeng 49(1):45-51

Vaseghi S, Baumeister A, Rizzi M, Reuss M (1999) In vivo dynamics of the pentose phosphate pathway in *Saccharomyces cerevisiae*. Metab Eng 1(2):128-40

Wellen KE, Thompson CB (2012) A two-way street: reciprocal regulation of metabolism and signalling. Nat Rev Mol Cell Biol 13(4):270-6

Yadav VG, De Mey M, Giaw Lim C, Kumaran Ajikumar P, Stephanopoulos G (2012) The future of metabolic engineering and synthetic biology: Towards a systematic practice. Metab Eng 14(3):233-241

Zhang B, Carlson R, Srienc F (2006) Engineering the monomer composition of polyhydroxyalkanoates synthesized in *Saccharomyces cerevisiae*. Appl Environ Microbiol 72(1):536-543

Österlund T, Nookaew I, Nielsen J (2012) Fifteen years of large scale metabolic modeling of yeast: Developments and impacts. Biotechnol Adv 30(5):979-988

Paper I

Toward design-based engineering of industrial microbes.

Tyo KEJ, Kocharin K, Nielsen J.

Curr Opinion Microbiol. 2010. 13(3):255-262.

Available online at www.sciencedirect.com
ScienceDirect
Current Opinion in Microbiology

Toward design-based engineering of industrial microbes

Keith EJ Tyo, Kanokarn Kocharin and Jens Nielsen

Engineering industrial microbes has been hampered by incomplete knowledge of cell biology. Thus an iterative engineering cycle of modeling, implementation, and analysis has been used to increase knowledge of the underlying biology while achieving engineering goals. Recent advances in Systems Biology technologies have drastically improved the amount of information that can be collected in each iteration. As well, Synthetic Biology tools are melding modeling and molecular implementation. These advances promise to move microbial engineering from the iterative approach to a design-oriented paradigm, similar to electrical circuits and architectural design. Genome-scale metabolic models, new tools for controlling expression, and integrated -omics analysis are described as key contributors in moving the field toward Design-based Engineering.

Address
Department of Chemical and Biological Engineering, Chalmers University of Technology, Göteborg SE-412 96, Sweden

Corresponding author: Nielsen, Jens (nielsenj@chalmers.se)

Current Opinion in Microbiology 2010, **13**:255–262

This review comes from a themed issue on
Ecology and Industrial Microbiology
Edited by Erick Vandamme

Available online 11th March 2010

1369-5274/$ – see front matter

DOI 10.1016/j.mib.2010.02.001

Introduction

Industrial microbiology has benefitted greatly from the introduction of recombinant DNA technologies, and the myriad of options that have hereby been enabled. These options have allowed a generation of engineers to splice DNA in many different ways, but even though recombinant DNA technology was developed in the early 1970s, many biotech challenges remain unsolved. Although we knew ***how*** to splice DNA, the past ~30 years have been spent trying to figure out ***what*** DNA to splice. In other engineering disciplines, such as electrical, civil, and chemical engineering, Design-based Engineering has enabled the construction of engineering devices (bridges, electric circuits, etc.) directly from plans, because of a largely complete mathematical understanding of the physics that govern these devices. Microbial engineering is qualitatively different, in that the objective to date has been to retrofit existing organisms, rather than design from scratch, to produce a product-of-interest using knowledge and models that can be limited in their predictive capabilities.

As such, microbial engineering has traditionally followed a cyclic pattern of modeling, implementation, and analysis (Figure 1a). Typically, available knowledge, for example, the biochemical reactions known in an organism, are used to develop a design strategy. Implementation of the strategies, such as extending a metabolic pathway to a new compound by introducing new enzymes, or knocking out competing pathways, is accomplished using recombinant DNA techniques consisting of plasmids or genomic alterations. Finally, the strain would be analyzed, sometimes only characterizing physiological properties and product yields. As models are limited and do not encompass all the activities of the cell, this process is inevitably iterative. Therefore, the knowledge gained from the previous analysis is used to refine the model, and the cycle begins again. Advances in Systems Biology leverage analysis and modeling to better define how a cell behaves in particular circumstances. Likewise, advances in Synthetic Biology are allowing implementation of novel gene circuits that are guided by predictive models of each molecular 'part.' Combined, these recent advances in Systems Biology and Synthetic Biology are changing the efficiency of this engineering cycle toward the goal of transitioning from *iterative* engineering (Figure 1a) to a linear *Design-based* Engineering (Figure 1b) where modeling and implementation are adequately sophisticated to achieve the design goal without iteration. In this review we will highlight techniques and tools that are helping to move us toward Design-based Engineering of microbes for industrial purposes.

Modeling

Models are a key asset to leverage in the design of microbes for a desired phenotype. Predictive models that describe relevant cellular processes can be used by engineers to rewire existing cellular processes toward a desired function. Genome-scale metabolic models (GSMMs) have been used extensively to predict changes in enzyme reaction rates (fluxes) in response to nutrient or genetic perturbations [1]. These models rely on firstly, conservation of mass through the network including electrons and secondly, cellular requirements for biomass to help predict how the cell will regulate metabolic pathways. Because these models predict changes in the metabolic network, they are of great use in predicting cellular alterations that will increase the production of a desired product [2]. These models can be used in combination

Figure 1

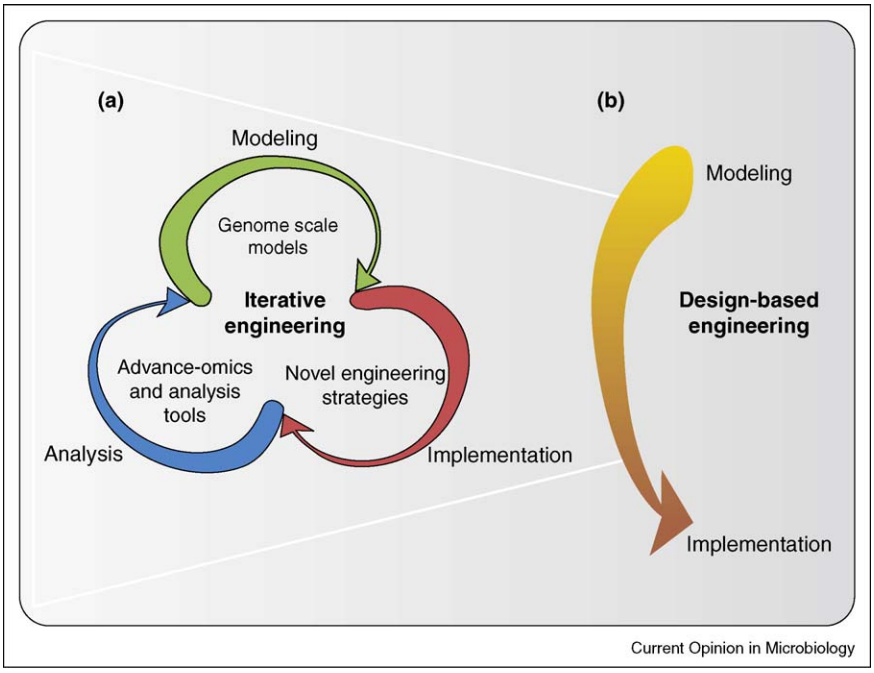

Transitioning from iterative to linear Design-based Engineering of industrial microbes. **(a)** Iterative engineering — genome-scale models describe the cellular processes under desired condition. These models guide implementation of engineering strategies. These implementations are characterized by -omics and integrated analysis tools, which are used to revise the model and improve predictive capability. **(b)** Design-based Engineering — models and implementation tools are reliable enough that the expected outcome is usually achieved, as in civil and electrical engineering. The transition from an iterative cycle to a linear Design-based Engineering will be accomplished by better modeling and implementation aided by enhanced analysis.

with metabolic optimization algorithms, such as OptKnock or OptGene, to scan through all possible gene knockouts in the cell, and identify knockouts that are predicted to increase production [3,4]. Improvement of production titers for a large number of products, including: lactic acid, L-valine, L-threonine, other amino acids, hydrogen, vanillin (see Ref. [2] for details), lycopene [5], ethanol [6], and sequiterpenes [7•] have been achieved using such models.

Stoichiometric models have been created for many industrially relevant microbes, through curating enzyme biochemistry literature and using comparative genomics approaches for organisms that have little biochemical evidence. Genome-scale metabolic models exist for a range of industrial microbes. Table 1 gives information for published industrial microbes. Because of the rapid drop in sequencing costs, models for new organisms are being added often. Currently models are being developed

Table 1

Genome-scale metabolic models of industrial microbes

Organism	Reactions	Metabolites	Genes	Regulation	Thermodynamics	Reference
Aspergillus nidulans	1095	732	666			[55]
A. niger	2168	1045	871			[56••]
A. oryzae	1846	1073	1314			[53•]
Bacillus subtilis	754	637	614			[57]
Corynebacterium glutamicum	495	408	411			[58]
Escherichia coli	2077	1039	1260	✓	✓	[12••]
Lactococcus lactis	621	422	358			[59]
Mannheimia succinicproducens	373	352	335			[60]
Saccharomyces cerevisiae	1446	1013	800			[61•]
	1489	972	805	✓		[10]
Streptomyces coelicolor	700	500	971			[62]

for *Penicillium chrysogenum* and *Pichia pastoris*, which will be useful for antibiotic and protein production. Many of the published models can be found at the Biochemical, Genetic, and Genomic (BiGG) database (http://bigg.ucsd.edu/) or the BioMet Toolbox (http://sysbio.se/BioMet/).

Although there is an increasing availability of stoichiometric models for a range of organisms, for *Escherichia coli* and *Saccharomyces cerevisiae*, additional model features are being added to improve the models predictive capabilities. The regulatory structure that controls the expression of different metabolic enzymes is not explicitly captured in stoichiometric models. In *E. coli*, Boolean logic representations of transcriptional regulation have been able to predict binary expression changes in response to various stimuli [8]. Such models contain at least some regulatory information for approximately half the metabolic reaction and can be trained using high-throughput phenotyping data and transcriptome measurements [9]. Similar efforts have been carried out in yeast, accounting for 55 transcription factors (TF) and nutrient conditions [10].

Another improvement has been identifying the reversibility/irreversibility of enzymatic reactions to constrain the model from predicting thermodynamically infeasible reactions. This is achieved by calculating the thermodynamic free energy of metabolites [11,12••]. Reactions that have a significant drop in free energy in the forward direction are irreversible, while reactions without significant changes in free energy will be reversible, and subject to mass action.

Currently, these models are limited to quantify metabolic fluxes, which surely are of significant value for biochemical production. However, many processes that may be of interest to engineers are not described by such models. In protein production, for example, various sorting/quality control processes are controlled by interactions with other proteins, not transcriptionally controlled, nor can these processes be predicted by mass action. Other processes, such as DNA repair, cell division, signaling pathways, stress responses, and trafficking between compartments have inputs and outputs that may be partially transcriptional in nature, but have many other interactions that cannot be described by current FBA-type models (a notable exception is the description of the JAK–STAT signaling pathway by stoichiometric models [13•]).

Protein–protein interaction networks provide a scaffold for models that describe nonmetabolic processes in the cell and are currently a useful resource for data analysis (described below). Such networks do not have the quantitative predictive power as GSMMs, but serve as scaffolds to identify which proteins may be relevant without specific knowledge of the mechanism. Protein interaction networks are available for several industrial organisms, such as *Bacillus subtilis*, *E. coli*, *S. cerevisiae*, and *S. pombe*, and are stored at BioGrid, a central repository for these and other types of interactions (www.thebiogrid.org) [14•]. These databases are being significantly upgraded by various efforts and this will lead to a more complete mapping of many cellular processes and move toward the usefulness of protein–protein interaction data in predicting cellular processes.

Implementation

Predictive models can offer hypotheses for improving the desired phenotype. In general, implementation has consisted of firstly, strong plasmid-based overexpression; secondly, knockout, or thirdly, introduction of a heterologous gene. As we move forward with more detailed models, it will be desirable to move from the binary options of strong overexpression and deletion to fine-tuned alteration of constitutive expression levels, as well as sophisticated responsive promoters to adjust protein expression through the course of the fermentation (Figure 2).

Well-characterized, robust expression systems will aid in this development. The Standard Biological Parts initiative (http://partsregistry.org/) is an open-source repository of biological 'parts' (promoters, ribosome-binding sites, reporters, etc.) with input/output data compiled for convenient use of the part [15••]. Abstracted parameters, such as polymerases per second (PoPs), are more useful in design than gfp fluorescence or β-galactosidase units that are commonly reported in research literature. This catalog relies on a cloning strategy called Biobricks which follows an ordered design experience that is less prone to user error than *ad hoc* cloning [16•]. Biobricks has been used by engineers with no cloning experience to design and implement cellular engineering strategies as can be seen by the student designs in the International Genetically Engineered Machine Competition (iGEM) [17].

New expression systems are being developed that expand the precision of expression levels and allow novel regulation. These approaches allow firstly, fine-tuned expression rather than just strong overexpression and secondly, scalability, because the control systems can be used orthogonally, allowing extensive multiplexing rather than only a few options.

Constitutive expression over a range of expression levels has been achieved through mutagenesis of existing promoters, followed by the characterization of the derived promoter library. This has been achieved in *E. coli* [18] and yeast [19] and the concept should be extendible to most relevant microorganisms. Expression strength can also be controlled by changing the copy number of tandem repeats on the chromosome using an approach called Chemically Induced Chromosomal Evolution (CIChE) [20•]. CIChE has the added advantage of stable

Figure 2

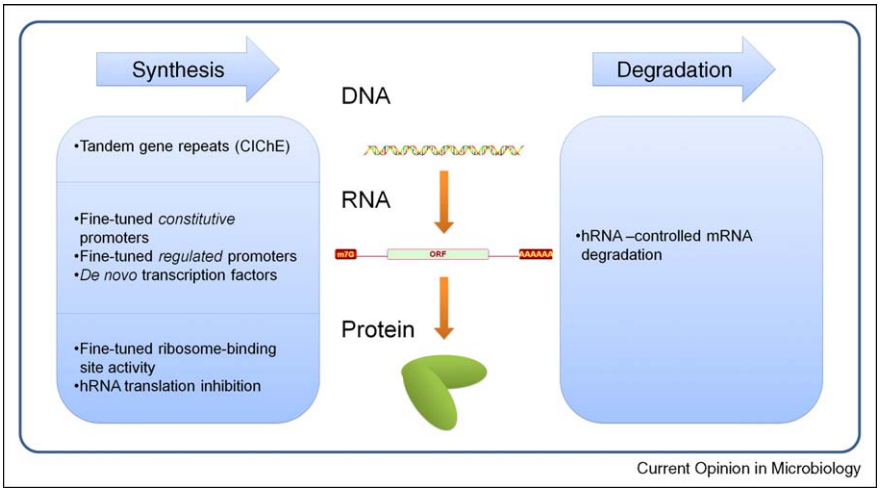

Biological 'parts' for controlling synthesis/degradation rates in the central dogma paradigm. Well-characterized biological components are necessary to control DNA, mRNA, and proteins in the cell. These biological components should be fine-tunable, independent of other implementations of the same control scheme, and robust in a variety of circumstances. The left column contains technologies that affect the synthesis rates, and the right column explains biological components that affect the degradation rates. Technologies are discussed in detail in the text. hRNA — hammerhead RNA.

copy numbers, whereas plasmid copy number can fluctuate significantly.

Beyond constitutive expression, regulatable promoters allow engineers to dynamically control expression levels in responses to environmental changes, making new bioprocessing strategies possible. Similar to the mutation-based diversification used to create the constitutive promoters, Ellis *et al.* have created libraries of tetracycline-responsive and lactose-responsive promoters in *E. coli* with altered response characteristics to their respective inducers [21•]. The researchers then design a gene circuit and implement it with components of the library, a simple example of Design-based Engineering. Nevoigt *et al.* have adjusted the oxygen sensitivity of the DAN1 promoter, allowing similar design possibilities [22].

De novo transcriptional regulatory networks can also be introduced into the cell, to coregulate different groups of genes in parallel. This has been achieved by evolving zinc-finger TF to recognize non-native promoter sequences [23•]. Conceptually, an unlimited number of TF/promoter combinations could be used independently to regulate genes (for a more extensive review of these possibilities, see [24]). Combined with the mutation-based diversification of promoter characteristics, a range of promoter strengths could be made for a heterologous zinc-finger TF in both prokaryotes and eukaryotes.

Besides mRNA synthesis, other processes can affect expression strength. Hammerhead RNA (hRNA) detectors/regulators can control mRNA stability and translation efficiency (see [25••] for an overview of RNA-based tools for controlling protein expression). These hRNAs can be evolved to detect a wide range of small molecule substrates, allowing different chemical inputs to affect protein synthesis. hRNAs are also scalable because different input/output hRNAs can operate without unintended cross-talk. Protein synthesis can also be controlled by altering the RBS and a recent model can be used to design specific translation activities [26•].

Other means of controlling cellular function have moved beyond controlling RNA/protein abundance or are based on inheritance. To improve flux through a metabolic pathway, Dueber *et al.* have developed a method to tether sequential heterologous enzymes in series [27]. By this, the pathways mimic the biological process of channeling, providing increased local concentrations of intermediates and decreased average concentrations which firstly, increases flux; secondly, decreases toxicity of intermediates; and thirdly, avoids undesired side reactions. Light-controlled conditional protein interactions can allow direct control over the activity of enzymes, independent of transcription/translation [28,29]. Finally, genetic stability can be problematic where intermediates or products of a heterologous pathway are toxic to the cell. By switching from plasmids to tandem gene repeats on the chromosome, the CIChE method can extend genetic stability by tenfold [20•].

Analysis

As models are not 100% predictive and molecular implementation may not perform as expected, the engineered cells must be analyzed after implementation. Over the

past decade, technological advancements have enabled -omics measurement, the characterization of all instances of a class of molecules in a cell. In the wake of this massive amount of data that is generated, model-based analytic tools are allowing researchers to compress high dimensionality data to simpler, biologically based insights, which can ultimately improve the model.

Transcriptomics examines the expression level of mRNAs at a specific physical condition. Various technologies have been developed to quantify the transcriptome, including hybridization (DNA microarray) and sequence-based approaches. The development of novel high-throughput sequencing methods has provided a new tool for both mapping and quantifying transcriptomes. This method, termed RNA-Seq (RNA sequencing), is being developed to profile transcriptomes and allows high-throughput sequencing of cDNA in order to quantify mRNA in the cell [30]. Willenbrock *et al.* have shown that RNA-Seq correlates well with traditional microarray hybridization using synthetic RNA samples [31]. As well, the sensitivity in terms of reproducibility and relative quantification were equivalent. As microarray analysis requires an available genome sequence, custom chips for each organism, and complex statistical tools, RNA-Seq, though a platform still under active development, overcomes these hybridization limitations, as well as enables analysis of sequence variants (e.g. SNPs [32]), and provides quantitative estimates of RNA abundance in the cell [33•].

Proteomics attempts to quantify the level of all proteins in the cell. In the past, mRNA levels were used as a (sometimes poor) proxy for protein levels. Nowadays, methods combining mass spectrometry and liquid chromatography, either gel-based or nongel-based protein separation, are used to improve complex proteome identification. Since proteomics methods were developed in the middle of 1990s, interactomics [34••,35] and phosphoproteomics [36] have also become interesting for many research applications, characterizing the state of a protein. Now, various methods are developed for proteomics such as MALDI-TOF for peptide mass finger printing and electrospray ionization (ESI), Fourier transform ion cyclotron resonance (FT-ICR) coupling with tandem mass spectrometry (MS/MS) for peptide identification. However, quantitative proteomic data must be validated by independent methods in order to overcome the heterogeneity of the biological samples [37]. Proteome analysis of *S. cerevisiae* response to carbon and nitrogen limitation was done by using shotgun approach, multidimensional protein identication technology (MudPIT), in combination with the metabolic or *in vitro* labeling of proteins. The comparison of transcript and protein levels clearly shows that upregulation in response to glucose limitation is transcriptionally controlled while upregulation in response to nitrogen limitation is controlled at the post-transcriptional level [38]. In a similar study the combination of transcriptome and proteome analysis by MudPIT allowed for global mapping of the regulatory network associated with the key protein kinase Snf1p in yeast [39].

Similar to proteomics, sophisticated mass spectrometry permits metabolomic studies. Metabolomics is achieved by quantifying cellular metabolites and systemically studying the unique chemical fingerprints that specific cellular processes leave behind. The methods coupling electrospray ionization with mass spectrometry are well developed and used for detecting the metabolomes in *S. cerevisiae*. With ESI-MS, up to 84% of the metabolites in *S. cerevisiae* can be identified [40]. A complete quantitative metabolomics workflow in a microplate format has recently been published [41•]. Although the protocol is developed and validated for *S. cerevisiae*, this protocol can be adapted and applied for high-throughput metabolome studies in different organisms.

With this massive flow of complex data from mRNA, protein, and metabolite levels, integrative analysis is crucial and needed to prevent bottlenecks during the analytical step [42•,43]. Integration comes from leveraging existing information about the cell through models (as described above) to interpret -omics data. At present, genotype-to-phenotype databases (G2P) are currently being improved using various integrative tools (Figure 3). The core modules for construction and improving genotype-to-phenotype databases include object model, exchange (data) format, ontology, globally unique identifier (GUID), and web service [44••]. According to the availability of databases, a great number of mathematical models and integrative strategies have been developed and established as Systems Biology tools to integrate and visualize multidimensional data, for examples PromoT [45], Metatool [46], PathSys and BiologicalNetworks [35], and YANAsquare [47]. Subnetwork analysis allows complex system with multistationarity such as cellular networks to be analyzed separately [48]. An algorithm to identify key metabolites and subnetwork structures in a biological response has been successfully developed by integrating transcriptome with topological information from genome-scale metabolic model without direct measurement of metabolite concentrations [49,50].

Many models are significantly revised after incorporating new biological information from the -omics analysis [51]. For example, a metabolic model of *A. niger* was significantly improved by combining metabolome and metabolic flux data with existing genome and literature data [52,53•]. By integrating metabolic flux and transcriptome data with both interaction networks and stoichiometric models, a new approach to correlate mRNA and metabolic flux data was developed [34••]. Through integrated

Figure 3

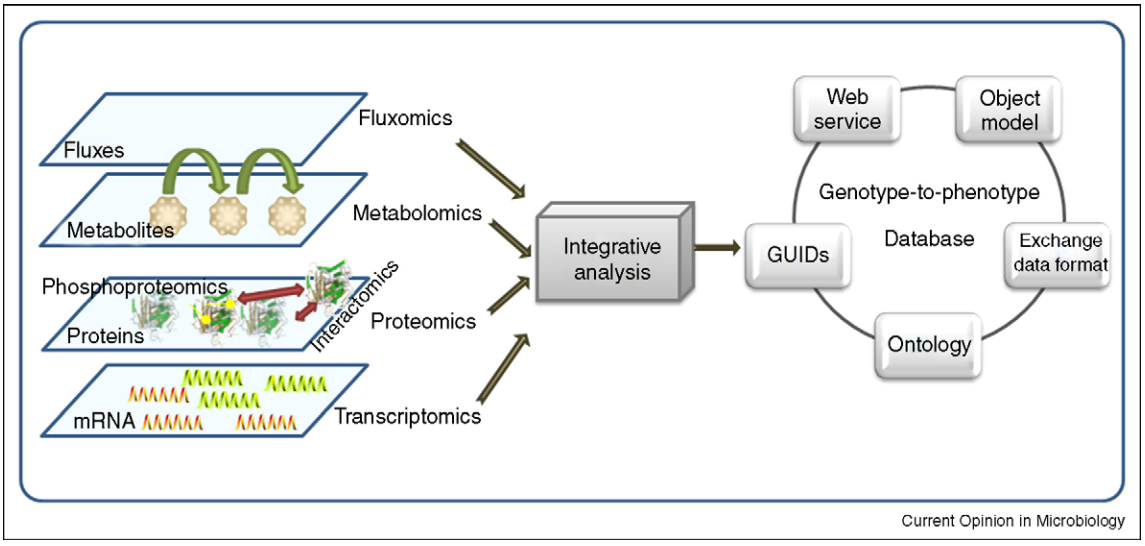

The conceptual work flow of integrated analysis of -omics data to formalize genotype-to-phenotype database. Advances in -omics measurement lead to the accumulation of high-throughput -omics data. With systematic and integrative analysis tools, genotype-to-phenotype database are currently being developed under the core modules outlined in this figure. Standardized object models and data formats facilitate the exchange of information between different data systems and are essential for unambiguous transmission of data between computers. A well-defined ontology enables the representation of domain-specific knowledge, as well as, the relationship between those domains and leads to powerful database searching. GUIDs solve data integration problems that result from ambiguity in name, or identity, of biological concepts and objects. Standard protocols for web service afford machine-to-machine interaction over the internet and simplify the task of exploring distributed data, forming the basis of the service-oriented architecture (SOA) [44••].

data analysis, a better understanding of the biological system is possible, allowing more realistic models to be developed for bio-based industries.

Conclusions and future directions

As synthetic genomes are quickly becoming a reality [54], we are then faced with an analogous question as 30 years ago. We know how to synthesize DNA, but what DNA should we synthesize? These research efforts mentioned here are qualitatively changing the nature of the cyclic engineering paradigm for industrial microbes. Thanks to increased analysis capability, much more information is gathered in each iteration. As well, with better models and molecular tools, better hypotheses and more controlled implementation is now possible.

Further developments in models that capture the change in metabolite concentrations will be useful in predicting flux distribution as well as potentially toxic levels of a particular metabolite. To improve molecular implementation, a larger catalog of well-characterized parts will need to be available to the research community. The standard biological part initiative has, thus far, been an open-source initiative. With suitable intellectual property security, private biological 'parts' companies could do rigorous characterization and sell 'components' to microbial engineers, significantly accelerating the accumulation of available parts. And finally, the use of -omics data to create phenotype-predictive models of protein–protein interactions would significantly extend the biological processes that could be engineered. In the end, the *far*, *far* end, experimental analysis may become an academic exercise for undergraduate, as is the state in electrical circuit design. At this point, we will have reached a paradigm of Design-based Engineering of industrial microbes.

Acknowledgements

We thank NIH F32 Kirschstein NRSA fellowship, Thailand Science and Technology Ministry, The Knut and Alice Wallenberg Foundation, and the Chalmers Foundation.

References and recommended reading

Papers of particular interest, published within the period of review, have been highlighted as:

- • of special interest
- •• of outstanding interest

1. Patil KR, Akesson M, Nielsen J: **Use of genome-scale microbial models for metabolic engineering**. *Curr Opin Biotechnol* 2004, **15**:64-69.

2. Feist AM, Palsson BO: **The growing scope of applications of genome-scale metabolic reconstructions using *Escherichia coli***. *Nat Biotechnol* 2008, **26**:659-667.

3. Patil KR, Rocha I, Forster J, Nielsen J: **Evolutionary programming as a platform for in silico metabolic engineering**. *BMC Bioinformatics* 2005, **6**:308.

4. Pharkya P, Burgard AP, Maranas CD: **OptStrain: a computational framework for redesign of microbial production systems**. *Genome Res* 2004, **14**:2367-2376.

5. Alper H, Miyaoku K, Stephanopoulos G: **Construction of lycopene-overproducing *E. coli* strains by combining systematic and combinatorial gene knockout targets**. *Nat Biotechnol* 2005, **23**:612-616.

6. Bro C, Regenberg B, Forster J, Nielsen J: **In silico aided metabolic engineering of *Saccharomyces cerevisiae* for improved bioethanol production**. *Metab Eng* 2006, **8**:102-111.

7. • Asadollahi MA, Maury J, Patil KR, Schalk M, Clark A, Nielsen J: **Enhancing sesquiterpene production in *Saccharomyces cerevisiae* through in silico driven metabolic engineering**. *Metab Eng* 2009, **11**:328-334.
This example uses a genome-scale model of *S. cerevisiae* to predict genomic alterations that will increase flux to isoprenoid precursors.

8. Covert MW, Palsson BO: **Transcriptional regulation in constraints-based metabolic models of *Escherichia coli***. *J Biol Chem* 2002, **277**:28058-28064.

9. Covert MW, Knight EM, Reed JL, Herrgard MJ, Palsson BO: **Integrating high-throughput and computational data elucidates bacterial networks**. *Nature* 2004, **429**:92-96.

10. Herrgard MJ, Lee BS, Portnoy V, Palsson BO: **Integrated analysis of regulatory and metabolic networks reveals novel regulatory mechanisms in *Saccharomyces cerevisiae***. *Genome Res* 2006, **16**:627-635.

11. Henry CS, Broadbelt LJ, Hatzimanikatis V: **Thermodynamics-based metabolic flux analysis**. *Biophys J* 2007, **92**: 1792-1805.

12. •• Feist AM, Henry CS, Reed JL, Krummenacker M, Joyce AR, Karp PD, Broadbelt LJ, Hatzimanikatis V, Palsson BO: **A genome-scale metabolic reconstruction for *Escherichia coli* K-12 MG1655 that accounts for 1260 ORFs and thermodynamic information**. *Mol Syst Biol* 2007, **3**:121.
One of the most advanced models to date. This *E. coli* model covers 28% of the genes in the genome and contains regulatory information and has been checked for thermodynamic consistency.

13. • Papin JA, Palsson BO: **The JAK–STAT signaling network in the human B-cell: an extreme signaling pathway analysis**. *Biophys J* 2004, **87**:37-46.
This paper implements a stoichiometric model typically used to model metabolism in a signaling pathway. This may be a useful way to model other cellular processes.

14. • Stark C, Breitkreutz BJ, Reguly T, Boucher L, Breitkreutz A, Tyers M: **BioGRID: a general repository for interaction datasets**. *Nucleic Acids Res* 2006, **34**:D535-D539.
BioGRID is an online resource for biological interactions. The database contains interaction data for many industrially relevant organisms, and contains physical as well as genetic interactions.

15. •• Canton B, Labno A, Endy D: **Refinement and standardization of synthetic biological parts and devices**. *Nat Biotechnol* 2008, **26**:787-793.
Standard biological parts will be essential to Design-based Engineering. This paper describes a strategy for cataloging parts in a way that is useful for cellular design.

16. • Shetty RP, Endy D, Knight TF Jr: **Engineering BioBrick vectors from BioBrick parts**. *J Biol Eng* 2008, **2**:5.
This paper describes the use of Biobricks as a platform for expressing proteins. The value of this approach is it systematizes the process, minimizing the opportunity for design errors that often plague cloning efforts.

17. Goodman C: **Engineering ingenuity at iGEM**. *Nat Chem Biol* 2008, **4**:13.

18. Alper H, Fischer C, Nevoigt E, Stephanopoulos G: **Tuning genetic control through promoter engineering**. *Proc Natl Acad Sci U S A* 2005, **102**:12678-12683.

19. Nevoigt E, Kohnke J, Fischer CR, Alper H, Stahl U, Stephanopoulos G: **Engineering of promoter replacement cassettes for fine-tuning of gene expression in *Saccharomyces cerevisiae***. *Appl Environ Microbiol* 2006, **72**:5266-5273.

20. • Tyo KE, Ajikumar PK, Stephanopoulos G: **Stabilized gene duplication enables long-term selection-free heterologous pathway expression**. *Nat Biotechnol* 2009, **27**:760-765.
Tandem genes offer a preferable approach to plasmids for multicopy expression of genes. CIChE allows high genetic stability, tunable expression, and does not require a selectable marker.

21. • Ellis T, Wang X, Collins JJ: **Diversity-based, model-guided construction of synthetic gene networks with predicted functions**. *Nat Biotechnol* 2009, **27**:465-471.
This study generated a library of promoters with different response properties to their inducers. These characterized promoters were used to design a genetic circuit directly from computer simulation.

22. Nevoigt E, Fischer C, Mucha O, Matthaus F, Stahl U, Stephanopoulos G: **Engineering promoter regulation**. *Biotechnol Bioeng* 2007, **96**:550-558.

23. • Beerli RR, Dreier B, Barbas CF 3rd: **Positive and negative regulation of endogenous genes by designed transcription factors**. *Proc Natl Acad Sci U S A* 2000, **97**:1495-1500.
Engineered zinc-finger proteins are a useful way to impose new regulation on genes. This system can work in both bacteria and fungi.

24. Lu TK, Khalil AS, Collins JJ: **Next-generation synthetic gene networks**. *Nat Biotechnol* 2009, **27**:1139-1150.

25. •• Win MN, Liang JC, Smolke CD: **Frameworks for programming biological function through RNA parts and devices**. *Chem Biol* 2009, **16**:298-310.
This paper describes the design strategies using RNA hammerheads. This strategy should have extensive use in a wide variety of organisms and in many applications.

26. • Salis HM, Mirsky EA, Voigt CA: **Automated design of synthetic ribosome binding sites to control protein expression**. *Nat Biotechnol* 2009, **27**:946-950.
A ribosome-binding site model is able to accurately predict translational activity, based on DNA sequence. This allows predictive ways to alter protein synthesis properties in a genetic circuit.

27. Dueber JE, Wu GC, Malmirchegini GR, Moon TS, Petzold CJ, Ullal AV, Prather KL, Keasling JD: **Synthetic protein scaffolds provide modular control over metabolic flux**. *Nat Biotechnol* 2009, **27**:753-759.

28. Levskaya A, Weiner OD, Lim WA, Voigt CA: **Spatiotemporal control of cell signalling using a light-switchable protein interaction**. *Nature* 2009, **461**:997-1001.

29. Levskaya A, Chevalier AA, Tabor JJ, Simpson ZB, Lavery LA, Levy M, Davidson EA, Scouras A, Ellington AD, Marcotte EM *et al.*: **Synthetic Biology: engineering *Escherichia coli* to see light**. *Nature* 2005, **438**:441-442.

30. Wang Z, Gerstein M, Snyder M: **RNA-Seq: a revolutionary tool for transcriptomics**. *Nat Rev Genet* 2009, **10**:57-63.

31. Willenbrock H, Salomon J, Sokilde R, Barken KB, Hansen TN, Nielsen FC, Moller S, Litman T: **Quantitative miRNA expression analysis: comparing microarrays with next-generation sequencing**. *RNA* 2009, **15**:2028-2034.

32. Barbazuk WB, Emrich SJ, Chen HD, Li L, Schnable PS: **SNP discovery via 454 transcriptome sequencing**. *Plant J* 2007, **51**:910-918.

33. • Tang F, Barbacioru C, Wang Y, Nordman E, Lee C, Xu N, Wang X, Bodeau J, Tuch BB, Siddiqui A *et al.*: **mRNA-Seq whole-transcriptome analysis of a single cell**. *Nat Methods* 2009, **6**:377-382.
Describe a method for single-cell gene expression profiling assay and compare mRNA-Seq with microarray techniques.

34. •• Moxley JF, Jewett MC, Antoniewicz MR, Villas-Boas SG, Alper H, Wheeler RT, Tong L, Hinnebusch AG, Ideker T, Nielsen J *et al.*: **Linking high-resolution metabolic flux phenotypes and transcriptional regulation in yeast modulated by the global regulator Gcn4p**. *Proc Natl Acad Sci U S A* 2009, **106**: 6477-6482.
An excellent example of model that correlates mRNA with metabolic data including interaction network and flux determination and the model is used to identify specific mechanisms in which genetic regulation mediates metabolic flux phenotype.

35. Baitaluk M, Qian X, Godbole S, Raval A, Ray A, Gupta A: **PathSys: integrating molecular interaction graphs for Systems Biology**. *BMC Bioinformatics* 2006, **7**:55.

36. Jacobs J, Monroe M, Qian W, Shen Y, Anderson G, Smith R: **Ultra-sensitive, high throughput and quantitative proteomics measurements**. *Int J Mass Spectrom* 2005, **240**:195-212.

37. Meyer HE, Stühler K: **High-performance proteomics as a tool in biomarker discovery**. *Proteomics* 2007, **7**:18-26.

38. Kolkman A, Daran-Lapujade P, Fullaondo A, Olsthoorn MMA, Pronk JT, Slijper M, Heck AJR: **Proteome analysis of yeast response to various nutrient limitations**. *Mol Syst Biol* 2006:2.

39. Usaite R, Jewett MC, Oliveira AP, Yates JR 3rd, Olsson L, Nielsen J: **Reconstruction of the yeast Snf1 kinase regulatory network reveals its role as a global energy regulator**. *Mol Syst Biol* 2009, **5**:319.

40. Højer-Pedersen J, Smedsgaard J, Nielsen J: **The yeast metabolome addressed by electrospray ionization mass spectrometry: initiation of a mass spectral library and its applications for metabolic footprinting by direct infusion mass spectrometry**. *Metabolomics* 2008, **4**:393-405.

41. • Ewald JC, Heux Sp, Zamboni N: **High-throughput quantitative metabolomics: workflow for cultivation, quenching, and analysis of yeast in a multiwell format**. *Anal Chem* 2009, **81**:3623-3629 Provide a recently developed protocol for high-throughput metabolome study..

42. • Prokisch H, Scharfe C, Camp DG II, Xiao W, David L, Andreoli C, Monroe ME, Moore RJ, Gritsenko MA, Kozany C *et al.*: **Integrative analysis of the mitochondrial proteome in yeast**. *PLoS Biol* 2004, **2**:e160 Propose the systematic integrative analysis of the mitochondrial proteome in *Saccharomyces cerevisiae* which is done by performing a comparative analysis of their proteomic dataset with gene expression analysis and quantitative deletion phenotype screening dataset by another research group..

43. Shields DC, O'Halloran AM: **Integrating genotypic data with transcriptomic and proteomic data**. *Comp Funct Genomics* 2002, **3**:22-27.

44. •• Thorisson GA, Muilu J, Brookes AJ: **Genotype–phenotype databases: challenges and solutions for the post-genomic era**. *Nat Rev Genet* 2009, **10**:9-18.
Review methods and relevant technologies which are required and currently improved for establishing genotype-to-phenotype databases.

45. Mirschel S, Steinmetz K, Rempel M, Ginkel M, Gilles ED: **PROMOT: modular modeling for Systems Biology**. *Bioinformatics* 2009, **25**:687-689.

46. von Kamp A, Schuster S: **Metatool 5.0: fast and flexible elementary modes analysis**. *Bioinformatics* 2006, **22**:1930-1931.

47. Schwarz R, Liang C, Kaleta C, Kuhnel M, Hoffmann E, Kuznetsov S, Hecker M, Griffiths G, Schuster S, Dandekar T: **Integrated network reconstruction, visualization and analysis using YANAsquare**. *BMC Bioinformatics* 2007, **8**:313.

48. Conradi C, Flockerzi D, Raisch Jr, Stelling Jr: **Subnetwork analysis reveals dynamic features of complex (bio)chemical networks**. *Proc Natl Acad Sci U S A* 2007, **104**:19175-19180.

49. Patil KR, Nielsen J: **Uncovering transcriptional regulation of metabolism by using metabolic network topology**. *Proc Natl Acad Sci U S A* 2005, **102**:2685-2689.

50. Oliveira A, Patil K, Nielsen J: **Architecture of transcriptional regulatory circuits is knitted over the topology of bio-molecular interaction networks**. *BMC Syst Biol* 2008, **2**:17.

51. Huang DW, Sherman BT, Lempicki RA: **Bioinformatics enrichment tools: paths toward the comprehensive functional analysis of large gene lists**. *Nucleic Acids Res* 2008. gkn923.

52. Andersen M, Nielsen M, Nielsen J: **Metabolic model integration of the bibliome, genome, metabolome and reactome of *Aspergillus niger***. *Mol Syst Biol* 2008, **4**:178.

53. • Vongsangnak W, Olsen P, Hansen K, Krogsgaard S, Nielsen J: **Improved annotation through genome-scale metabolic modeling of *Aspergillus oryzae***. *BMC Genomics* 2008, **9**:245.
Developed annotation strategy in this paper allows a genome-scale model of *Aspergillus oryzae* to be revised and reconstructed. This improved annotation reduces the number of hypothetical proteins and newly predicted genes are assigned to new putative functions in the model.

54. Gibson DG, Benders GA, Andrews-Pfannkoch C, Denisova EA, Baden-Tillson H, Zaveri J, Stockwell TB, Brownley A, Thomas DW, Algire MA *et al.*: **Complete chemical synthesis, assembly, and cloning of a *Mycoplasma genitalium* genome**. *Science* 2008, **319**:1215-1220.

55. David H, Ozcelik IS, Hofmann G, Nielsen J: **Analysis of *Aspergillus nidulans* metabolism at the genome-scale**. *BMC Genomics* 2008, **9**:163.

56. •• Andersen MR, Nielsen ML, Nielsen J: **Metabolic model integration of the bibliome, genome, metabolome and reactome of *Aspergillus niger***. *Mol Syst Biol* 2008, **4**:178.
This model was built using a variety of data sources beyond genomic sequence and biochemical evidence. As built, this model demonstrates that sophisticated models can now be developed rapidly using Systems Biology approaches.

57. Park S, Schilling C, Palsson B: **Compositions and methods for modeling *Bacillus subtilis* metabolism**. US Patent 2003.

58. Kjeldsen KR, Nielsen J: **In silico genome-scale reconstruction and validation of the *Corynebacterium glutamicum* metabolic network**. *Biotechnol Bioeng* 2009, **102**:583-597.

59. Oliveira AP, Nielsen J, Forster J: **Modeling *Lactococcus lactis* using a genome-scale flux model**. *BMC Microbiol* 2005, **5**:39.

60. Hong SH, Kim JS, Lee SY, In YH, Choi SS, Rih JK, Kim CH, Jeong H, Hur CG, Kim JJ: **The genome sequence of the capnophilic rumen bacterium *Mannheimia succiniciproducens***. *Nat Biotechnol* 2004, **22**:1275-1281.

61. • Nookaew I, Jewett MC, Meechai A, Thammarongtham C, Laoteng K, Cheevadhanarak S, Nielsen J, Bhumiratana S: **The genome-scale metabolic model iIN800 of *Saccharomyces cerevisiae* and its validation: a scaffold to query lipid metabolism**. *BMC Syst Biol* 2008, **2**:71.
A recent genome-scale model of yeast. It specifically accounts for lipid metabolism and is useful in the study of lipid disease states.

62. Borodina I, Krabben P, Nielsen J: **Genome-scale analysis of *Streptomyces coelicolor* A3(2) metabolism**. *Genome Res* 2005, **15**:820-829.

Paper II

Chemical induced chromosomal evolution in *Saccharomyces cerevisiae*.

Kocharin K, Tyo KEJ, Siewers V, Nielsen J

(Manuscript in preparation)

Chemical Induced Chromosomal Evolution in *Saccharomyces cerevisiae*

Kanokarn Kocharin[1], Keith E.J. Tyo[1,2], Verena Siewers[1], Jens Nielsen[1,*]

[1] Department of Chemical and Biological Engineering
Chalmers University of Technology
SE-412 96 Göteborg, Sweden

[2] Department of Chemical and Biological Engineering
Northwestern University,
Evanston, IL 60208, USA

Manuscript in preparation for:
MicrobiologyOpen

Draft as of:
28 September 2012

*Corresponding author:
Department of Chemical and Biological Engineering
Chalmers University of Technology
Kemivägen 10
SE-412 96 Göteborg, Sweden

Telephone: +46 31 772 3804
Fax: +46 31 772 3801
email: nielsenj@chalmers.se

Abstract

Current methods for high copy expression of heterologous genes in yeast mostly rely on episomal plasmids stabilized by auxotrophic markers, which do not work well in complex media. In these systems, maintaining a high copy number is crucial, which has hampered efforts to express enzymes and other proteins at desirable levels in the production of drugs, biofuels, and industrial enzymes. Chemically Induced Chromosomal Evolution (CIChE) is a novel expression system that achieves high copy numbers of recombinant genes in the genome without the need for a selectable marker. This strategy has been recently developed in bacteria. Here, we present progress on engineering and characterizing CIChE constructs in *Saccharomyces cerevisiae* and applications to the production of the heterologous protein, insulin precursors. A CIChE integration construct, containing a selectable marker, a site homologous to yeast genomic DNA and the gene(s) of interest, was designed and cloned. Chromosomal integration of the constructs and subsequent growth in increasing antibiotic challenges resulted in several tandem repeats with up to eight copies. Using CIChE with adaptive evolution in G418 resulted in multiple copies similar to delta integration methods and demonstrated good genetic stability. Therefore, yeast CIChE should be useful for engineering yeast and serves as the basis for developing CIChE in other industrially interesting eukaryotes.

Key Words

Ty, tandem integration, homologous recombination, adaptive evolution

Introduction

The yeast *Saccharomyces cerevisiae* is a widely used cell factory due to its long term use in the food, beverage and biotech industry, as well as the availability of extensive physiological data and the availability efficient genetic manipulation methods. Expression of heterologous genes or over-expression of native genes in *S. cerevisiae* can be achieved either by using an autonomously replicating extrachromosomal plasmid or by direct integration of the foreign DNA into the yeast chromosome. Vectors based on the yeast 2 micron plasmid are generally used for expression of heterologous DNA because of the high copy number, approximately 10-20 per cell and moderate stability under selection pressure (Jayaram et al. 2004; Cui et al. 2009; Ghosh et al. 2006).

However, plasmid instability leads to productivity loss during long term cultivation (Kilonzo et al. 2009; Caunt et al. 1988). Three processes during cell duplication have been studied and modeled to explain the mechanisms of plasmid loss, (i) segregational instability, (ii) structural instability and (iii) allele segregation (Impoolsup et al. 1989; Friehs 2004; Patnaik 2000; Parker and Di Biasio 1987; Löser and Ray 1996; Veit and Fangman 1988). Tyo et al. showed that a drastic decrease in productivity in plasmid carrying strains was a result of randomness in plasmid inheritance and could not be mitigated by decreasing mutation rates or applying selection pressure (Tyo et al. 2009).

Many strategies have been studied to circumvent the instability problem regarding plasmid based expression systems. Immobilization of plasmid carrying cells has been studied to improve the stability during cultivation (Guillán et al. 1998). Up to 50% improvement of plasmid stability and enzymatic expression was observed in an immobilized recombinant strain (Lú Chau

et al. 2000). Also different feeding strategies were developed and applied to stabilize plasmids in fed-batch cultivation (Zhang et al. 2002; Cheng et al. 1997).

Integration into the chromosome is an alternative way to implement stable expression of heterologous DNA even though in most cases only one copy of foreign DNA is integrated into the genome resulting in generally low expression levels (PlessisDujon 1993). Homologous recombination into the long terminal repeats (LTRs) of Ty retrotransposons (e.g. delta or sigma elements) sequences and ribosomal DNA sequences has allowed multiple integrations and increased expression (Sakai et al. 1990; Boeke et al. 1991; Fujii et al. 1990). The Ty sequences are dispersed throughout the genome and these elements have been well characterized for their mobility, size and occurrence in the genome (Boeke et al. 1988; Boeke et al. 1985; Garfinkel et al. 1988; Garfinkel et al. 2005; Cameron et al. 1979). Several studies have pointed out the potential of using delta elements in combination with *neo*^{r}, which confers resistance to G418 antibiotic, for DNA integration (Wang et al. 1996; Oliveira et al. 2007; Lee and Silva 1996; Parekh et al. 1996; Lang-Hinrichs et al. 1989). Different methods were applied in order to select transformants with different numbers of integration events. Multi-copy transformants were selected after plating on different concentrations of G418 media (Parekh et al. 1996; Wang et al. 1996). These strategies are dependent on the usage of high concentrations of integrative plasmids and the copy number is set after transformation.

Chemical induced chromosomal evolution (CIChE) has been proposed for improving the stability and the productivity during long term selection-free heterologous pathway expression in *Escherichia coli* (Tyo et al. 2009). This expression system produces many tandem repeats during the gradual increase of selective pressure and then stabilized by blocking homologous recombination through deletion of *recA* in *E.coli* . No selection pressure is required to maintain

the recombinant strain after CIChE. By applying CIChE in *E. coli*, approximately 40 copies could be obtained and the productivity of polyhydroxybutyrate and lycopene was improved compared to a plasmid based expression system.

Here, we employed the CIChE adaptive evolution strategy in *S. cerevisiae*. It was evaluated for the tunability of the copy number of the integrated construct in the genome. Finally, genetic stability of the resulting strains expressing insulin precursor was validated compared with a plasmid based expression system during long-term cultivation.

Materials and Methods

Strains and media

S. cerevisiae CEN.PK 113-5D (*MAT***a** *HIS3 TRP1 LEU2 SUC2 MAL2-8 ura3–52*; provided by P. Kötter, Frankfurt, Germany) was used as the host strain for all CIChE experiments. Plasmids were maintained and propagated in *E. coli* DH5α. The preparation and transformation of competent *E. coli* cells was performed according with standard protocols (SambrookRussell 2006). Lysogeny broth was used for cultivation of *E. coli*. YPD medium contained 10 $g \cdot L^{-1}$ yeast extract, 20 $g \cdot L^{-1}$ peptone and 20 $g \cdot L^{-1}$ glucose was used for routine culturing of *S. cerevisiae* and for amplification of CIChE constructs. YPD-G418 medium for CIChE was prepared by adding various amount of filter-sterilized G418 (Sigma-Aldrich, St. Louis, MO) to obtain final G418 concentrations from 0.1 to 51.2 $g \cdot L^{-1}$. Medium containing 20 $g \cdot L^{-1}$ glucose, 6.7 $g \cdot L^{-1}$ yeast nitrogen base (Formedium, Hunstanton, UK), 13.125 $g \cdot L^{-1}$ potassium dihydrogen phosphate (adjusted to pH 6) and SD-2X SCAA amino acid supplement at this final concentration: 190 $mg \cdot L^{-1}$ Arg, 108 $mg \cdot L^{-1}$ Met, 52 $mg \cdot L^{-1}$ Tyr, 290 $mg \cdot L^{-1}$ Ile, 440

mg·L^{-1} Lys, 200 mg·L^{-1} Phe, 1260 mg·L^{-1} Glu, 400 mg·L^{-1} Asp, 390 mg·L^{-1} Val, 220 mg·L^{-1} Thr, 130 mg·L^{-1} Gly, 400 mg·L^{-1} Leu, 40 mg·L^{-1} Trp, 140 mg·L^{-1} His and 0 mg·L^{-1} Ser was used as a minimal medium for the study of insulin production in *S. cerevisiae* (WittrupBenig 1994). Electrophoresis-grade bovine serum albumin (BSA) (Sigma-Aldrich) was prepared at 25 g·L^{-1} in water, filter-sterilized and added to the minimal media at the final concentration of 1 g·L^{-1} in order to prevent protein degradation during cultivation.

Plasmid construction

Plasmid pJEF1105 containing the bacterial *neo*^{r} gene adjacent to the δ element derived from the 3' end of the yeast Ty1 retrotransposon was kindly provided by Dr. Jef D. Boeke (Boeke et al. 1988). DNA coding for an insulin precursor with leader sequence for correct secretory processing (Kjeldsen et al. 1999) was codon optimized for expression in yeast (GenScript, Piscataway, NJ) and cloned into p426GPD resulted in p426-YapIns (detailed description in Tyo et al., 2011). Plasmid pSP-GM2 with a P_{TEF1}-P_{PGK1} bidirectional promoter was generously provided from Siavash Partow (Partow et al. 2010). Plasmid pBluescript SK II (+) (Stratagene, La Jolla, CA) was digested with *Aat*II and ligated with the *his3*Δ1 sequence which was isolated from genomic DNA of *S. cerevisiae* CEN.PK 113.11C using primers KK001/KK002. This derived plasmid, pBluSKP-his, was PCR amplified with KK003/KK004 to obtain a fragment containing origin of replication, ampicillin resistance marker and *his3*Δ1 with restriction sites for *Kpn*2I and *Mfe*I at the respective ends. Plasmid pSP-GM2 was digested with *Kpn*2I and *Mfe*I and ligated with the derived PCR fragment from pBluSKP-his. The resulting plasmid, pSP-GM2-his, was digested with *Asc*I and *Mfe*I and ligated with the *neo*^{r} marker which was isolated from plasmid pJEF1105 using primers KK005/KK006 and named pCIChE-KK001.

pCIChE-KK001 was further digested with *Aat*II and *Asc*I and ligated with the cassette containing delta sequence and *neo*^{r} marker amplified from pJEF1105 using primers KK005/KK007. The resulting construct, pCIChE-KK003, was used as a general integration platform (plasmid map in Figure 1). Insulin cassette, contained A-subunit, C-peptide and B-subunit, was amplified from p426GPD-YapIns with KK009/KK010 and was inserted into the *Sal*I site of pCIChE-KK003, downstream of the constitutive P_{TEF1} promoter of pCIChC-KK003 to create CIChE-KK003-Ins. A 2 micron based expression system for insulin production was generated for comparative studies. The insulin cassette was amplified from p426GPD-YapIns using primers KK008/KK010 and inserted into the *Sal*I/*Bam*HI sites of pSP-GM2 to create pSP-GM2-Ins. The primers used for plasmid and strain construction are listed in Table1.

Yeast transformation

S. cerevisiae transformations were performed by the LiAc procedure of Ito et al. with the following modifications (Ito et al. 1983, Wang et al. 1996). pCIChE-KK003-Ins was linearized with *Nco*I prior the yeast transformation. Single-stranded salmon sperm DNA (50 μg per transformation) was added together with 5-10 μg of linearized integrating plasmid, and the heat shock time at 42°C was extended from 5 to 15 min. After heat shock, the cell suspension (ca. 0.4 mL) was mixed with 2.7 mL of YPD medium and incubated at 30°C for 18 h with shaking. 50-100 μL of the culture was then plated on a selective YPD-G418 plate (0.1 $g \cdot L^{-1}$ G418).

Evolutionary process for CIChE strain

A colony was collected from the YPD-G418 plate and grown in 5 ml culture tube with YPD plus G418 at 0.2 $g \cdot L^{-1}$. When the strain reached late exponential phase (~24 h), 1 % of the culture was transferred to fresh YPD medium containing 0.4 $g \cdot L^{-1}$ of G418. These evolution steps

were repeated doubling the G418 concentration with each transfer until the concentration was 51.2 $g \cdot L^{-1}$. CIChE strains were collected at different concentrations of G418 and characterized for growth and metabolic activity in 25 ml media in 125 ml shake flask cultivation at 30 °C with minimal medium contained SD-2XSCAA and supplemented with G418 concentrations equivalent to the evolutionary level. Specific growth rates of the CIChE strains were calculated from cell density monitored by A_{600} with a GeneSys-20 spectrophotometer (Thermo Scientific, MA, USA).

Characterization of CIChE strains after the evolution process

Strains evolved from different concentration of G418 were grown in minimal media contained SD-2X SCAA with the G418 concentrations that match the evolutionary level. Metabolites including glucose, ethanol, glycerol, and acetate were quantified from culture filtrate by HPLC (Dionex-HPLC, Sunnyvale, CA) equipped with an Aminex HPX 87H ion exclusion column (300 mm x 7.8 mm, Bio-Rad Laboratories, Hercules, CA) which was operated at 45 °C, and a flow rate of 0.6 $mL \cdot min^{-1}$ of 5 mM H_2SO_4 using a refractive index detector and UV detector for sugar and organic acids, respectively. Insulin was measured by a modification of the assay by Snel and co-worker (SnelDamgaard 1988). 1 mL of cell culture was centrifuged at 4000 x g for 4 min. 8 parts supernatant was added to 1 part 0.1 N HCl and 5.5 mM sodium azide and stored at 4°C until measurement. The insulin precursor concentration was determined by HPLC using a Luna 5µ C18 (250mm x 4.6 mm) (Phenomenex, USA) column and gradient-based elution. Buffer A contained 50% acetonitrile in water and Buffer B contained 68 mM phosphoric acid, 0.2 M sodiumsulphate and 10% (w/v) acetonitrile in water, and HPLC was run with 25 µL injections at 1 $mL \cdot min^{-1}$ and 50 °C. Gradient protocol: 80% B for 10 min. Linear

gradient from 80% B to 40% B over 10 min. Hold at 40% B for 5 min and then to 80% B for 3 min to reequilibrate for next sample. Recombinant human insulin purchased from Sigma-Aldrich was used as a standard for the quantification of insulin precusor. Insulin standards eluted at 22.6 min and insulin precursor at 20.0 min. HPLC peaks were verified by SDS-PAGE. At mid-log phase, samples contained 5 ml culture from strains that evolved with different concentrations of G418 were harvested and the pellet was kept at -20 °C for further DNA extraction and copy number measurement. 3 ml culture was harvested and transferred into 50 ml centrifuge tube containing ice. Cell pellet after centrifuge at 3000 x g was rapidly frozen with liquid nitrogen and kept at -80 °C as RNA samples for further qPCR analysis on gene expression experiment.

Genetic stability assay

Strains were grown in minimal medium contained SD-2X SCAA in the absence of selection pressure in order to investigate genetic stability and measure insulin productivity during long term cultivation (over 50 generations). The yeast CIChE strains were cultivated in the absence of G418, while a strain harboring the 2 micron plasmid (pSP-GM2-Ins) was grown in medium supplemented with uracil (20 $mg \cdot L^{-1}$) in order to grow the strain under non selective conditions. Both strains were grown in 25 ml in 250 ml Erlenmeyer flasks at 30 °C. After the cultures had reached stationary phase (typically 24 hrs), 250 μL were diluted into fresh 25 mL of minimal medium contained SD-2X SCAA . This was repeated 5 times (at 10, 20, 30, 40 and 50 generations). At each point, genomic DNA and plasmid DNA were purified and copy numbers were measured by qPCR. *ACT1*, *TAF10* and *ALG9* were used as reference genes for normalization of *neo*^{r} expression level (Teste et al. 2009).

Quantitative PCR

The traditional DNA purification method using phenol-chloroform-isoamyl alcohol (25:24:1) to purify DNA adapted from Lorincz was applied to all samples (Lorincz 1984). RNA samples were extracted using the RNeasy Mini kit (Qiagen, Hilden, Germany). DNA and RNA concentration was quantified spectrophotometrically using a BioPhotometer (Eppendorf, Hamburg, Germany). RNA quality (RIN) was determined using an Agilent 2100 Bioanalyzer. Oligo–dT primers were used in the reverse transcriptase reaction for cDNA synthesis. All qPCR experiments were performed with the Stratagene Mx3005P qPCR system (Agilent Technologies, Santa Clara, CA). Oligonucleotide primers for qPCR were designed with Primer3 (v.0.4.0) software (RozenSkaletsky 2000). The reactions were carried out in 25 μL using Brilliant II SYBR Green QPCR master mix (Agilent Technologies) and primer concentrations of 400 nM. The number of TAF10 from each sample was measured in the same qPCR experiment and used for *neo*^{r} normalization. In order to compare of the difference in copy numbers between CIChE construct and the episomal plasmid, 144 bp from ampicillin marker was selected as a target for qPCR amplification. The absolute copy numbers were determined by relating the Cq values of the unknown sample to the standard curves using the equation of the standard curve trend line. Duplicate measurements on triplicate biological samples were used to calculate the average copy number and standard deviation. The primers used in the qPCR experiments are listed in Table2.

Southern blot analysis

Southern hybridization was conducted according to Evans et al (Evans et al. 1994). Yeast genomic DNA was isolated from the CIChE strain evolved in 0.2 g/L G418. Approximately 10 μg DNA digested with restriction enzymes *Sac*I and *Sph*I were separated by gel electrophoresis

through a 1% agarose gel and were transferred onto a nylon membrane (Amersham Hybond- N+, GE Healthcare, Little Chalfont, UK) by downward capillary action using the TurboBlotter system (Whatman Schleicher & Schuell, Keene, NH). The *neo*^{r} cassette in the CIChE construct was used as probe binding region. DNA probe, PCR amplified 1-kb *neo*^{r} fragment, was labeled with alkaline phosphatase using the AlkPhos direct labeling system (Amersham) and hybridized to the membrane. Chemiluminescence detection was performed with the CDP-Star detection system (Amersham) according to the procedure provided by the manufacturer.

Results

Characterization of CIChE strain

The CIChE construct was integrated into the genome of *S. cerevisiae* containing (i) an expression cassette for insulin precursor as target product, (ii) *neo*^{r} as a tunable and selectable marker and (iii) delta element sequences flanking both sides of the construct for homologous recombination (Figure 1a). These flanking delta element sequences allowed homologous recombination to occur during the evolutionary process when the primary transformant was subcultured in increasing G418 concentrations (Figure 1b). The primary strain was obtained by direct selection for G418 resistance on YPD supplemented with the lowest G418 concentration, 0.1 g/L G418. As reported before, the copy number of *neo*^{r} in transformed yeast cells is tunable and proportional to the concentration of G418 applied for selection (Parekh et al. 1996, Wang et al. 1996). Therefore, the selection was first performed with the lowest concentration of G418 in order to obtain a parental strain with a low copy number of the CIChE construct in the genome. Evolution of the primary transformant was accomplished by subculturing in YPD supplemented

with increasing concentrations of G418 from 0.1-51.2 $g \cdot L^{-1}$. Figure 2 shows the change in copy number with increasing G418 concentration. To evaluate the tunability of the *neo*^{r} copy number it was determined for the different concentrations of G418 used during the evolutionary process using quantitative PCR (qPCR). A general trend of increasing copy number was observed up to a G418 concentration of 3.2 $g \cdot L^{-1}$. The copy number detected tended to increase from the strain evolved from 0.2 to 3.2 $g \cdot L^{-1}$ G418, starting at about 4 and ending at about 9 copies per cell. At higher G418 concentrations the copy number did not increase further with increasing G418 antibiotic concentration (Figure 2), but instead decreased again The lack of a further copy number increase of *neo*^{r} is contradictory to the tunability of *neo*^{r} found in previous studies (Parekh et al. 1996, Wang et al. 1996).

Evaluation of the physiological properties of the evolved CIChE strains was performed in shake flask cultivation with minimal medium contained SD-2XSCAA supplemented with different concentrations of G418. Specific growth rate, glucose consumption and insulin production rate were examined. The specific growth rates of CIChE strains isolated from 0.2 $g \cdot L^{-1}$ G418 to 12.8 $g \cdot L^{-1}$ G418 was 0.26 h^{-1} with a coefficient of variation of less than 1% (data not shown) however the CIChE strains isolated from higher concentration of G418, 25.1 and 51.2 $g \cdot L^{-1}$ G418, showed lower specific growth rates, 0.19 and 0.15 h^{-1}, respectively. These are the specific growth rates in the G418 concentrations they were selected from. The same trend was observed for the biomass yield on glucose and the insulin production rate as shown in Figure 3. The biomass yield calculated from the amount of biomass produced from 1 g of glucose was 0.08-0.1 $g \cdot g\ Glucose^{-1}$, typical of growth on high concentrations of glucose. The maximum insulin concentrations measured in the supernatants of the CIChE strain cultures were 1.3 to 2.8

mg·L^{-1} at different cultivation times depending on the strain. In most CIChE strains, insulin started to be produced from the middle of the exponential phase (50-60 h) but in CIChE strain evolved from 25.2 and 51.2 g·L^{-1} G418, insulin could not be detected.

As increased G418 resistance was observed while the *neo*^{r} copy number was not changed in the strains selected at high G418 conditions, we hypothesized that there were changes in the *neo*^{r} expression level. We therefore extracted mRNA from different CIChE strains isolated from 0.1, 0.4, 1.6, 6.4, 12.8, 25.6 and 51.2 g·L^{-1} G418 to quantify the expression level of *neo*^{r}. Three fold differences in *neo*^{r} expression level were detected for the parental strain isolated from 0.1 g·L^{-1} G418 and the strain isolated from 51.2 g·L^{-1} G418 (Figure 4). This result showed that although the number of *neo*^{r} copies in the chromosome remained constant when the concentration of G418 was increased, the expression level of *neo*^{r} increased.

Since Ty1 retrotransposons can transpose through an RNA intermediate (Boeke et al. 1985) and disperse throughout the yeast genome, the delta element of the Ty1 retrotransposon was used as homologous recombination site when the CIChE construct was integrated into the genome. Southern blot analysis was conducted in order to elucidate the pattern of delta integration in the CIChE strain - namely, to determine if the copies of the CIChE cassette were distributed throughout the genome or in tandem repeats. Genomic DNA from the CIChE strain isolated from 0.2 g·L^{-1} G418 was digested with *Sac*I and *Sph*I and blotted onto the membrane. A 1 kb PCR fragment of the *neo*^{r} cassette was used as probe and genomic DNA from *S. cerevisiae* CEN.PK113-5D was used as negative control and compared with the CIChE strain. Southern blot analysis revealed that a single band was detected, i.e. although the delta element from Ty1 was the homologous recombination site, CIChE was tandemly integrated at one position in the

genome (Figure 5). This result concurs with previous results showing that delta integration preferably occurs in tandem repeats compared to a random distribution throughout the genome (Parekh et al. 1996, PlessisDujon 1993, Wang et al. 1996).

Evaluation of genetic stability

Plasmids typically require selection pressure for maintenance. Even with selection pressure, episomal plasmid copy numbers can vary significantly. We evaluated the long-term productivity (in terms of recombinant insulin precursor production) and copy number of the CIChE strain, as compared to a strain containing an analogous episomal plasmid, in the absence of selective pressure. The CIChE strain was grown in the absence of G418 and the strain containing the 2 micron based plasmid with a *URA3* marker was grown with 20 mgL^{-1} uracil supplemented to the medium. The specific growth rate was 0.259±0.001 and 0.262±0.004 h^{-1} for the plasmid carrying strain and the CIChE strain in the absence of selection pressure, respectively. The insulin precursor production rate in the 2 micron plasmid based strain with selection pressure was 0.0637±0.0003 $mg{\cdot}L^{-1}h^{-1}$, which is higher than both for the CIChE strain and the plasmid carrying strain grown in the absence of selection pressure (0.0291±0.002 and 0.0456±0.001 $mg{\cdot}L^{-1}h^{-1}$, respectively). The copy number of the 2 micron plasmid strain and the CIChE strain were measured and compared for the stability during long term cultivation (50 generations with a doubling time of approximately 2.5-3 h) (Figure 6). Even though the copy number looks fairly constant for the CIChE strain, ANOVA analysis of the copy number over time showed a p-value of less than 0.05 and it is therefore concluded that the stability was significantly different among this sample group, perhaps with a slight decreasing trend. Although the plasmid carrying strain

showed a higher productivity of insulin precursor, the plasmid copy number fluctuated significantly during the cultivations.

Discussion

The yeast 2 micron plasmid is a multicopy circular DNA element that can propagate itself autonomously independent of the host nuclear DNA. Despite the convenience of using plasmids for heterologous gene expression, plasmid loss during long term cultivation especially in a continuous process can be a significant problem in terms of loss of productivity in an industrial production processes. Therefore, many strategies have been developed to improve the genetic stability during long term cultivation. Integration of genes directly into the yeast chromosome is one approach that has been investigated in order to avoid the segregational instability related to 2 micron based expression systems.

The prokaryotic *neo*^{r} gene, which confer a resistance to the aminoglycoside antibiotic G418, has been used as a selectable marker in many vectors used for yeast transformation (Lee and Silva 1996; Oliveira et al. 2007; Parekh et al. 1996; Scorer et al. 1994; Wang et al. 1996). One property of *neo*^{r} is the level of expression correlates with the concentration of G418 it can inactivate. In this study, *neo*^{r} was used as a tunable marker in delta integration of a CIChE construct into the yeast genome. In order to obtain the primary transformant, the LiAc transformation procedure according to Ito et al. (1983) was modified by adding an 18 hour incubation step after PEG treatment in order to allow the expression of *neo*^{r} before plating directly on G418 YPD selective plates. In this study, the primary transformant was selected from the lowest concentration of G418 in order to increase the probability of obtaining the lowest number of integrated CIChE constructs. By having a strain with a low copy number initially, it

allowed us to evaluate the evolutionary process during the iterative subculturing in increasing concentrations of G418.

The CIChE approach is based on the assumption that an increase in the antibiotic concentration will result in selection for cells with an increased copy number of the expression cassette. From this study, it appears that an increased resistance to G418 can evolve by the mechanism at low G418 concentrations. When the mRNA level of *neo*^{r} from different evolved CIChE strains was evaluated, it was shown that the CIChE strain grown at the highest concentration of G418, had a 3-fold higher transcription level compared to the primary transformant, which did not correlate with the copy number of *neo*^{r} in the genome. Also in rat 2 fibroblasts, no correlation between the occurrence of G418 resistance and the number of copies or integration sites of *neo*^{r} was observed (Quinto et al. 1992).

According to the result of the unchanged copy number at higher G418 concentrations during the evolution of the CIChE strain, especially above 3 $g \cdot L^{-1}$ G418, it appears that mechanisms other than increased copy number account for the increased resistance. It is possible that mutations leading to the higher transcription levels of the *neo*^{r} gene were sufficient to provide for the increased resistance. This might however also be due to the occurrence of spontaneous resistance to G418 in this yeast strain due to chromosomal mutations. Even though the mechanism of spontaneous resistance of G418 in yeast is still unclear, the occurrence of spontaneous resistance in this study could have been faster than the evolutionary process of CIChE. This limitation in the evolutionary process using an antibiotic resistance marker can be improved by the use of other inducible resistance marker such as *CUP1* which mediates resistance to high concentrations of copper and cadmium (Keil and McWilliams 1993; Koller et al. 2000; Welch et al. 1990).

Ty elements are well studied in yeast and are frequently used to facilitate the introduction of foreign DNA into the host. In this study, the delta element from the Ty1 retrotransposon was used as integration site in order to promote homologous recombination of the integration construct during the evolutionary process. However, the pattern of integrated constructs was found to be in a tandem repeat manner instead of random integration into different delta sequence. This result is consistent with findings by Wang and coworkers (Wang et al. 1996), but different from what was observed by Boeke and coworkers (Boeke et al. 1988) who found integration at multiple sites in the genome, which may lead to further lack of correlation of gene expression and copy number due to varying expression levels at different chromosomal sites. Even though the copy number obtained by CIChE is less than the maximum copy number reported in previous studies ; (Parekh et al. 1996), it is in the same range as the number of episomal plasmids per cell detected in this study. The maximum copy number of the CIChE construct found in this study is approximately 10 copies per genome. This number might be limited for several reasons, e.g. the size of the insert after integration in a tandem repeat manner may limit homologous recombination and affect genome integrity (Scheifele et al. 2009) or there may be limitation in recombinase enzyme resulting in insufficient recombination (Nagy 2000).

Finally, genetic stability was analyzed. Here we were both concerned with (a) an overall loss of copy number over time and (b) a high degree of variability in copy number. Various recombinant techniques were developed to overcome the segregational instability related to 2 micron plasmid based expression systems. Integration of genes directly into the yeast chromosome is one approach that has been investigated in this study and the genetic stability of CIChE was compared with a 2 micron plasmid expression system. CIChE was found to be more stable compare than the 2 micron plasmid which tended to vary during long term cultivation (50

generation) in the absence of selection pressure. The relatively good stability of the CIChE strain is different from findings by Wang and coworkers, who observed that the copy number of the delta integration changed over time due to homologous recombination of the entire integrated sequence during long term cultivations (Wang et al. 1996). We therefore believe that we have shown the potential of CIChE in the development of stable multi-copy strains with chromosomal integration.

Acknowledgements

We acknowledge the Thailand Science and Technology Ministry, the Chalmers Foundation, the Knut and Alice Wallenberg Foundation, the European Research Council (grant no. 247013) and the NIH Kirschstein NRSA Postdoctoral Fellowship (F32 GM083647-01) for funding.

References

Boeke, J., H. Xu and G. Fink. 1988. A general method for the chromosomal amplification of genes in yeast. Science 239: 280-282.

Boeke, J. D., D. J. Eichinger and G. Natsoulis. 1991. Doubling Ty1 element copy number in *Saccharomyces cerevisiae*: Host genome stability and phenotypic effects. Genetics 129: 1043-1052.

Boeke, J. D., D. J. Garfinkel, C. A. Styles and G. R. Fink. 1985. Ty elements transpose through an RNA intermediate. Cell 40: 491-500.

Cameron, J. R., E. Y. Loh and R. W. Davis. 1979. Evidence for transposition of dispersed repetitive DNA families in yeast. Cell 16: 739-751.

Caunt, P., A. Impoolsup and P. F. Greenfield. 1988. Stability of recombinant plasmids in yeast. J. Biotechnol. 8: 173-192.

Cheng, C., Y. L. Huang and S. T. Yang. 1997. A novel feeding strategy for enhanced plasmid stability and protein production in recombinant yeast fedbatch fermentation. Biotechnol. Bioeng. 56: 23-31.

Cui, H., S. K. Ghosh and M. Jayaram. 2009. The selfish yeast plasmid uses the nuclear motor *Kip1*p but not *Cin8*p for its localization and equal segregation. J. Cell. Biol. 185: 251-264.

Evans, M., A. Bertera and D. Harris. 1994. The Southern blot. Mol. Biotechnol. 1: 1-12.

Friehs, K., (2004) Plasmid copy number and plasmid stability. In: New trends and developments in Biochemical Engineering. Springer Berlin / Heidelberg. 22-192.

Fujii, T., K. Kondo, F. Shimizu, H. Sone, J. Tanaka and T. Inoue. 1990. Application of a ribosomal DNA integration vector in the construction of a brewer's yeast having alpha-acetolactate decarboxylase activity. Appl. Environ. Microbiol. 56: 997-1003.

Garfinkel, D. J., M. F. Mastrangelo, N. J. Sanders, B. K. Shafer and J. N. Strathern. 1988. Transposon tagging using Ty elements in yeast. Genetics 120: 95-108.

Garfinkel, D. J., K. M. Nyswaner, K. M. Stefanisko, C. Chang and S. P. Moore. 2005. Ty1 copy number dynamics in *Saccharomyces*. Genetics 169: 1845-1857.

Ghosh, S. K., S. Hajra, A. Paek and M. Jayaram. 2006. Mechanisms for chromosome and plasmid segregation. Ann. Rev. Biochem. 75: 211-241.

Guillán, A., T. Lú Chau, E. Roca, M. J. Núñez and J. M. Lema. 1998. Plasmid stability in recombinant *Saccharomyces cerevisiae* expressing the *EXG1* gene in free and immobilized cultures. Prog. Biotechnol. 15: 611-618.

Impoolsup, A., P. Caunt and P. F. Greenfield. 1989. Effect of growth rate on stability of a recombinant plasmid during continuous culture of *Saccharomyces cerevisiae* in non-selective medium. J. of Biotechnol. 10: 171-180.

Ito, H., Y. Fukuda, K. Murata and A. Kimura. 1983. Transformation of intact yeast cells treated with alkali cations. J. Bacteriol. 153: 163-168.

Jayaram, M., S. Mehta, D. Uzri and S. Velmurugan. 2004. Segregation of the yeast plasmid: similarities and contrasts with bacterial plasmid partitioning. Plasmid 51: 162-178.

Keil, R. L. and A. D. McWilliams. 1993. A gene with specific and global effects on recombination of sequences from tandemly repeated genes in *Saccharomyces cerevisiae*. Genetics 135: 711-718.

Kilonzo, P., A. Margaritis and M. Bergougnou. 2009. Plasmid stability and kinetics of continuous production of glucoamylase by recombinant *Saccharomyces cerevisiae* in an airlift bioreactor. J. Ind. Microbiol. Biotechnol. 36: 1157-1169.

Kjeldsen, T., A. Frost Pettersson and M. Hach. 1999. The role of leaders in intracellular transport and secretion of the insulin precursor in the yeast *Saccharomyces cerevisiae*. J. Biotechnol. 75: 195-208.

Koller, A., J. Valesco and S. Subramani. 2000. The *CUP1* promoter of *Saccharomyces cerevisiae* is inducible by copper in *Pichia pastoris*. Yeast 16: 651-656.

Lang-Hinrichs, C., D. Berndorff, C. Seefeldt and U. Stahl. 1989. G418 resistance in the yeast *Saccharomyces cerevisiae* comparison of the neomycin resistance genes from Tn5 and Tn903. Appl. Microbiol. Biotechnol. 30: 388-394.

Lee, F. W. F. and N. A. Silva. 1996. Application of Ty1 for cloned gene insertion: amplification of a large regulated expression cassette in *Saccharomyces cerevisiae*. Appl. Microbiol. Biotechnol. 44: 620-623.

Lorincz, A. 1984. Quick preparation of plasmid DNA from yeast. Focus. 6.

Lú Chau, T., A. Guillán, E. Roca, M. J. Núñez and J. M. Lema. 2000. Enhancement of plasmid stability and enzymatic expression by immobilising recombinant *Saccharomyces cerevisiae*. Biotechnol. Lett. 22: 1247-1250.

Löser, C. and P. Ray. 1996. Modelling the stability of the pBR322 plasmid derivative pBB210 in *Escherichia coli* TG1 under non-selective and selective conditions. Acta Biotechnol. 16: 271-282.

Nagy, A. 2000. Cre recombinase: The universal reagent for genome tailoring. Genesis. 26: 99-109.

Oliveira, C., J. A. Teixeira, N. Lima, N. A. Da Silva and L. Domingues. 2007. Development of stable flocculent Saccharomyces cerevisiae strain for continuous *Aspergillus niger* β-galactosidase production. J. Biosci. Bioeng. 103: 318-324.

Parekh, R. N., M. R. Shaw and K. D. Wittrup. 1996. An integrating vector for tunable, high copy, stable integration into the dispersed Ty δ sites of *Saccharomyces cerevisiae*. Biotechnol. Prog. 12: 16-21.

Parker, C. and D. DiBiasio. 1987. Effect of growth rate and expression level on plasmid stability in *Saccharomyces cerevisiae*. Biotechnol. Bioeng. 29: 215-221.

Partow, S., V. Siewers, S. Bjørn, J. Nielsen and J. Maury. 2010. Characterization of different promoters for designing a new expression vector in *Saccharomyces cerevisiae*. Yeast 27: 955-964.

Patnaik, P. R. 2000. An evaluation of models for the effect of plasmid copy number on bacterial growth rate. Biotechnol Lett. 22: 1719-1725.

Plessis, A. and B. Dujon. 1993. Multiple tandem integrations of transforming DNA sequences in yeast chromosomes suggest a mechanism for integrative transformation by homologous recombination. Gene 134: 41-50.

Quinto, H., G. Scala, M. Mallardo, A. Arcucci, M. R. Ruocco and F. De Lorenzo. 1992. Spontaneous and mutagen-mediated amplification of a neo gene integrated at different genomic sites in *rat 2* fibroblasts. Carcinogenesis 13: 439-445.

Rozen, S. and H. Skaletsky. 2000. Primer3 on the WWW for general users and for biologist programmers. Methods in molecular biology (Clifton, N.J.). 132: 365-386.

Sakai, A., Y. Shimizu and F. Hishinuma. 1990. Integration of heterologous genes into the chromosome of *Saccharomyces cerevisiae* using a delta sequence of yeast retrotransposon Ty. Appl. Microbiol. Biotechnol. 33: 302-306.

Sambrook, J. and D. W. Russell. 2006. The Inoue method for preparation and transformation of competent *E. Coli*: "Ultra-competent" cells. Cold Spring Harb Protoc. 2006: pdb.prot3944-.

Scheifele, L. Z., G. J. Cost, M. L. Zupancic, E. M. Caputo and J. D. Boeke. 2009. Retrotransposon overdose and genome integrity. Proc. Natl Acad. Sci. USA. 106: 13927-13932.

Scorer, C. A., J. J. Clare, W. R. McCombie, M. A. Romanos and K. Sreekrishna. 1994. Rapid selection using G418 of high copy number transformants of *Pichia pastoris* for high-level foreign gene expression. Nat. Biotech. 12: 181-184.

Snel, L. and U. Damgaard. 1988. Proinsulin heterogeneity in pigs. Horm. Metab. Res. 20: 476,480.

Teste, M.-A., M. Duquenne, J. Francois and J.-L. Parrou. 2009. Validation of reference genes for quantitative expression analysis by real-time RT-PCR in *Saccharomyces cerevisiae*. BMC Molecular Biology. 10: 99.

Tyo, K. E. J., P. K. Ajikumar and G. Stephanopoulos. 2009. Stabilized gene duplication enables long-term selection-free heterologous pathway expression. Nat. Biotechnol. 27: 760-765.

Wang, X., Z. Wang and N. A. Da Silva. 1996. G418 Selection and stability of cloned genes integrated at chromosomal δ sequences of *Saccharomyces cerevisiae*. Biotechnol. Bioeng. 49: 45-51.

Veit, B. E. and W. L. Fangman. 1988. Copy number and partition of the *Saccharomyces cerevisiae* 2 micron plasmid controlled by transcription regulators. Mol. Cell. Biol. 8: 4949-4957.

Welch, J. W., D. H. Maloney and S. Fogel. 1990. Unequal crossing-over and gene conversion at the amplified *CUP1* locus of yeast. Mol. Gen. Genet. 222: 304-310.

Wittrup, K. D. and V. Benig. 1994. Optimization of amino-acid supplements for heterologous protein secretion in *Saccharomyces cerevisiae*. Biotechnol. Tech. 8: 161-166.

Zhang, X., Z. Xia, B. Zhao and P. Cen. 2002. Enhancement of plasmid stability and protein productivity using multi-pulse, fed-batch culture of recombinant *Saccharomyces cerevisiae*. Biotechnol. Lett. 24: 995-998.

Tables

Table 1 Oligonucleotides and their sequences

Name	Sequence (5' -3')
KK-001 his (f)	TCGACGTCACAGAGCAGAAAGCCCTA
KK-002 his (r)	CAGACGTCCTTTGGTGGAGGGAACAT
KK-003 OAH (f)	AGTCCGGAACTCAAAGGCGGTAATACGGTTATCCACAG
KK-004 OAH (r)	ATCAATTGTAGCATGCGGAACAACACTCAACCCTATCTGA
KK-005 neoR (f)	TGGCGCGCCCTAACAAATGGATTCATTAGATCCGTTACATTGC
KK-006 neoR (r)	CACAATTGGTTGATTTCTATTCCAACATACCACCCATAA
KK-007 deltaneoR (r)	TCGACGTCTCCAATTGTGCATTAGGAAGCAGCCCAGTAGTA
KK-008 YapIns-B (f)	GAGGATCCAACACCAGAACTTAGTTTCGACGGATTCTAG
KK-009 YapIns-S (f)	AGGTCGACACACCAGAACTTAGTTTCGACGG
KK-010 YapIns-S (r)	TGGTCGACGTGACATAACTAATTACATGACTCG

Restriction sites are underlined.

Table2 Oligonucleotides and their sequences used in QPCR experiments

Name	Description	Sequence (5' -3')
KKQ-neoR (f)	QPCR to measure copy number of neo^r	CAGTTTAGTCTGACCATCTCATCTGTA
KKQ-neoR (r)	QPCR to measure copy number of neo^r	AAACAGTAATACAAGGGGTGTTATGAG
KKQ-TAF10 (f)	QPCR to normalize neo^r copy number in genome or amplicillin in plasmid	TACCCGAATTTACAAGAAAAGATAAGA
KKQ-TAF10 (r)	QPCR to normalize neo^r copy number in genome or amplicillin in plasmid	ATTTCTGAGTAGCAAGTGCTAAAAGTC
KKQ-ACT1 (f)	QPCR to normalize neo^r copy number and neo^r expression level	ATCAAACAGAGAAAAGATGACTCAAAT
KKQ-ACT1 (r)	QPCR to normalize neo^r copy number and neo^r expression level	ATCAAGTAGTCAGTCAAATCTCTACCG
KKQ-ALG9 (f)	QPCR to normalize neo^r copy number and neo^r expression level	CACGGATAGTGGCTTTGGTGAACAATT AC
KKQ-ALG9 (r)	QPCR to normalize neo^r copy number and neo^r expression level	TATGATTATCTGGCAGCAGGAAAGAAC TTGGG

KKQ-AmpR (f)	QPCR to measure copy number of ampicillin in genome or plasmid	GAGTTACATGATCCCCCATGTT
KKQ-AmpR (r)	QPCR to measure copy number of ampicillin in genome or plasmid	TTACGGATGGCATGACAGTAAG
KK-TAF10 (f)	amplification of TAF10 as template for standard curve	GATTTTGAGGAAGATTACGATGCGGA
KK-TAF10 (r)	amplification of TAF10 as template for standard curve	CGTTCACCGTCAGAACAACTTTGCT
KK-003 OAH (s)	amplification of *amp*^{R} as template for standard curve	AGTCCGGAACTCAAAGGCGGTAATACG GTTATCCACAG
KK-004 OAH (a)	amplification of *amp*^{R} as template for standard curve	ATCAATTGTAGCATGCGGAACAACACT CAACCCTATCTGA
KK-005 neoR (f)	amplification of *neo*^{r} as template for standard curve	TGGCGCGCCCTAACAAATGGATTCATT AGATCCGTTACATTGC
KK-007 deltaneoR (r)	amplification of *neo*^{r} as template for standard curve	TCGACGTCTCCAATTGTGCATTAGGAA GCAGCCCAGTAGTA

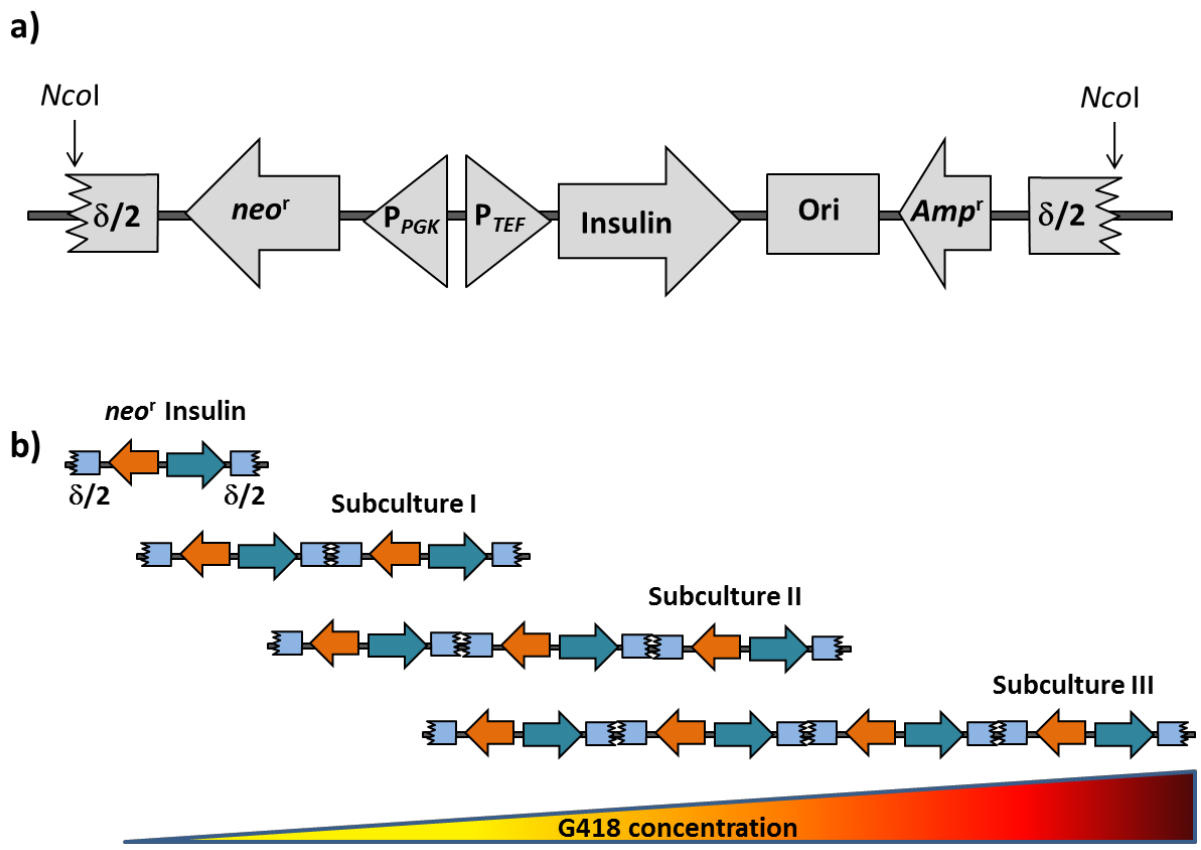

Figure 1: Yeast CIChE integration cassette and schematic illustration of the evolutionary process. (a) Integrated CIChE construct with *neo*^{r} and insulin precursor gene flanked by delta sequence. (b) CIChE process by subculturing in increasing G418 concentration and the pattern of tandem chromosomal integration. See Materials and Methods for details.

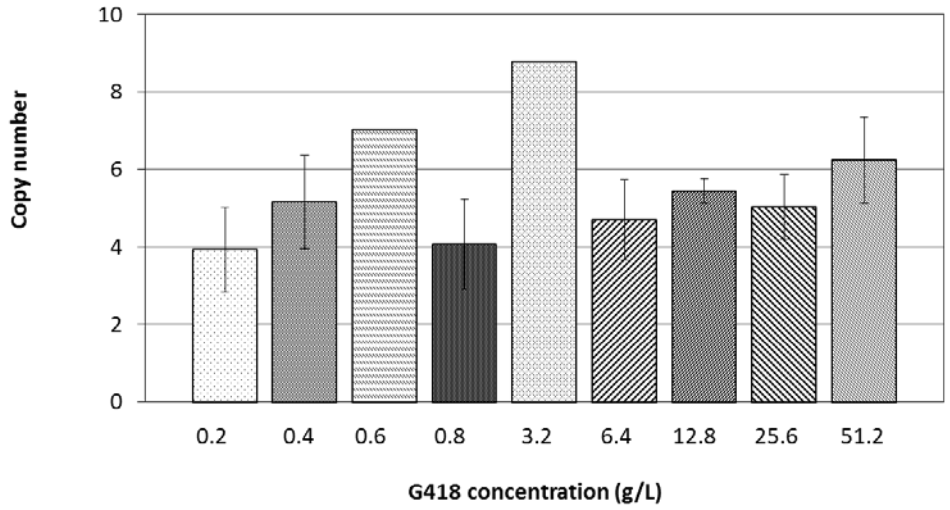

Figure 2: *Neo*^{r} copy number measurement. The copy number of *neo*^{r} in the genome of strains isolated from different concentration of G418 was determined by qPCR using single copy gene *TAF10* for normalization.

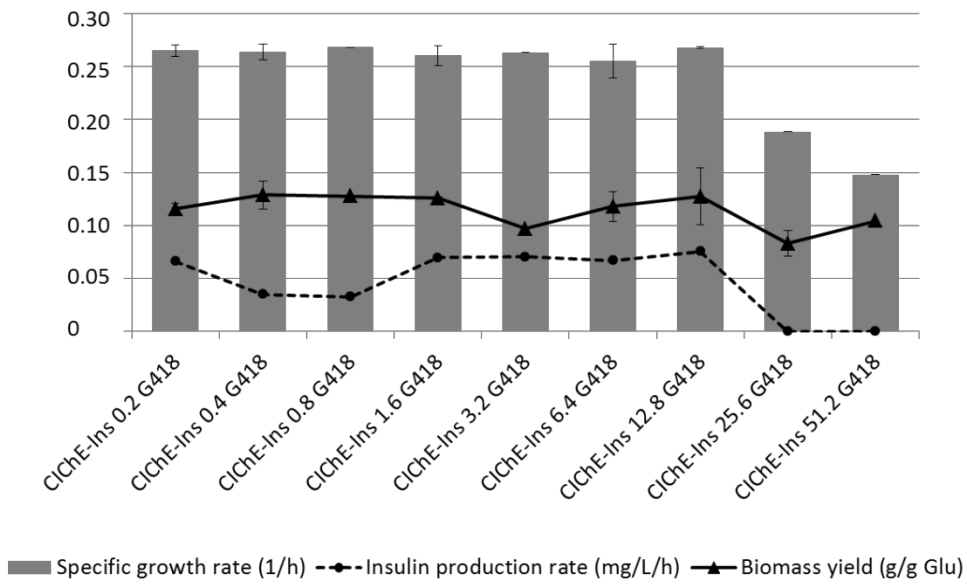

Figure 3: Specific growth rate, insulin precursor production rate and biomass yield of CIChE strains isolated at different concentrations of G418.

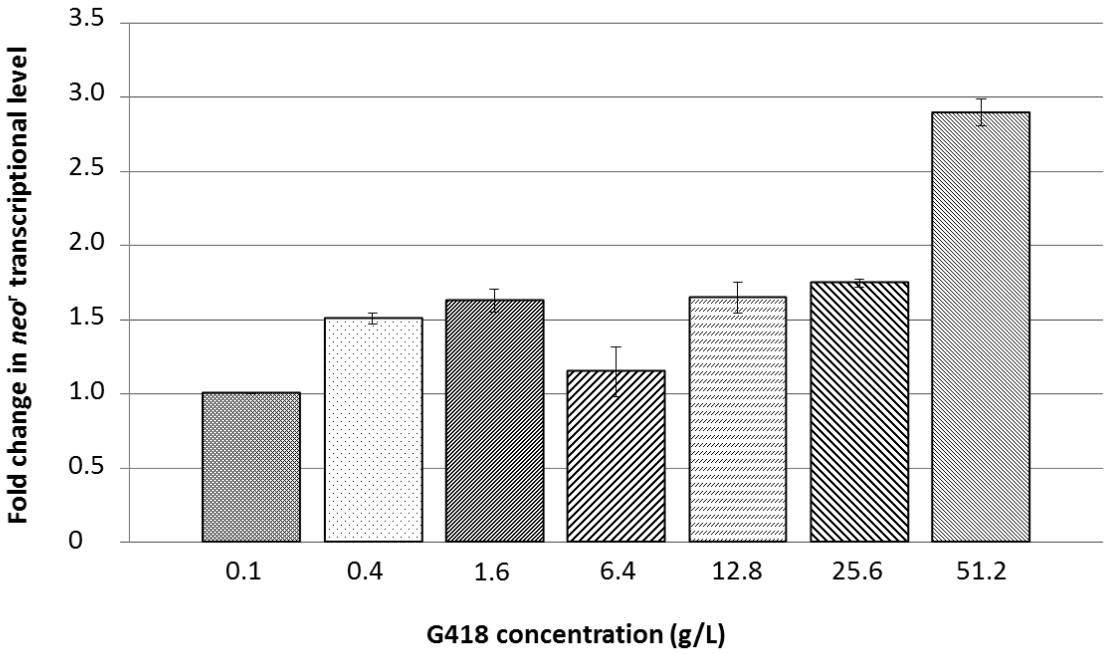

Figure 4: Comparison of *neo*^{r} transcription levels. RNA extracted from evolved strains at different concentration of G418 was examined by qRT-PCR. *TAF10*, *ALG9* and *ACT1* were used as reference genes to normalize the transcript level of *neo*^{r}.

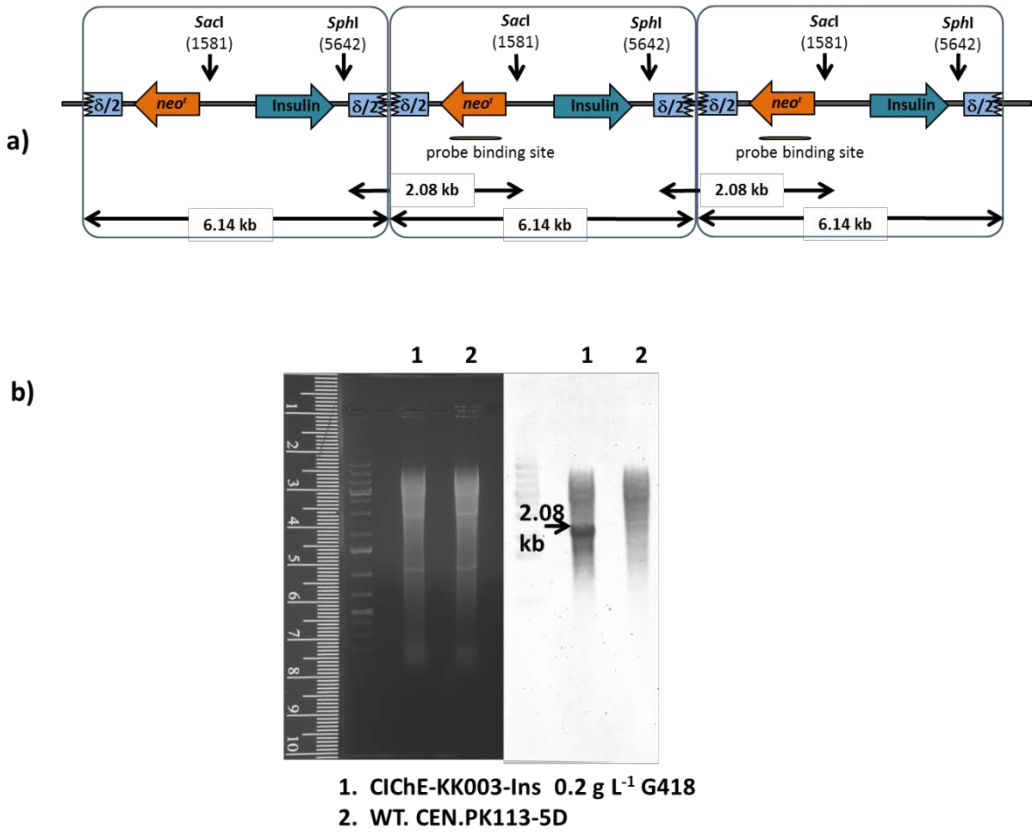

Figure 5: Southern blot analysis of CIChE strain. (a) Schematic presentation of tandem integrated CIChE construct (b) Genomic DNA of strains CIChE-KK003-Ins 0.2 g L^{-1} G418 and CEN.PK113-5D was subjected to restriction enzyme digestion with *Sac*I and *Sph*I and separated by gel electrophoresis followed by hybridization with a probe containing a 1-kb *neo*^{r} fragment.

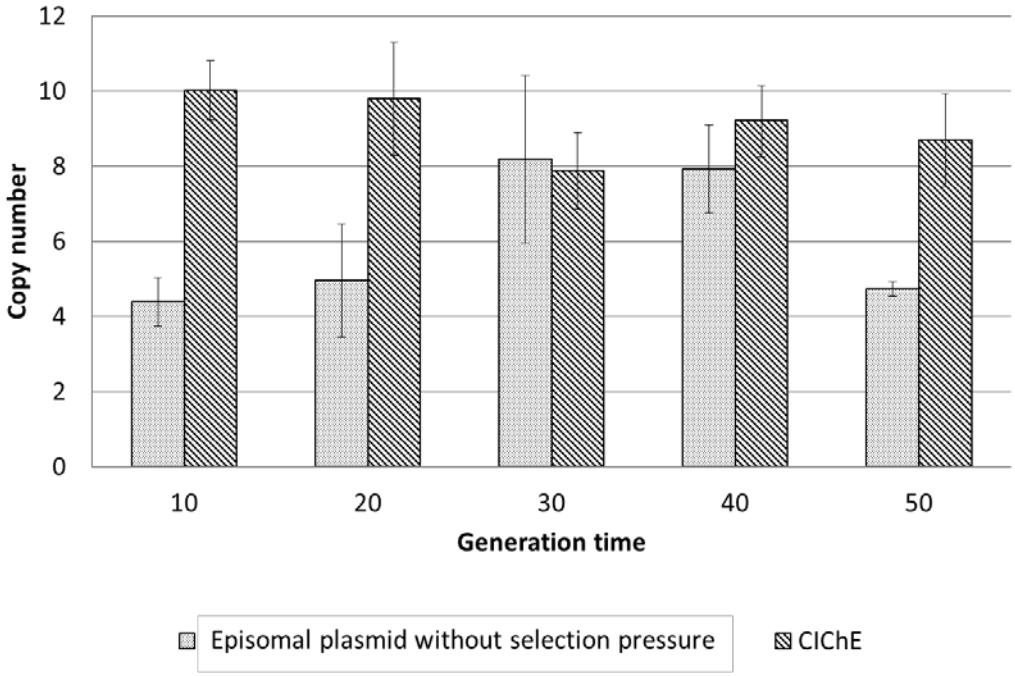

Figure 6: Genetic stability analysis. Copy number of *neo*^{r} in ClChE strain and episomal plasmid carrying strain was determined by qPCR after different numbers of generation in the absence of selection pressure.

Paper III

Engineering of acetyl-CoA metabolism for the improved production of polyhydroxybutyrate in *Saccharomyces cerevisiae*.

Kocharin K, Chen Y, Siewers V, Nielsen J.

AMB Express. 2012. 2(1):52.

AMB Express
a SpringerOpen Journal

ORIGINAL ARTICLE Open Access

Engineering of acetyl-CoA metabolism for the improved production of polyhydroxybutyrate in *Saccharomyces cerevisiae*

Kanokarn Kocharin, Yun Chen, Verena Siewers and Jens Nielsen*

Abstract

Through metabolic engineering microorganisms can be engineered to produce new products and further produce these with higher yield and productivities. Here, we expressed the bacterial polyhydroxybutyrate (PHB) pathway in the yeast *Saccharomyces cerevisiae* and we further evaluated the effect of engineering the formation of acetyl coenzyme A (acetyl-CoA), an intermediate of the central carbon metabolism and precursor of the PHB pathway, on heterologous PHB production by yeast. We engineered the acetyl-CoA metabolism by co-transformation of a plasmid containing genes for native *S. cerevisiae* alcohol dehydrogenase (*ADH2*), acetaldehyde dehydrogenase (*ALD6*), acetyl-CoA acetyltransferase (*ERG10*) and a *Salmonella enterica* acetyl-CoA synthetase variant (acs^{L641P}), resulting in acetoacetyl-CoA overproduction, together with a plasmid containing the PHB pathway genes coding for acetyl-CoA acetyltransferase (*phaA),* NADPH-linked acetoacetyl-CoA reductase *(phaB)* and poly(3-hydroxybutyrate) polymerase (*phaC)* from *Ralstonia eutropha* H16. Introduction of the acetyl-CoA plasmid together with the PHB plasmid, improved the productivity of PHB more than 16 times compared to the reference strain used in this study, as well as it reduced the specific product formation of side products.

Keywords: Polyhydroxybutyrate, Acetyl coenzyme A, *Saccharomyces cerevisiae*, Pathway engineering

Introduction

Poly-(R)-3-hydroxybutyrate (PHB) is the most common type of polyhydroxyalkanoates (PHAs) synthesized and accumulated by microorganisms like *Ralstonia eutropha* (also known as *Cupriavidus necator, Wautersia eutropha*, *Alcaligenes eutrophus*), *Bacillus megaterium* or *Pseudomonas* sp. as carbon and energy storage material in response to conditions of physiological stress (Steinbuchel et al. 1993). Biodegradable PHB is a linear polyester consisting solely of the stereospecific monomer, (R)-3-hydroxybutyric acid. It belongs to the group of short chain length PHAs consisting of C_3-C_5 hydroxyacid monomers. (Hankermeyer and Tjeerdema 1999; Melchiors et al. 1994). The biosynthesis pathway of PHB involves three enzymes and their sequential reactions (Breuer et al. 2002; Carlson et al. 2002; Steinbüchel 2001; Steinbüchel and Hein 2001). The first enzyme of the pathway is acetyl-CoA *C*-acetyltransferase [EC 2.3.1.9], encoded by *phaA*, which catalyzes the condensation of two acetyl-CoA molecules to form acetoacetyl-CoA (Peoples and Sinskey 1989b). The next step is the reduction of acetoacetyl-CoA to (R)-3-hydroxybutyryl-CoA, which is catalyzed by NADPH-dependent acetoacetyl-CoA reductase [EC 1.1.1.36] encoded by *phaB* (Peoples and Sinskey 1989b). Finally, PHA synthase [EC 2.3.1.-] encoded by *phaC*, catalyzes the polymerization of (R)-3-hydroxybutyryl-CoA monomers to PHB (Peoples and Sinskey 1989a).

The natural PHB producers like *R. eutropha*, *Bacillus megaterium* or *Pseudomonas sp.* are known to produce and accumulate PHB as a storage compound in response to nutrient imbalance caused by growth under conditions of carbon source excess but limitation in other essential nutrients (Steinbüchel and Hein 2001; Trotsenko and Belova 2000). Instead of employing the natural PHB producers, which can depolymerize PHB and use it as a secondary energy source, metabolic engineering can be used to transfer the PHB biosynthetic pathway to alternative hosts that may have advantage over the natural PHB producers, in particular the lack of enzymes for PHB

* Correspondence: nielsenj@chalmers.se
Department of Chemical and Biological Engineering, Chalmers University of Technology, Kemivägen 10, SE-412 96 Göteborg, Sweden

depolymerization (Uchino and Saito 2006). Furthermore, by transferring to alternative hosts one may take advantage of a range of technologies developed for general platform cell factories like *Escherichia coli* and *Saccharomyces cerevisiae*. Thus, there have been a range of studies where PHB production has been evaluated in *E. coli* and further metabolic engineering has been carried out with the objective to improve the productivity. In a metabolic and kinetic study, a recombinant *E. coli* strain producing PHB was examined and compared to the native PHB producer, *R. eutropha*, and this study revealed that the PHB flux was highly sensitive to the acetyl-CoA/CoA ratio, the total acetyl-CoA plus CoA concentration and pH (van Wegen et al. 2001). In recombinant *E. coli*, a mutation in *arcA* encoding a protein that regulates aerobic respiration under microaerobic conditions resulted in higher amounts of PHB accumulated in the cell (Nikel et al. 2006). Low-agitation conditions had a positive effect on PHB synthesis from glycerol in recombinant *E. coli* carrying the *phaCAB* operon and *phaP* encoding a granule-associated protein (phasin) (de Almeida et al. 2010). Several studies also attempted to synthesize PHB in plants according to the aim to produce high amounts of PHB at lower costs compared to microbial fermentation, particularly in plant plastids where the biosynthesis of fatty acids from acetyl-CoA occurs (Bohmert et al. 2000; Nawrath et al. 1994; Petrasovits et al. 2012). However, the growth of some of these transgenic plants was inhibited, possibly due to the metabolic burden of PHB synthesis (Poirier et al. 1992).

The benefits of using S. cerevisiae as a model for producing PHB is that the molecular machinery of *S. cerevisiae* is well studied and as the most widely used eukaryal microorganism for industrial production of fuels and chemicals it is an attractive cell factory platform. Furthermore, its genome has been very well characterized and genome scale metabolic models have been reconstructed (Goffeau 2000; Nookaew et al. 2008). For these reasons, several attempts have been made to evaluate *S. cerevisiae* as a cell factory for PHB production (Breuer et al. 2002; Dimster-Denk and Rine 1996; Leaf et al. 1996; Marchesini et al. 2003; Zhang et al. 2006). Synthesis of PHB in *S. cerevisiae* has initially been demonstrated by expressing only bacterial polyhydroxybutyrate synthase (Leaf et al. 1996). This PHB synthesis approach is successful because of the activity of native thiolase and reductase enzymes involved in the synthesis of D-3-hydroxybutyryl-CoA in *S. cerevisiae.* However, the yield obtained in this study was very low when compared with the expression of all three genes of the PHB biosynthesis pathway (Breuer et al. 2002; Carlson et al. 2002; Carlson and Srienc 2006). Thiolase enzymes in *S. cerevisiae* exist and function in three different compartments, in mitochondria and peroxisomes for fatty acid β-oxidation and in the cytoplasm for the mevalonate pathway (Hiser et al. 1994). However, only the cytoplasmic thiolase participates in PHB biosynthesis. Many approaches have been followed to improve the production of PHB in yeast. Srienc and co-workers performed elementary mode analysis of a *S. cerevisiae* containing the PHB synthesis pathway in order to identify new metabolic engineering targets (Carlson et al. 2002). The analysis suggested that the introduction of the ATP citrate-lyase reaction and the transhydrogenase reaction can improve the theoretical PHB carbon yield (Carlson et al. 2002). Acetyl-CoA serves as the precursor for the PHB biosynthesis pathway and increasing the availability of acetyl-CoA was proposed to improve PHB production (Carlson and Srienc 2006; Suzuki et al. 2002). However, using enzyme inhibitors to reduce its consumption by other pathways or feeding of the substrate during cultivation would result in increasing production costs and may not be feasible for industrial applications. Here, we demonstrated metabolic pathway engineering by co-transformation of a plasmid containing the PHB biosynthesis pathway and an acetyl-coenzyme A (acetyl-CoA) boost plasmid designated to improve the availability of cytoplasmic acetyl-CoA and hereby improve the productivity of PHB in *S. cerevisiae*.

Materials and methods

Strains, media, and culture conditions

Plasmids were maintained and propagated in *E. coli* DH5α. The preparation of competent *E. coli* cells and their transformation were performed according to standard protocols (Sambrook and Russell 2006). Lysogeny broth (LB) medium was used for routine culturing of *E. coli* (Bertani 1951) and 80 mg L^{-1} ampicillin was added to LB when needed. *S. cerevisiae* strain CEN.PK113-11C (*MAT*a *SUC2 MAL2-8*^{c} *ura3-52 his3-Δ1;* provided by P. Kötter, Frankfurt, Germany) was used as the background strain for evaluation of the polyhydroxybutyrate pathway. Plasmid containing yeast strains were selected on synthetic dextrose (SD) medium, prepared with 6.7 g L^{-1} yeast nitrogen base without amino acids (YNB-AA) (Formedium, Hunstanton, UK) and 20 g L^{-1} glucose with complete supplement mixture (CSM) lacking uracil and/or histidine (Formedium) where appropriate.

Plasmid construction and yeast transformation

The detailed construction of pIYC04 as a background plasmid and pIYC08 as acetyl-CoA boost plasmid is described by Chen et al. (Chen et al. 2012). The primers used for plasmid construction are listed in Table 1. The PHB biosynthesis pathway was introduced into CEN.PK 113-11C by using another multi-copy plasmid based on pSP-GM2 containing a P_{TEF1}-P_{PGK1} bidirectional promoter (Partow et al. 2010). The PHB biosynthesis pathway genes *phaA*, *phaB* and *phaC* were synthesized based on the genes from *R. eutropha* H16 and codon optimized for expression in *S. cerevisiae* by DNA 2.0

Table 1 Oligonucleotides used in this study

No.	Sequence (5' -3')
1	TACAATTGCTATTATTATCCTGCTCAGTGGTACTT
2	TCCAATTGTCAGTGAGCGAGGAAGCGGAAGAG
3	TTCGTTCTTCCTTCTGTTCGGAGATTAC
4	GGAACAGGAGTATTGCCTTTCAAGTAGTTATC

Restriction sites are underlined.

(Menlo Park, CA, USA). *PhaA* was cloned into pSP-GM2 into the *Spe*I/*Sac*I sites between the *PGK1* promoter and the *ADH1* terminator. Then, *PhaB* was cloned into *the BamHI/Sal*I sites between the *TEF1* promoter and the *CYC1* terminator of the same vector to yield pSP-GM2-phaAB. *PhaC* was cloned into the MCS of pSP-GM2 vector the *TEF1* promoter and the *CYC1* terminator. The fragment of *phaC* together with the *TEF1* promoter and the CYC1 terminator was amplified using primer 1 and 2 and ligated into pSP-GM2-phaAB using the *Mfe*I restriction site resulting in pKK01. The direction of *phaC* insertion was confirmed by colony PCR with primer 3 and 4. Yeast transformation was performed by using the lithium acetate/single-stranded carrier DNA/ polyethylene glycol method (Gietz and Woods 2002). Strain SCKK005 was constructed by transforming plasmids pKK01 and pIYC04 into strain CEN.PK113-11C. Plasmids pKK01 and pIYC08 were co-transformed into strain CEN.PK113-11C for the construction of SCKK006. Strain SCKK009 and SCKK010 were constructed by co-transformation of plasmids pKK01 and pIYC08 into SIYC32 and SCIYC33, respectively. The construction of the *cit2Δ* strain (SCIYC32) and the *mls1Δ* strain (SCIYC33) are described by Chen et al. (Chen et al. 2012). Strains used in this study are summarized in Table 2. The metabolic pathway and plasmid maps are illustrated in Figure 1.

Shake flask cultivation

The pre-cultures for shake flask cultivations were prepared by inoculation of 5 mL modified minimal medium in a 14 mL culture tube and grown at 30°C and 180. The modified minimal medium for shake flask cultivations was prepared as follows: 5 $g \cdot L^{-1}$ $(NH_4)_2SO_4$; 3 $g \cdot L^{-1}$ KH_2PO_4; 0.5 $g \cdot L^{-1}$ $MgSO_4 \cdot 7H_2O$; 1 $mL \cdot L^{-1}$ of trace metal solution and vitamin solution (see below) with an initial pH of 6.5. 45 mL of defined minimal medium in a 100 mL unbaffled flask were inoculated with an amount of pre-culture that resulted in a final optical density of 0.02 at 600 nm (OD_{600}). The culture was grown at 30°C with 180 rpm in an orbital shaking incubator and samples were taken at 40, 80 and 120 h to determine PHB production.

Bioreactor cultivation

PHB production was evaluated in defined minimal media with the following composition: 5 $g \cdot L^{-1}$ $(NH_4)_2SO_4$; 3 g L^{-1} KH_2PO_4; 0.5 g L^{-1} $MgSO_4 \cdot 7H_2O$; 1 mL L^{-1} trace metal solution (pH 4.0: 15.0 g L^{-1} EDTA (sodium salt); 0.45 g L^{-1} $ZnSO_4 \cdot 7H_2O$; 1 g L^{-1} $MnCl_2 \cdot 2H_2O$; 0.3 g L^{-1} $CoCl_2 \cdot 6H_2O$; 0.3 g L^{-1} $CuSO_4 \cdot 5H_2O$; 0.4 g L^{-1} $Na_2MoO_4 \cdot 2H_2O$; 0.45 g L^{-1} $CaCl_2 \cdot 2H_2O$; 0.3 g L^{-1} $FeSO_4 \cdot 7H_2O$; 0.1 g L^{-1} H_3BO_3, and 0.10 g L^{-1} KI). The pH was adjusted to 5 by adding 2 M KOH and autoclaved separately from the carbon source solution. Glucose was added at a concentration of 20 g L^{-1}. Vitamin solution (pH 6.5: 0.05 g L^{-1} biotin; 0.2 g L^{-1} ρ-amino benzoic acid; 1 g L^{-1} nicotinic acid; 1 g L^{-1} Ca-pantothenate; 1 g L^{-1} pyridoxine-HCl; 1 g L^{-1} thiamine-HCl and 25 g L^{-1} myo-inositol) was filter sterilized and aseptically added to the medium after autoclaving at the concentration of 1 mL L^{-1}. Batch cultivations were carried out in 1.2 L bioreactors. The pre-cultures were prepared using the same culture conditions as for shake flask cultivation. 700 mL of defined minimal medium were inoculated with an amount of pre-culture that resulted in a final OD_{600} of 0.02. The temperature was kept at 30°C and the pH was adjusted to 5.00 ± 0.05 using 2 M KOH.

Analytical methods

Culture samples of 10 mL volume were centrifuged at 5,311 × g and 4°C for 5 min and the pellets were washed once with distilled water and centrifuged at 14,000 × g

Table 2 Yeast strains and plasmids used in this study

Strain	Genotype or relevant feature(s)	Plasmid	Source
CEN.PK 113-11C	*MATa SUC2 MAL2-8^c ura3-52 his3-Δ1*	-	P. Kötter[a]-
SCKK005	*MATa SUC2 MAL2-8^c ura3-52 his3-Δ1*	pIYC04/pKK01	This study
SCKK006	*MATa SUC2 MAL2-8^c ura3-52 his3-Δ1*	pIYC08/pKK01	This study
SCIYC32	*MATa SUC2 MAL2-8^c ura3-52 his3-Δ1 cit2Δ*	-	(Chen et al. 2012)
SCIYC33	*MATa SUC2 MAL2-8^c ura3-52 his3-Δ1 mls1Δ*	-	(Chen et al. 2012)
SCKK009	*MATa SUC2 MAL2-8^c ura3-52 his3-Δ1 cit2Δ*	pIYC08/pKK01	This study
SCKK010	*MATa SUC2 MAL2-8^c ura3-52 his3-Δ1 mls1Δ*	pIYC08/pKK01	This study

[a] Institute of Microbiology, J.W. Goethe Universität, Frankfurt, Germany.

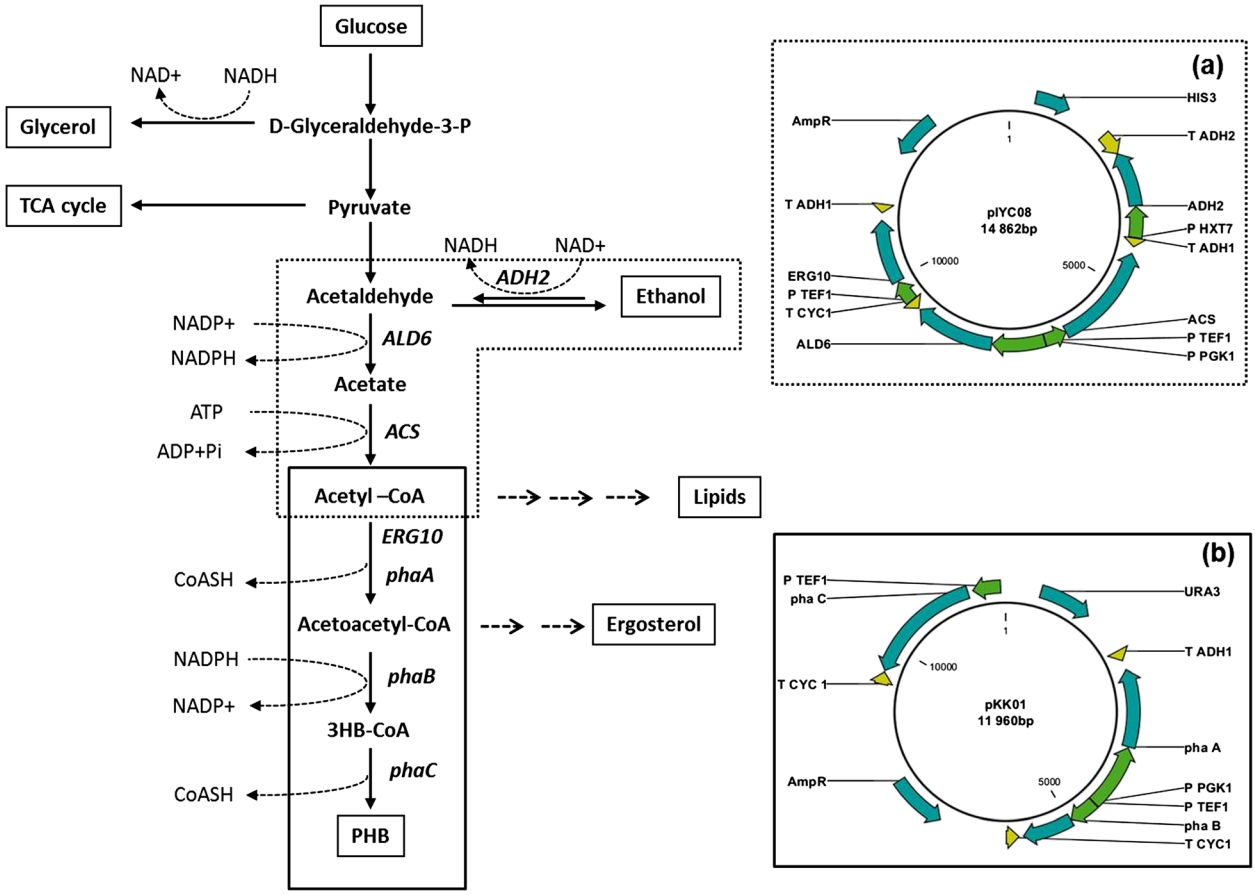

Figure 1 Schematic pathway and plasmid maps for polyhydroxybutyrate production in *S. cerevisiae*. (**a**) Acetyl-CoA boost plasmid (pIYC08) containing *ADH2*: alcohol dehydrogenase, *ALD6*: aldehyde dehydrogenase, *ACS*: acetyl-CoA synthetase variant and *ERG10*: acetyl-CoA acetyltransferase. (**b**) PHB plasmid (pKK01) containing PHB genes from *R. eutropha*, *phaA*: acetyl-CoA acetyltransferase, *phaB*: NADPH-linked acetoacetyl coenzyme A (acetyl-CoA) reductase and *phaC*: poly(3-hydroxybutyrate) polymerase. P and T in the plasmid map represent promoter and terminator, respectively.

for 1 min. To lyophilize the biomass, the recovered cell pellet was immediately frozen by immersion in liquid nitrogen followed by lyophilization under vacuum (Christ Alpha 2–4 LSC, Shropshire, UK). The cell dry weight was determined and the pellet kept at 4°C for further analysis.

Metabolites including glucose, ethanol, glycerol, and acetate were quantified in the culture supernatant using an Ultimate 3000 HPLC (Dionex, Sunnyvale, CA, USA) equipped with an Aminex HPX 87 H ion exclusion column (300 mm × 7.8 mm, Bio-Rad Laboratories, Hercules, CA, USA) which was operated at 45°C and a flow rate of 0.6 mL min^{-1} of 5 mM H_2SO_4 using a refractive index detector and UV detector for analysis of sugars and organic acids, respectively.

PHB was analyzed as described previously (Karr et al. 1983; Tyo et al. 2006). 10–20 mg of dried cells were weighed and boiled in 1 mL of concentrated sulfuric acid for 60 min and then diluted with 4 mL of 14 mM H_2SO_4. Samples were centrifuged (15 min, 16,000 × g) to remove cell debris, and the supernatant was analyzed using an Ultimate 3000 HPLC (Dionex) equipped with an Aminex HPX-87 H ion exclusion column (300 × 7.8 mm; Bio-Rad Laboratories) and UV detector. Commercially available PHB (Sigma-Aldrich, St. Louis, MO), processed in parallel with the samples, was used as a standard. The HPLC was operated at 60°C and a flow rate of 0.6 mL min^{-1} of 5 mM H_2SO_4.

The total lipid extraction method was adapted from Bligh and Dyer (Bligh and Dyer 1959). Briefly, 15 mg of freeze-dried cell pellets were treated with 1 unit μL^{-1} zymolyase in 1 mL digestion buffer (1.2 M glycerol, 100 mM sodium thioglycolate, 50 mM Tris-sulfate, pH 7.5) at 37°C for 15 min, followed by centrifugation at 3000 rpm for 3 min. The mixture of collected spheroplasts was spiked with cholesterol as internal standard, 7 ml of chloroform:methanol (2:1, v/v) were added and shaken vigorously at room temperature and 500 rpm for 30 min. 1.7 mL of 0.73%

NaCl was added to the mixture prior centrifugation at 3500 rpm for 5 min at 4°C. The lower (organic) phase was collected and the upper phase was re-extracted with 5 mL of chloroform-methanol (85:15 v/v). The lower (organic) phase was collected and pooled with the previous organic fraction and kept at −20°C for further HPLC analysis.

Lipid separation and quantification were performed using the method modified from Silversand and Haux (Silversand and Haux 1997). Lipid separation was accomplished using an Ultimate 3000 HPLC (Dionex) equipped with a Corona charged aerosol detector (CAD) (Dionex) connected with nitrogen gas at 35 psi gas pressure. A 20 μL volume of each sample was injected into a Luna 5 μm HILIC 200 Å 250 × 4.6 mm LC column (Phenomenex, Torrance, CA). The flow-rate was 0.8 $mL \cdot min^{-1}$ and the column temperature was kept at 25°C during all runs. A gradient flow with 3 solvents (solvent A, 99:1 by vol. of hexane/acetic acid, solvent B 70:29:1, by vol. of hexane/isopropanol/acetic acid, solvent C 85:14:1, by vol. of isopropanol/water/acetic acid) was applied for the separation of lipids. Triethylamine (0.08%) was added to solvent B and solvent C for better separation. The HPLC system was equilibrated with 99% solvent A. The gradient profile started from 3% solvent B at 7 min, reached 10% solvent B in 1 min and ended at 100% solvent B in 15 min, while solvent C was kept at 0% from 0 min to 15 min. This gradient profile is used for separation of triacylglycerol (TAG), free fatty acids, cholesterol (as internal standard) and ergosterol. After 15 min, solvent A was kept at 0% until 35 min. Meanwhile, an increase of solvent C to 65% from 15 min to 32 min was applied for separation of phospholipids (phosphatidylethanolamine, phosphatidylinositol, phosphatidylcholine, phosphatidylserine, phosphatidic acid). After that, solvent C was decreased to 0% from 32 min to 35 min and 100% solvent B was applied to the system. After 40 min, 99% solvent A was run for 5 min in order to equilibrate and stabilize the system for the measurement of the next sample. A logarithmic plot of peak area versus the concentration of each lipid standard was used to generate a calibration curve. The slope determined from the log-log plot was further used for lipid quantification (Nair and Werling 2009).

Results

Characterization of PHB-producing *S. cerevisiae*

The engineered *S. cerevisiae* strains were preliminary studied for growth and PHB production in shake flasks as shown in Figure 2. Co-expression of beta-ketothiolase, acetoaetyl-CoA reductase and PHA synthase results in PHB accumulation in *S. cerevisiae* as observed in previous studies (Breuer et al. 2002; Carlson et al. 2002; Carlson and Srienc 2006). In this study, the 3 genes involved in the PHB pathway were expressed from a single vector in order to avoid the heterogeneity of plasmid distribution. *S. cerevisiae* carrying the PHB plasmid and an empty *HIS3* plasmid (strain SCKK005) and a strain carrying the PHB plasmid and the acetyl-CoA boost plasmid (SCKK006) were characterized and evaluated for the productivity of PHB. The acetyl-CoA boost plasmid contains 4 genes, *ADH2*, *ALD6*, acs^{L641P} and *ERG10*, involved in channeling carbon from ethanol to acetyl-CoA. In the acetyl-CoA boost plasmid, *ALD6*, acs^{L641P} and *ERG10* are controlled by constitutive promoters, P_{TEF1} and P_{PGK1}, respectively, while *ADH2* is under control of the P_{HXT7} promoter which is strongly de-repressed under glucose depletion (Partow et al. 2010; Reifenberger et al. 1995; Sedlak and Ho 2004).

CIT2 encoding peroxisomal citrate synthase catalyzes the conversion of oxaloacetate and acetyl-CoA to citrate and plays role in acetate metabolism. *MLS1* encoding malate synthase catalyzes the conversion of glyoxylate and acetyl-CoA to malate in the glyoxylate shunt. Deletion of *CIT2* and *MLS1* affect the integrity of the glyoxylate shunt and will therefore reduce the drain of acetyl-CoA through this pathway and hereby possibly affect the availability of cytosolic acetyl-CoA. Thus, the effect of *CIT2* and *MLS1* deletion on PHB production was also investigated. The biomass yield of *cit2Δ* (SCKK009) was less than that of *mls1Δ* (SCKK010), and the biomass yield for both the deletion strains were lower than those of the non-deletion reference strain without the acetyl-CoA plasmid (SCKK005) and the non-deletion strain with the acetyl-CoA plasmid (SCKK006) (see Figure 2a). The biomass yield of the deletion strains, SCKK009 and SCKK010, was lower than that of non-deletion strains, SCKK005 and SCKK006, due to the impaired C_2 carbon utilization. The recombinant strain with both the acetyl-CoA boost plasmid and the PHB plasmid (SCKK006) produced an 18 times higher final concentration of PHB (at 120 h) compared to the reference strain, SCKK005 (Figure 2b). Besides that, the amount of accumulated PHB in SCKK009 and SCKK010 was less than SCKK006. Although, *mls1Δ* (SCKK010) gave lower biomass yield than the reference, it gave higher PHB titer compare to the non-deletion reference strain (SCKK005) when the deletion strain carried the acetyl-CoA plasmid. This result showed the combined effect of *mls1Δ* together with the utilization of acetyl-CoA plasmid on the availability of acetyl-CoA and the influence of the deletion on PHB production. The consumption rate of ethanol in the deletion strains, especially in *cit2Δ* (SCKK009), was slower than for the non-deletion strain as the residual amount of ethanol was detected after 80 h of cultivation (Figure 2c). In addition, more than 6.5 $g\ L^{-1}$ of acetate was detected in the medium after 120 of fermentation of SCKK009, which is clear evidence for the impaired C_2 metabolism. Due to the negative impact of *CIT2* and *MLS1* deletion on growth and PHB production, the recombinant strains SCKK005 and

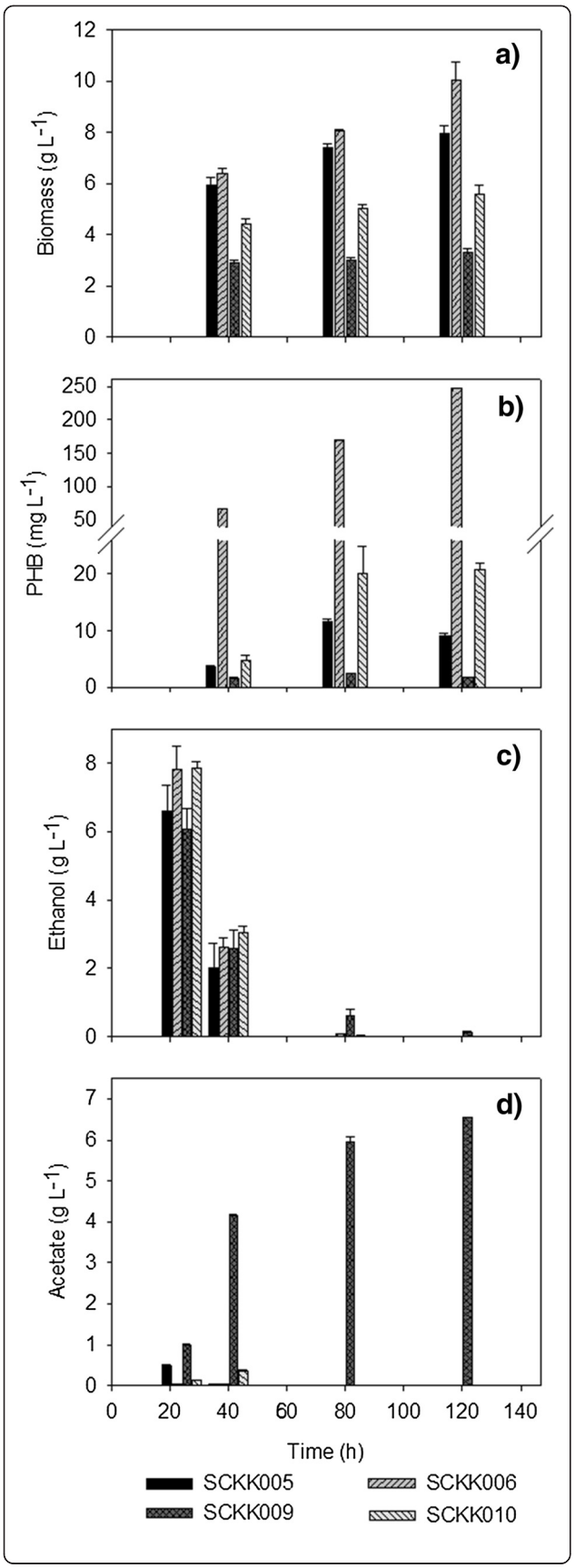

Figure 2 Measurements of biomass and PHB from shake flask cultivations in a modified minimal medium with 20 g L^{-1} glucose as carbon source. Strain SCKK005 harbors an empty plasmid (pIYC04) and the PHB plasmid (pKK01), strain SCKK006 harbors an acetyl-CoA boost plasmid (pIYC08) and the PHB plasmid (pKK01), SCKK009 and SCKK010 harbor pIYC08 and pKK01 and carry a *CIT2* and *MLS1* deletion, respectively.

SCKK006 without gene deletions were selected for further characterization in bioreactors.

Kinetic studies of the PHB-producing *S. cerevisiae* strains were carried out in aerobic bioreactor cultivation. The production and accumulation of PHB coincided with the depletion of glucose and the increase in ethanol concentration during the glucose consumption phase. SCKK005 and SCKK006 demonstrated a similar growth profile as shown in Figure 3. Kinetic parameters and yields on glucose and ethanol are summarized in Table 3. There was no significant difference in the maximum specific growth rates of SCKK005 and SCKK006, which were 0.27 ± 0.02 h^{-1} and 0.28 ± 0.00 h^{-1}, respectively. The glucose consumption rate of SCKK006 was higher than that of SCKK005. However, a slightly lower biomass yield on glucose of SCKK006 was observed. The strain carrying the acetyl-CoA boost plasmid showed the capability to increase the carbon flux from ethanol to the PHB pathway as the PHB yield on ethanol in SCKK006 was significantly higher than that of SCKK005 In the ethanol phase, the PHB yield on ethanol in SCKK006 was 6.09 ± 1.44 mg (g EtOH)$^{-1}$, which was approximately 25-fold higher than for SCKK005 that had a yield of 0.22 ± 0.04 mg (g EtOH)$^{-1}$. The maximum PHB titer detected during the ethanol phase in SCKK005 was 1.85 mg·L^{-1} while SCKK006, which contained both the PHB biosynthesis and the acetyl-CoA boost plasmid, reached a titer of 43.11 mg·L^{-1} after 36 h of batch fermentation. In SCKK005, the PHB level remained at the same concentration until the end of fermentation while the PHB titer in SCKK006 tended to decrease after 50 h.

Comparison of specific productivities in pathway engineered strains

The effect of the acetyl-CoA boost plasmid was clearly seen during growth in the glucose phase when SCKK006 started to produce and accumulate PHB with a yield of PHB on glucose of 0.13 ± 0.02 mg (g glc)$^{-1}$, higher than that of SCKK005 as previously shown in Table 3. Figure 4 shows the consumption of glucose and the formation of ethanol, glycerol and acetate measured during growth in an aerobic batch bioreactor. A maximum glycerol concentration of 1.33 ± 0.06 g·L^{-1} was observed in SCKK006, while a lower glycerol concentration, 0.86 ± 0.01 g·L^{-1}, was observed in SCKK005. This result indicates the influence of *ADH2* overexpression in order to convert ethanol to acetaldehyde thus resulting in a small increase in NADH

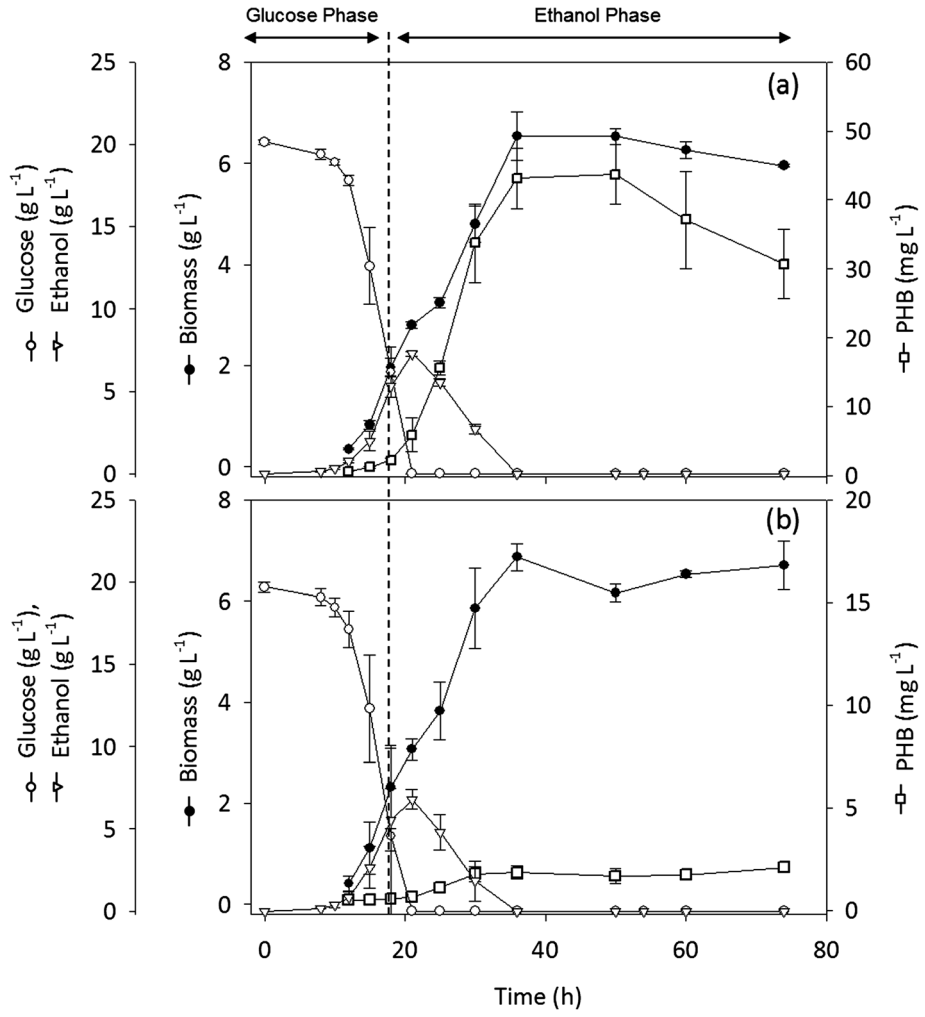

Figure 3 Fermentation profile of *S. cerevisiae* producing PHB in aerobic batch bioreactor cultivation using a chemically defined medium with 20 g L^{-1} glucose as carbon source. (**a**) SCKK006: *S. cerevisiae* harboring an acetyl-CoA boost plasmid (pIYC08) and the PHB plasmid (pKK01). (**b**) SCKK005: *S. cerevisiae* harboring an empty plasmid (pIYC04) and the PHB plasmid (pKK01).

production, which triggers the formation of glycerol for redox balancing in the cytosol (Bakker et al. 2001). On the other hand, the maximum acetate concentration of 0.42 ± 0 g·L^{-1} detected in SCKK005 was 3 times higher than the acetate concentration of 0.12 ± 0.01 g·L^{-1} detected in SCKK006. Therefore, the different concentrations of glycerol and acetate detected during growth on glucose are most likely a consequence of introducing the acetyl-CoA boost plasmid in the PHB producing strain.

To further explore carbon channeling from glucose to PHB and use of acetyl-CoA for lipid synthesis we measured phospholipids, triacylglycerols, free fatty acids and ergosterol in the cells. Using these measurements we calculated the specific productivities (r_p) of ethanol, glycerol, PHB, triacylglycerols (TAG), ergosterol, phospholipids and free fatty acids as directly and non-directly acetyl-CoA derived products during growth on glucose using the maximum specific growth rate (μ_{max}) and the product yield coefficient.

Table 3 Yields and kinetic parameters obtained from batch cultivations

	Unit	SCKK005	SCKK006
Maximum specific growth rate	h^{-1}	0.27 ± 0.02	0.28 ± 0.00
Glucose consumption rate	g (g DW h)$^{-1}$	1.80 ± 0.09	2.24 ± 0.33
Biomass yield on glucose	g (g glc)$^{-1}$	0.15 ± 0.01	0.13 ± 0.02
Ethanol yield on glucose	g (g glc)$^{-1}$	0.35 ± 0.05	0.35 ± 0.07
Glycerol yield on glucose*	g (g glc)$^{-1}$	0.05 ± 0.00	0.07 ± 0.00
Acetate yield on glucose*	g (g glc)$^{-1}$	0.02 ± 0.00	0
PHB yield on glucose*	mg (g glc)$^{-1}$	0.02 ± 0.01	0.13 ± 0.02
Biomass yield on ethanol	g (g EtOH)$^{-1}$	0.46 ± 0.27	0.45 ± 0.08
PHB yield on ethanol*	mg (g EtOH)$^{-1}$	0.22 ± 0.04	6.09 ± 1.44

The values were calculated from at least triplicate fermentations ($n \geq 3$) and represent as mean ± SD.
* The values are significantly difference at p-value ≤ 0.05.

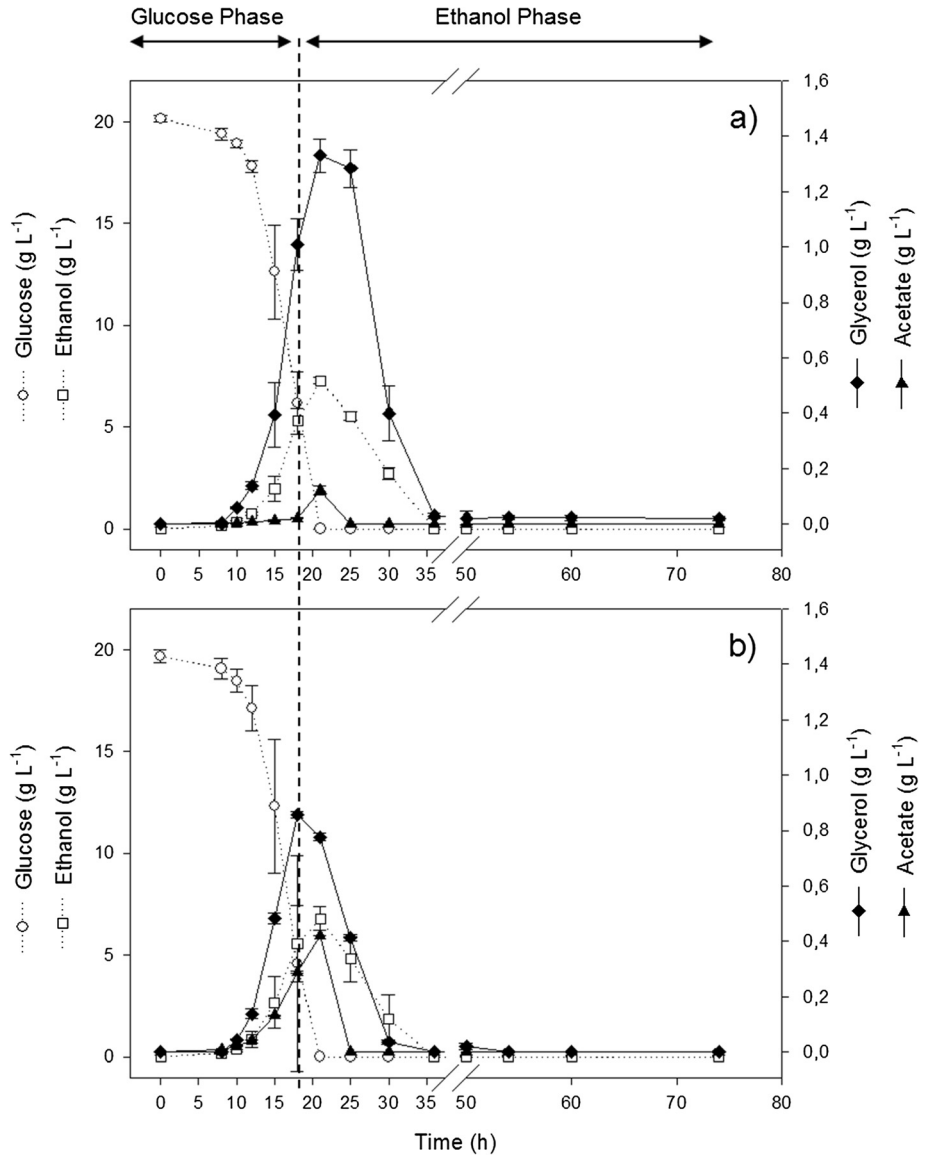

Figure 4 Time profile of glucose consumption and ethanol, glycerol and acetate formation during batch bioreactor cultivation of a) SCKK006 and b) SCKK005 in a chemically define minimal medium with 20 g L^{-1} glucose as carbon source. SCKK006: *S. cerevisiae* harboring an acetyl-CoA boost plasmid (plYC08) and the PHB plasmid (pKK01). and SCKK005: *S. cerevisiae* harboring an empty plasmid (plYC04) and the PHB plasmid (pKK01), respectively.

The biomass yield coefficient (Y_{sx}) and the product yield coefficient (Y_{sp}) are defined as the amount of substrate (s) consumed for the formation of biomass (x) or other metabolites (p) such as ethanol, acetate or PHB. The specific product formation rate was calculated by using the equation: $r_p = \mu_{max} \cdot \frac{Y_{sp}}{Y_{sx}}$ and the specific glucose consumption rate was calculated by using the equation: $r_s = \frac{\mu_{max}}{Y_{sx}}$. Figure 5 illustrates a simplified pathway with the calculated fluxes during growth on glucose. The mean value ± SD from at least triplicate fermentations is reported. The carbon from glucose was mainly directed to ethanol as the major product in *S. cerevisiae*. The impact of using the acetyl-CoA boost plasmid was clearly associated with a higher specific productivity of PHB in SCKK006 as well as the lower specific productivities of triacylglycerol and phospholipids as other acetyl-CoA derived products. The higher specific productivity of glycerol in SCKK006 revealed the collateral effect of *ADH2* over-expression as mentioned above. The specific productivity of ergosterol, which is also derived from acetoacetyl-CoA, an intermediate in the PHB pathway, was lower in SCKK006 than in SCKK005, which shows that the heterologous PHB pathway is clearly able to compete for acetoacetyl-CoA otherwise used for biosynthesis of

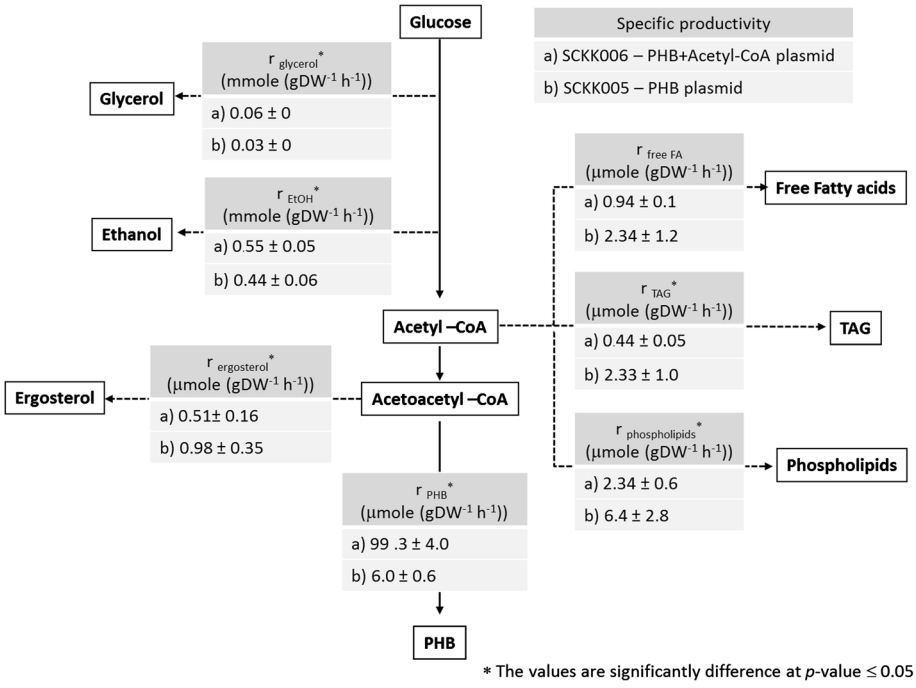

Figure 5 Comparison of specific fluxes in SCKK006 and SCKK005 during growth on glucose in aerobic batch bioreactor cultivation with 20 g L^{-1} glucose as carbon source. SCKK006 is *S. cerevisiae* harboring an acetyl-CoA boost plasmid (pIYC08) and the PHB plasmid (pKK01). SCKK005 is *S. cerevisiae* harboring an empty plasmid (pIYC04) and the PHB plasmid (pKK01). The fluxes towards the different lipids were calculated from measurement of the lipid composition of the biomass and the maximum specific growth rate. The mean value ± SD from at least triplicate fermentations are reported.

ergosterol. Finally, as a result of employing the acetyl-CoA boost plasmid to channel carbon from ethanol to the PHB pathway, the specific productivity of PHB in the glucose phase in the strain carrying the acetyl-CoA boost plasmid (SCKK006) was 99.3 ± 4 μmole (g DW^{-1} h^{-1}), 16.5 times higher compared to the strain carrying the empty acetyl-CoA plasmid (SCKK005).

Discussion

The addition of precursor molecules to the fermentation medium has been shown to improve the formation of many biological products, e.g. supplementation with glucosamine as precursor resulted in improved hyaluronic acid production by *E. coli* (Mao et al. 2009) and supplementation with specific amino acids enhanced heterologous protein production by *S. cerevisiae* (Görgens et al. 2005). Extra feeding of acetate (0.5 g·L^{-1} with pH adjusted to 4.5) and panthothenate (1000 μg·L^{-1}) as a precursors of acetyl-CoA were tested by Carlson and Srienc in order to increase PHB accumulation in *S. cerevisiae* (Carlson and Srienc 2006). Feeding a combination of acetate and pantothenate was found to improve PHB production by approximately 45% over the control. Instead of feeding precursors to improve the productivity, which would increase the costs of PHB production, we focused on pathway engineering to increase the supply of the precursor for PHB production and hereby improve the economic feasibility of a process using *S. cerevisiae*.

The native *ADH2* in *S. cerevisiae* is a glucose-repressible alcohol dehydrogenase. It catalyzes the oxidation of ethanol to acetaldehyde only when glucose becomes depleted from the medium. In order to activate the reaction catalyzed by *ADH2* when glucose was completely consumed, the *HXT7* promoter was selected to control *ADH2* in the acetyl-CoA plasmid. Although the *HXT7* promoter is a glucose-repressible promoter, we select the *HXT7* promoter based on its strong expression level especially during the ethanol phase. Therefore, *ADH2* under control of the *HXT7* promoter ensures the conversion of ethanol to acetyldehyde and is responsible for the initial step in the utilization of ethanol as carbon source. *ALD6* encoding cytosolic aldehyde dehydrogenase is involved in the conversion of acetaldehyde to acetate. This enzyme utilizes $NADP^+$ as the preferred coenzyme. As a result, *ALD6* over-expression might help providing NADPH, a required cofactor for PHB production (Boubekeur et al. 2001). There are two acetyl-CoA synthetase in *S. cerevisiae*, encoded by *ACS1* and *ACS2*. Both of these enzymes catalyze ATP-dependent activation of acetate to acetyl-CoA. The expression of *ACS1* is subjected to glucose repression while *ACS2* can be expressed during growth on glucose where it is likely to be responsible for cytosolic

acetyl-CoA production. However, the regulation of both enzymes is complex and hence over-expression is believed necessary to increase the flux towards acetyl-CoA. In the native host *Salmonella enterica,* mutations at Leu-641 of acetyl CoA synthetase (Acs), prevent the acetylation by acetyltransferase bypassing the need for sirtuin deacetylase activity and maintain the enzyme in an active state during growth on acetate. (Starai et al. 2005). Enhancing acetyl-CoA supply by engineering the pyruvate dehydrogenase bypass through over-expression of acetaldehyde dehydrogenase in combination with introduction of a *S. enterica* acetyl CoA synthetase variant (L641P) in *S. cerevisiae*, was successful demonstrated to improve the productivity of isoprenoids in yeast (Shiba et al. 2007).

CIT2, the peroxisomal citrate synthase and *MLS1*, the cytosolic malate synthase are key enzymes of the glyoxylate shunt and hereby affect acetate metabolism (Kunze et al. 2006; Lee et al. 2011). Deletion of *CIT2* and *MLS1* in order to improve the availability of cytosolic acetyl-CoA was investigated for its impact on PHB production. However, this deletion strategy resulted in the impaired metabolism due to the incapability to utilize C_2 carbon via the glyoxylate shunt in *cit2Δ* and *mls1Δ* strains. The deletion strains have only the tricarboxylic acid cycle (TCA cycle) to utilize C_2 carbon for energy production whereas the biosynthesis of C_4 dicarboxylic acids required as precursors for amino acids biosynthesis cannot take place, resulting in lack of growth (Chen et al. 2012). This is reflected by a much reduced biomass yield in the *cit2Δ* strain. In the *mls1Δ* strain (SCKK009), less acetate was accumulated in the medium compared to the *cit2Δ* strain and acetate was slowly consumed until the end of fermentation. This might be due to the activity of the homolog malate synthase encoded by *DAL7* (Hartig et al. 1992). Moreover, the deletion of *CIT2* affect acetate metabolism and reduced the efficiency of acetyl-CoA synthetase, both native acetyl-CoA synthetase and the additional acetyl-CoA synthetase, to catalyze the ATP-dependent activation of acetate to acetyl-CoA thus resulting in more than 6.5 g/L^{-1} of acetate accumulated in the *cit2Δ* strain and no further biomass production after glucose is completely consumed (after 24 hr). Besides that, the PHB titer was drastically decreased as compared to the non-deletion strain, SCKK006.

The comparison of the specific productivities in the PHB producing strains revealed that employing the acetyl-CoA boost plasmid helps in directing carbon towards the PHB pathway. Although, there was a difference in PHB yield when the PHB strains, SCKK005 and SCKK006, were cultivated in bioreactors. This might be explained by the cultivation condition in the bioreactor which favors the growth of *S. cerevisiae* rather than PHB production. Thus, the maximum specific growth rate in shake flasks was 0.18-0.20 h^{-1} while the maximum specific growth rate in the bioreactors was 0.27-0.28 h^{-1}. Although the PHB yield from the bioreactors was less than shake flask cultivation the difference in PHB productivity between SCKK005 and SCKK006 clearly showed the effect of employing the acetyl-CoA plasmid for PHB production. Therefore, the flux from glucose to PHB was analyzed by using the information from aerobic batch bioreactor cultivations. For this analysis free fatty acids, TAG, phospholipids and ergosterol were considered as side products of PHB production. From this analysis we found that over-expression of *ERG10* together with *phaA* significantly reduced the specific productivities of TAG and phospholipids as side products compared to the reference strain which does not have over-expression of *ERG10*. Although increased production of acetyl-CoA might lead to fatty acid or lipid synthesis, our study show that when the cells contain a heterologous pathway to PHB flux is actually directed towards PHB rather than towards lipids. Thus, we can conclude that enhancement of acetyl-CoA production by co-expression of genes on the acetyl-CoA boost plasmid improved the productivity of PHB during growth on glucose and further enhanced the productivity of PHB approximately 16.5 times bioreactor cultivations and reduce the flux from acetyl-CoA to lipids.

Competing interests

The authors declare that they have no competing interest.

Authors' contributions

JN and KK participated in the design of the study. JN and VS supervised the project and edited manuscript. YC contributed the plasmid, pIYC08, used in this study. KK performed the experimental work, analyzed the data and wrote the manuscript. All authors read and approved the final manuscript.

Acknowledgements

We thank Chalmers Foundation and the Knut and Alice Wallenberg Foundation for funding part of this work. We also acknowledge the Thailand Science and Technology Ministry for providing a stipend to KK.

Received: 8 September 2012 Accepted: 12 September 2012
Published: 25 September 2012

References

Bakker BM, Overkamp KM, van Maris AJA, Kötter P, Luttik MAH, van Dijken JP, Pronk JT (2001) Stoichiometry and compartmentation of NADH metabolism in *Saccharomyces cerevisiae*. FEMS Microbiol Rev 25(1):15–37

Bertani G (1951) Studies on lysogenesis I. J Bacteriol 62(3):293–300

Bligh EG, Dyer WJ (1959) A rapid method of total lipid extraction and purification. Can J Biochem Physiol 37(8):911–917

Bohmert K, Balbo I, Kopka J, Mittendorf V, Nawrath C, Poirier Y, Tischendorf G, Trethewey RN, Willmitzer L (2000) Transgenic *Arabidopsis* plants can accumulate polyhydroxybutyrate to up to 4% of their fresh weight. Planta 211(6):841–845

Boubekeur S, Camougrand N, Bunoust O, Rigoulet M, Guérin B (2001) Participation of acetaldehyde dehydrogenases in ethanol and pyruvate metabolism of the yeast Saccharomyces cerevisiae. Eur J Biochem 268(19):5057–5065

Breuer U, Terentiev Y, Kunze G, Babel W (2002) Yeasts as producers of polyhydroxyalkanoates: Genetic engineering of *Saccharomyces cerevisiae*. Macromol Bioscie 2(8):380–386

Carlson R, Fell D, Srienc F (2002) Metabolic pathway analysis of a recombinant yeast for rational strain development. Biotechnol Bioeng 79(2):121–134

Carlson R, Srienc F (2006) Effects of recombinant precursor pathway variations on poly[(R)-3-hydroxybutyrate] synthesis in. J Biotechnol 124(3):561–573

Chen Y, Siewers V, Nielsen J (2012) Profiling of cytosolic and peroxisomal acetyl-CoA metabolism in *Saccharomyces cerevisiae*. PLoS One 7(8):e42475

de Almeida A, Giordano AM, Nikel PI, Pettinari MJ (2010) Effects of aeration on the synthesis of poly(3-hydroxybutyrate) from glycerol and glucose in recombinant *Escherichia coli*. Appl Environ Microbiol 76(6):2036–2040

Dimster-Denk D, Rine J (1996) Transcriptional regulation of a sterol-biosynthetic enzyme by sterol levels in *Saccharomyces cerevisiae*. Mol Cell Biol 16(8):3981–3989

Gietz RD, Woods RA (2002) Transformation of yeast by lithium acetate/single-stranded carrier DNA/polyethylene glycol method. Methods Enzymol 350:87–96

Goffeau A (2000) Four years of post-genomic life with 6000 yeast genes. FEBS Lett 480(1):37–41

Görgens JF, van Zyl WH, Knoetze JH, Hahn-Hägerdal B (2005) Amino acid supplementation improves heterologous protein production by *Saccharomyces cerevisiae* in defined medium. Appl Microbiol Biotechnol 67(5):684–691

Hankermeyer CR, Tjeerdema RS (1999) Polyhydroxybutyrate: Plastic made and degraded by microorganisms. In: Ware GW (ed) Revi Environ Contam Toxicol, vol 159. Springer, New York, pp 1–24

Hartig A, Simon MM, Schuster T, Daugherty JR, Yoo HS, Cooper TG (1992) Differentially regulated malate synthase genes participate in carbon and nitrogen metabolism of *S. cerevisiae*. Nucleic Acids Res 20(21):5677–5686

Hiser L, Basson ME, Rine J (1994) ERG10 from *Saccharomyces cerevisiae* encodes acetoacetyl-CoA thiolase. J Biol Chem 269(50):31383–31389

Karr DB, Waters JK, Emerich DW (1983) Analysis of poly-beta-hydroxybutyrate in *Rhizobium japonicum* bacteroids by ion-exclusion high-pressure liquid chromatography and UV detection. Appl Environ Microbiol 46(6):1339–1344

Kunze M, Pracharoenwattana I, Smith SM, Hartig A (2006) A central role for the peroxisomal membrane in glyoxylate cycle function. Biochim Biophys Acta 1763(12):1441–1452

Leaf TA, Peterson MS, Stoup SK, Somers D, Srienc F (1996) *Saccharomyces cerevisiae* expressing bacterial polyhydroxybutyrate synthase produces poly-3-hydroxybutyrate. Microbiol 142(Pt 5):1169–1180

Lee YJ, Jang JW, Kim KJ, Maeng PJ (2011) TCA cycle-independent acetate metabolism via the glyoxylate cycle in *Saccharomyces cerevisiae*. Yeast 28(2):153–166

Mao Z, Shin H-D, Chen R (2009) A recombinant *E. coli* bioprocess for hyaluronan synthesis. Appl Microbiol Biotechnol 84(1):63–69

Marchesini S, Erard N, Glumoff T, Hiltunen JK, Poirier Y (2003) Modification of the monomer composition of polyhydroxyalkanoate synthesized in *Saccharomyces cerevisiae* expressing variants of the beta-oxidation-associated multifunctional enzyme. Appl Environ Microbiol 69(11):6495–6499

Melchiors M, Keul H, Höcker H (1994) Synthesis of highly isotactic poly[(R)-3-hydroxybutyrate] by ring-opening polymerization of (R, R, R)-4,8,12-trimethyl-1,5,9-trioxacyclododeca-2,6,10-trione. Macromol Rapid Commun 15(6):497–506

Nair LM, Werling JO (2009) Aerosol based detectors for the investigation of phospholipid hydrolysis in a pharmaceutical suspension formulation. J Pharm Biomed Anal 49(1):95–99

Nawrath C, Poirier Y, Somerville C (1994) Targeting of the polyhydroxybutyrate biosynthetic pathway to the plastids of *Arabidopsis thaliana* results in high levels of polymer accumulation. PNAS 91(26):12760–12764

Nikel PI, Pettinari MJ, Galvagno MA, Méndez BS (2006) Poly(3-hydroxybutyrate) synthesis by recombinant *Escherichia coli arcA* mutants in microaerobiosis. Appl Environ Microbioly 72(4):2614–2620

Nookaew I, Jewett MC, Meechai A, Thammarongtham C, Laoteng K, Cheevadhanarak S, Nielsen J, Bhumiratana S (2008) The genome-scale metabolic model iIN800 of *Saccharomyces cerevisiae* and its validation: a scaffold to query lipid metabolism. BMC Syst Biol 2:71

Partow S, Siewers V, Bjorn S, Nielsen J, Maury J (2010) Characterization of different promoters for designing a new expression vector in *Saccharomyces cerevisiae*. Yeast 27(11)):646–955

Peoples OP, Sinskey AJ (1989a) Poly-beta-hydroxybutyrate (PHB) biosynthesis in *Alcaligenes eutrophus* H16. Identification and characterization of the PHB polymerase gene (phbC). J Biol Chem 264(26):15298–15303

Peoples OP, Sinskey AJ (1989b) Poly-beta-hydroxybutyrate biosynthesis in *Alcaligenes eutrophus* H16, Characterization of the genes encoding beta-ketothiolase and acetoacetyl-CoA reductase. J Biol Chem 264(26):15293–15297

Petrasovits LA, Zhao L, McQualter RB, Snell KD, Somleva MN, Patterson NA, Nielsen LK, Brumbley SM (2012) Enhanced polyhydroxybutyrate production in transgenic sugarcane. Plant Biotechnol J 10(5):569–578

Poirier Y, Dennis D, Klomparens K, Nawrath C, Somerville C (1992) Perspectives on the production of polyhydroxyalkanoates in plants. FEMS Microbiol Lett 103(2–4):237–246

Reifenberger E, Freidel K, Ciriacy M (1995) Identification of novel HXT genes in *Saccharomyces cerevisiae* reveals the impact of individual hexose transporters on glycolytic flux. Mol Microbiol 16(1):157–167

Sambrook J, Russell DW (2006) The Inoue method for preparation and transformation of competent *E. Coli*: "Ultra-competent" cells. Cold Spring Harb Protoc (2):3944

Sedlak M, Ho NW (2004) Characterization of the effectiveness of hexose transporters for transporting xylose during glucose and xylose co-fermentation by a recombinant *Saccharomyces yeast*. Yeast 21(8):671–684

Shiba Y, Paradise EM, Kirby J, Ro DK, Keasling JD (2007) Engineering of the pyruvate dehydrogenase bypass in *Saccharomyces cerevisiae* for high-level production of isoprenoids. Metab Eng 9(2):160–168

Silversand C, Haux C (1997) Improved high-performance liquid chromatographic method for the separation and quantification of lipid classes: application to fish lipids. J Chromatogr B Biomed Sci Appl 703(1–2):7–14

Starai VJ, Gardner JG, Escalante-Semerena JC (2005) Residue Leu-641 of acetyl-CoA synthetase is critical for the acetylation of residue Lys-609 by the protein acetyltransferase enzyme of *Salmonella enterica*. J Biol Chem 280(28):26200–26205

Steinbuchel A, Hustede E, Liebergesell M, Pieper U, Timm A, Valentin H (1993) Molecular basis for biosynthesis and accumulation of polyhydroxyalkanoic acids in bacteria. FEMS Microbiol Rev 10(3–4):347–350

Steinbüchel A (2001) Perspectives for biotechnological production and utilization of biopolymers: Metabolic engineering of polyhydroxyalkanoate biosynthesis pathways as a successful example. Macromol Biosci 1(1):1–24

Steinbüchel A, Hein S (2001) Biochemical and molecular basis of microbial synthesis of polyhydroxyalkanoates in microorganisms. In: Babel W, Steinbüchel A (eds) Adv BiochemEng/Biotechnol, vol 71. Springer Berlin, Heidelberg, pp 81–123

Suzuki Y, Kurano M, Arai Y, Nakashita H, Doi Y, Usami R, Horikoshi K, Yamaguchi I (2002) Enzyme Inhibitors to increase poly-3-hydroxybutyrate production by transgenic tobacco. Biosci Biotechnol Biochem 66(12):2537–2542

Trotsenko YA, Belova LL (2000) Biosynthesis of poly(3-Hydroxybutyrate) and poly (3-hydroxybutyrate-co-3-hydroxyvalerate) and its regulation in bacteria. Microbiol 69(6):635–645

Tyo KE, Zhou H, Stephanopoulos GN (2006) High-throughput screen for poly-3-hydroxybutyrate in *Escherichia coli* and *Synechocystis sp*. Strain PCC6803. Appl Environ Microbiol 72(5):3412–3417

Uchino K, Saito T (2006) Thiolysis of poly(3-hydroxybutyrate) with polyhydroxyalkanoate synthase from *Ralstonia eutropha*. J Biochem 139(3):615–621

van Wegen RJ, Lee S-Y, Middelberg APJ (2001) Metabolic and kinetic analysis of poly(3-hydroxybutyrate) production by recombinant *Escherichia coli*. Biotechnol Bioeng 74(1):70–81

Zhang B, Carlson R, Srienc F (2006) Engineering the monomer composition of polyhydroxyalkanoates synthesized in *Saccharomyces cerevisiae*. Appl Environ Microbiol 72(1):536–543

doi:10.1186/2191-0855-2-52
Cite this article as: Kocharin *et al.*: Engineering of acetyl-CoA metabolism for the improved production of polyhydroxybutyrate in *Saccharomyces cerevisiae*. *AMB Express* 2012 **2**:52.

Paper IV

Specific growth rate and substrate dependent polyhydroxybutyrate production in *Saccharomyces cerevisiae*.

Kocharin K, Nielsen J. (Manuscript accepted for publication in AMB Express)

Specific growth rate and substrate dependent polyhydroxybutyrate production in *Saccharomyces cerevisiae*.

Kanokarn Kocharin, Jens Nielsen*

Department of Chemical and Biological Engineering
Chalmers University of Technology
SE-41296 Göteborg, Sweden

Manuscript in preparation for:
[AMB express]

Draft as of:
9 March 2013

*Corresponding author:
Department of Chemical and Biological Engineering
Chalmers University of Technology
Kemivägen 10
SE-412 96 Göteborg, Sweden

Telephone: +46 31 772 3804
Fax: +46 31 772 3801
Email: nielsenj@chalmers.se

Abstract

Production of the biopolymer polyhydroxybutyrate (PHB) in *Saccharomyces cerevisiae* starts at the end of exponential phase particularly when the specific growth rate is decreased due to the depletion of glucose in the medium. The specific growth rate and the type of carbon source (fermentable/non-fermentable) have been known to influence the cell physiology and hence affect the fermentability of *S. cerevisiae*. Since the production of PHB utilizes the cytosolic acetyl-CoA as a precursor, therefore *S. cerevisiae* employed in this study is a strain with the enhanced cytosolic acetyl-CoA supply. Growth and PHB production at different specific growth rates were evaluated on glucose, ethanol and the mixture of glucose and ethanol. Ethanol is the carbon source yielding higher PHB production compared to glucose since it can be directly used for cytosolic acetyl-CoA production and hence serves as a precursor for PHB production. According to the economical competence, the mixed substrate was shown for its capability to compensate between growth and PHB production and the highest volumetric productivity of PHB obtained at the dilution rate of 0.1 h^{-1} was 8.23 $mg/L \cdot h^{-1}$.

Key Words

Polyhydroxybutyrate, *Saccharomyces cerevisiae*, Specific growth rate

Introduction

Saccharomyces cerevisiae is a biotechnologically important microorganism. The well-established knowledge and the availability of genome data have led to its versatile use as a cell factory for many industrial products (Ostergaard et al. 2000). Process optimization for production of various industrial products such as biofuels, fine and bulk chemicals in *S. cerevisiae* has been studied by several research groups (de Jong et al. 2012; Hong and Nielsen 2012; Nevoigt 2008; Ostergaard et al. 2000; Steen et al. 2008). This reveals the physiological adaptability of *S. cerevisiae* to a highly variable environment. According to a respiratory-fermentative metabolism in *S. cerevisiae*, the type (fermentable/non fermentable) and concentration of carbon source as well as the availability of oxygen are the important factors driving the metabolic pattern in the yeast. In order to improve productivity for any products in *S. cerevisiae*, it is substantial to know the relationship between growth and product formation.

The bacterial PHB biosynthesis pathway has previously been introduced into the yeast's genome and *S. cerevisiae* has been evaluated as a cell factory for PHB production (Breuer et al. 2002; Dimster-Denk and Rine 1996; Leaf et al. 1996; Marchesini et al. 2003; Zhang et al. 2006). The production of PHB in *S. cerevisiae* starts at the end of the exponential growth phase specifically when glucose is depleted from the medium. (Carlson et al. 2002; Kocharin et al. 2012). From our earlier work, we demonstrated that PHB production can be improved by co-transformation of the plasmid containing the PHB biosynthesis pathway with an acetyl-coenzyme A (acetyl-CoA) boost plasmid designated to improve the availability of cytoplasmic acetyl-CoA (Kocharin et al. 2012). However, a difference in the productivity when the production was scaled up from shake flask to bioreactor cultivation was observed. We suspected that the higher growth rate obtained in the bioreactor has an effect on PHB

production. It is known that the specific growth rate influences the physiology of *S. cerevisiae* hence affecting the fermentative capacity, TCA activity and other metabolic activities (Blank and Sauer 2004; Frick and Wittmann 2005; Van Hoek et al. 1998). Therefore, the difference in specific growth rate is hypothesized to be responsible for the lower PHB production in the bioreactor cultivation. In the present study, we employ a chemostat cultivation system to investigate PHB production at different dilution rates (which correspond to different specific growth rates). Furthermore, we assess PHB production in *S. cerevisiae* grown on the different carbon sources, glucose, ethanol and a mixture of glucose and ethanol.

Materials and Methods

Strains and pre-culture conditions

S. cerevisiae harboring the acetyl-CoA boost plasmid and the PHB plasmid (SCKK006) was used in this study. The acetyl-CoA plasmid contained four genes; alcohol dehydrogenase (*ADH2*) and acetaldehyde dehydrogenase (*ALD6*), acetyl-CoA C-acetyltransferase (*ERG10*) and acetyl-CoA synthetase (acs^{L641P}) from *Streptococcus mutans*. The details in the acetyl-CoA boost plasmid are described by Chen and co-workers (Chen et al. 2013). The PHB plasmid (pKK01) contained three PHB genes from *Ralstonia eutropha*, *PhaA* (β-ketothiolase), *PhaB* (acetoacetyl-CoA reductase) and *PhaC* (polyhydroxyalkanoate synthase). All of the heterologous genes were codon optimized for better expression in *S. cerevisiae*. The details on strain construction have been described previously (Kocharin et al. 2012).

The pre-cultures for bioreactor cultivations were prepared by inoculation of 5 mL of a defined minimal medium in a 14 mL culture tube with a single colony and grown at 30ºC and

180 rpm in an orbital shaking incubator. After 15 h, the culture was transferred into 50 mL of defined minimal medium in a 500 mL baffled flask and grown at 30ºC with 180 rpm in an orbital shaking incubator. The minimal medium for pre-culture cultivations had the same composition as the medium used for bioreactor cultivation.

Chemostat bioreactor cultivation

PHB production was evaluated in defined minimal media (Verduyn et al. 1992) prepared as follows (per liter): $(NH_4)_2SO_4$, 5 g;KH_2PO_4, 3 g; $MgSO_4 \cdot 7H_2O$, 0.5 g; trace metal solution, 1 mL; and vitamin solution,1 mL, with an initial pH of 6.5. Glucose was autoclaved separately from the minimal medium and later added to the media at the concentration of 20 g/L. The trace metal solution consisted of the following (per liter): EDTA (sodium salt) 15 g; $ZnSO_4 \cdot 7H_2O$, 0.45 g; $MnCl_2 \cdot 2H_2O$, 1 g; $CoCl_2 \cdot 6H_2O$, 0.3 g; $CuSO_4 \cdot 5H_2O$, 0.3 g; $Na_2MoO_4 \cdot 2H_2O$, 0.4 g; $CaCl_2 \cdot 2H_2O$, 0.45 g; $FeSO_4 \cdot 7H_2O$, 0.3 g; H_3BO_3, 0.1 g and KI, 0.1 g. The pH of the trace metal solution was adjusted to 4.0 with 2 M NaOH. The vitamin solution contained (per liter): biotin, 0.05 g; ρ-amino benzoic acid, 0.2 g; nicotinic acid, 1 g; Ca-pantothenate, 1 g; pyridoxine-HCl, 1 g; thiamine-HCl, 1 g and myo-inositol, 25 g. The pH of the vitamin solution was adjusted to pH 6.5 prior filter sterilization.

The bioreactor was inoculated with an amount of pre-culture that resulted in a final OD_{600} of 0.02. When the glucose and ethanol during batch cultivation was almost completely consumed, the feeding systems for the chemostat operations were started. The aerobic chemostat was performed in 1.0 L stirrer-pro vessels (DasGip, Jülich, Germany) with a working volume of 0.5 L. The temperature was controlled at 30°C using a bioBlock integrated heating and cooling thermo well. Agitation was maintained at 600 rpm using an

overhead drive stirrer with one Rushton impeller. The air flow rate was kept at 1 vvm. The pH was maintained constant at 5.0 by the automatic addition of 2 M KOH. Dissolved oxygen was monitored and maintained above 30% saturation. All the feed media had the same composition and were prepared as described above except for the carbon source. The carbon sources used were 100% glucose, 100% ethanol and a mixture of glucose and ethanol at the ratio of 1:2. The carbon sources in the feed medium were prepared based on the C-molar concentration of 20 g/L glucose (0.666 Cmol/L) as in the medium used during batch cultivation. Therefore, feed media with 15.32 g/L ethanol, and a mixture of 6.35 g/L glucose and 10.21 g/L of ethanol were prepared yielding a final carbon concentration of 0.666 Cmol/L. To obtain a dilution rate of 0.05 h^{-1}, 0.1 h^{-1}, 0.15 h^{-1} and 0.2 h^{-1}, the inlet medium was fed at 25 ml/h, 50 mL/h, 75 mL/h and 100 mL/h respectively. Samples were taken when the fermentation reached the steady state, defined by constant values of carbon dioxide transfer rate (CTR), oxygen transfer rate (OTR) and biomass concentration.

Cell mass determination

Culture samples of 10 mL volume were centrifuged at 5,000 rpm and 4°C for 5 min and the pellets were washed once with distilled water and centrifuged at 14,000 g for 1 min. The recovered cell pellet was immediately frozen by immersion in liquid nitrogen followed by lyophilization under vacuum (Christ Alpha 2-4 LSC, Shropshire, UK). The dry cell weight was determined and the pellet kept at 4°C for further analysis.

Metabolite analysis

Metabolites including glucose, ethanol, glycerol, and acetate were quantified in the culture supernatant using an Ultimate 3000 HPLC (Dionex, Sunnyvale, CA, USA) equipped with an Aminex HPX 87H ion exclusion column (300 mm x 7.8 mm, Bio-Rad Laboratories,

Hercules, CA, USA) which was operated at 45°C and a flow rate of 0.6 mL/min of 5 mM H_2SO_4 using a refractive index detector and UV detector for analysis of sugars and organic acids, respectively.

PHB was analyzed as described previously (Karr et al. 1983; Tyo et al. 2006). 10-20 mg of dried cells were weighed and boiled in 1 mL of concentrated sulfuric acid for 60 min and then diluted with 4 mL of 14 mM H_2SO_4. Samples were centrifuged (15 min, 16,000 × g) to remove cell debris, and the supernatant was analyzed using an Ultimate 3000 HPLC (Dionex) equipped with an Aminex HPX-87H ion exclusion column (300 × 7.8 mm; Bio-Rad Laboratories) and UV detector. Commercially available PHB (Sigma-Aldrich, St. Louis, MO), processed in parallel with the samples, was used as a standard. The HPLC was operated at 60°C and a flow rate of 0.6 mL/min of 5 mM H_2SO_4.

Results

PHB production at different dilution rates.

In this study, we employed a chemostat cultivation technique to investigate PHB production at different specific growth rates of an engineered *S. cerevisiae* strain, SCKK006, in which genes from the ethanol degradation pathway were overexpressed in order to enhance the supply for acetyl-CoA used as a precursor for PHB production. Besides, we also investigated the production of PHB when the engineered strain was grown on different carbon sources. In batch cultures, the maximum specific growth rate of SCKK006 on glucose in a defined minimal medium with 20 g/L glucose as carbon source was 0.34 h^{-1}. Kinetic parameters and yields during batch cultivation are reported in Table 1. The ethanol yield and glycerol yield on glucose were 0.2293 Cmol/Cmol and 0.0241 Cmol/Cmol, respectively. Detectable amounts of pyruvate, succinate and acetate were observed during the batch cultivation. When

the ethanol was almost completely depleted from the medium (observed by a drop of the carbon dioxide profile measured from the exhaust gas via a gas analyzer), the chemostat cultivation was started.

The chemostat cultivation was operated at different dilution rates ranging from 0.05 h^{-1} to 0.2 h^{-1} with the feed medium containing different carbon sources. The physiological parameters are reported in Table 2. When the feed medium contained glucose as the sole carbon source, ethanol was detected when the dilution rate was higher than 0.1 h^{-1}. This reveals a respiro-fermentative metabolism of *S. cerevisiae* grown at high dilution rate or high sugar content even in aerobic cultivation with excess oxygen (Hanegraaf et al. 2000). At a dilution rate higher than 0.15 h^{-1}, a very small amount of glycerol (<10 mg/L) was observed. The highest biomass yield, 0.57 Cmol/Cmol was found at a dilution rate of 0.1 h^{-1}. At dilution rates higher than 0.1 h^{-1}, the biomass yield tended to decrease. The highest PHB yield was also observed at a dilution rate of 0.1 h^{-1}, 3.67 Cmmol/Cmol substrate.

When the feed medium contained ethanol as the sole carbon source, the highest biomass yield and PHB yield on substrate, 0.45 Cmol/Cmol and 8.5 Cmmol/Cmol, was observed when the chemostat was operated at the dilution rate of 0.05 h^{-1}. The biomass yield and the PHB yield tended to decrease when increasing the dilution rate. At dilution rates higher than 0.05 h^{-1}, ethanol accumulated and progressively increased in the medium when the dilution rate was increased. When the chemostat was operated at 0.15 h^{-1}, after 5 residence time, the amount of ethanol accumulated in the medium almost reached the level of the ethanol in the feed. When the chemostat was operated at a dilution rate of 0.2 h^{-1}, the biomass decreased and become zero or washout within 3 resident times.

When glucose and ethanol were used as substrates, the biomass yield and PHB yield on the mixed-substrate in the feed medium was calculated based on the C-moles of consumed substrate. The maximum biomass yield, 0.48 ± 0.02 Cmol/Cmol, and the maximum PHB

yield, 9.97 ± 0.07 Cmmol/Cmol, were obtained when the mixed-substrate was fed at 0.05 h^{-1}. Moreover, no accumulation of ethanol was observed when the chemostat was operated at 0.05 h^{-1} while 0.16-0.28 Cmol/L of ethanol were observed when the chemostat was operated at dilution rates higher than 0.05 h^{-1}. The amount of accumulated ethanol on the mixed-substrate was similar to the amount of ethanol accumulated in the medium when the chemostat was fed with ethanol alone before the washout occurred The biomass yield on substrate was substantially decreased when the dilution rate was increased on all substrates used in this study.

PHB production in *S. cerevisiae* grown on different carbon sources

Comparing substrate utilization at the same dilution rate, glucose showed the highest biomass yield on substrate in all dilution rates investigated in this study, followed by the mixed-substrate and ethanol, respectively. The maximum PHB content, 18.34 mg/gDW, was obtained when the mixed substrate was used in the feed at a dilution rate of 0.05 h^{-1}. Comparing either glucose or ethanol as sole carbon source, ethanol alone resulted in a ~3 times higher PHB yield when the chemostat was operated at D= 0.05 h^{-1}although it led to a lower biomass yield on substrate. When the feed medium contained glucose and ethanol as carbon sources, the highest PHB yield was obtained compared to using a single carbon source as a substrate. Comparing the overall volumetric productivities in Figure 1, the mixed-substrate at a dilution rate of 0.1 h^{-1} revealed the highest volumetric productivity, 8.23 mg/L·h^{-1}. When ethanol was produced during growth on glucose or was accumulated when using ethanol or the mixed-substrate containing ethanol as a feed medium, the volumetric productivity could not improve. However, when glucose was fed at a dilution rate of 0.2 h^{-1}, a slight increased in the volumetric productivity of PHB was observed.

Discussion

In *S. cerevisiae*, high specific growth rate and high sugar concentration trigger the production of ethanol, even during a fully aerobic cultivation. In this study, when the chemostat was operated at dilution rates of 0.15 h^{-1} and 0.2 h^{-1}, ethanol was produced in the medium as an evidence of a respiro-fermentative metabolism of *S. cerevisiae*, which can ferment glucose at a high dilution rate (Duntze et al. 1969; Hanegraaf et al. 2000; Maaheimo et al. 2001). When using glucose as a carbon source in the feed medium, a high growth rate (corresponding to a high dilution rate) reduces the flux distribution to the pentose phosphate pathway, which might lower the NADPH concentration (Frick and Wittmann 2005). Since NADPH is required in the PHB biosynthesis pathway, higher specific growth rates might influence the availability of NADPH and thus substantially lower PHB production. Moreover, the production of PHB consumes only the cytosolic acetyl-CoA which is in this case produced mainly from the overexpression of the ethanol degradation pathway (Figure 2a). Therefore, the PHB yield on glucose was lower than the PHB yield on ethanol. Besides, a small amount of glycerol was produced in order to maintain the redox balance when ethanol was produced from glucose feeding at higher dilution rates. In this study, a lower biomass yield on ethanol was observed compared to the biomass yield on glucose at all dilution rates. However, the PHB yield on ethanol was higher compared with using only glucose in the feed medium. This might be due to the fact that ethanol in the feed replaces pyruvate as the direct source for cytosolic acetyl-CoA production hence resulting in a higher Y_{sPHB} compared to glucose (Figure 2b). When *S. cerevisiae* is grown on ethanol, the synthesis of biomass and the TCA intermediates requires the activity of the glyoxylate and gluconeogenesis pathway (de Jong-Gubbels et al. 1995; Maaheimo et al. 2001) and this might result in the lower biomass yield compared to glucose. When *S. cerevisiae* is grown in a mixed-substrate, glucose and ethanol,

glucose phosphorylation still occurs while malate synthase, which convert glyoxylate to malate in the glyoxylate cycle, replaces pyruvate carboxylase in the synthesis of TCA intermediates and ethanol serves as the main source for cytosolic acetyl-CoA production (de Jong-Gubbels et al. 1995) (Figure 2c). Therefore, the mixed-substrate used in this study resulted in higher biomass and PHB yields on substrate compared to the use of a single substrate in the feed medium. However, when the mixed-substrate was fed at a dilution rate higher than 0.05 h^{-1}, ethanol started to accumulate ranging from 0.16 Cmol/L to 0.2 Cmol/L. The accumulated ethanol at higher dilution rates affected the ratio of glucose and ethanol in the bioreactor, thus influencing the overall regulation of the central carbon metabolism (de Jong-Gubbels et al. 1995) and eventually led to the washout. In conclusion, ethanol is the better carbon source for PHB production in yeast compared to glucose since it can be directly used for acetyl-CoA production and hence served as a precursor for PHB production. In terms of productivity and economic feasibility, to compromise between growth of *S. cerevisiae* and PHB production, feeding of a mixed-substrate at the appropriate ratio between glucose and ethanol where no ethanol would accumulate at the dilution rate of 0.1 h^{-1} would result in a maximum PHB production.

Acknowledgements

We thank Chalmers Foundation and the Knut and Alice Wallenberg Foundation for funding part of this work. We also acknowledge the Thailand Science and Technology Ministry for providing a stipend to KK.

Competing interest

The authors declare that they have no competing interest.

References

Blank LM, Sauer U (2004) TCA cycle activity in *Saccharomyces cerevisiae* is a function of the environmentally determined specific growth and glucose uptake rates. Microbiol 150(Pt 4):1085-93

Breuer U, Terentiev Y, Kunze G, Babel W (2002) Yeasts as producers of polyhydroxyalkanoates: Genetic engineering of *Saccharomyces cerevisiae*. Macromol Biosci 2(8):380-386

Carlson R, Fell D, Srienc F (2002) Metabolic pathway analysis of a recombinant yeast for rational strain development. Biotechnol Bioeng 79(2):121-34

Chen Y, Daviet L, Schalk M, Siewers V, Nielsen J (2013) Establishing a platform cell factory through engineering of yeast acetyl-CoA metabolism. Metab Eng 15(0):48-54

de Jong-Gubbels P, Vanrolleghem P, Heijnen S, van Dijken JP, Pronk JT (1995) Regulation of carbon metabolism in chemostat cultures of *Saccharomyces cerevisiae* grown on mixtures of glucose and ethanol. Yeast 11(5):407-18

de Jong B, Siewers V, Nielsen J (2012) Systems biology of yeast: enabling technology for development of cell factories for production of advanced biofuels. Curr Opin Biotechnol 23(4):624-30

Dimster-Denk D, Rine J (1996) Transcriptional regulation of a sterol-biosynthetic enzyme by sterol levels in *Saccharomyces cerevisiae*. Mol Cell Biol 16(8):3981-9

Duntze W, Neumann D, Gancedo JM, Atzpodien W, Holzer H (1969) Studies on the regulation and localization of the glyoxylate cycle enzymes in S*accharomyces cerevisiae*. Eur J Biochem / FEBS 10(1):83-9

Frick O, Wittmann C (2005) Characterization of the metabolic shift between oxidative and fermentative growth in *Saccharomyces cerevisiae* by comparative ^{13}C flux analysis. Microb Cell Fact 4(1):30

Hanegraaf PP, Stouthamer AH, Kooijman SA (2000) A mathematical model for yeast respiro-fermentative physiology. Yeast 16(5):423-37

Hong KK, Nielsen J (2012) Metabolic engineering of *Saccharomyces cerevisiae*: a key cell factory platform for future biorefineries. Cell Mol Life Sci : 69(16):2671-90

Karr DB, Waters JK, Emerich DW (1983) Analysis of poly-β-hydroxybutyrate in *Rhizobium japonicum* bacteroids by ion-exclusion high-pressure liquid chromatography and UV detection. Appl Environ Microbiol 46(6):1339-44

Kocharin K, Chen Y, Siewers V, Nielsen J (2012) Engineering of acetyl-CoA metabolism for the improved production of polyhydroxybutyrate in *Saccharomyces cerevisiae*. AMB Express 2(1):52

Leaf TA, Peterson MS, Stoup SK, Somers D, Srienc F (1996) *Saccharomyces cerevisiae* expressing bacterial polyhydroxybutyrate synthase produces poly-3-hydroxybutyrate. Microbiol 142 (Pt 5):1169-80

Maaheimo H, Fiaux J, Cakar ZP, Bailey JE, Sauer U, Szyperski T (2001) Central carbon metabolism of *Saccharomyces cerevisiae* explored by biosynthetic fractional ^{13}C labeling of common amino acids. Eur J Biochem / FEBS 268(8):2464-79

Marchesini S, Erard N, Glumoff T, Hiltunen JK, Poirier Y (2003) Modification of the monomer composition of polyhydroxyalkanoate synthesized in *Saccharomyces cerevisiae* expressing variants of the β-oxidation-associated multifunctional enzyme. Appl Environ Microbiol 69(11):6495-9

Nevoigt E (2008) Progress in metabolic engineering of *Saccharomyces cerevisiae*. Microbiol Mol Biol Rev 72(3):379-412

Ostergaard S, Olsson L, Nielsen J (2000) Metabolic Engineering of *Saccharomyces cerevisiae*. Microbiol Mol Biol Rev 64(1):34-50

Steen E, Chan R, Prasad N, Myers S, Petzold C, Redding A, Ouellet M, Keasling J (2008) Metabolic engineering of *Saccharomyces cerevisiae* for the production of n-butanol. Microb Cell Fact 7(1):36

Tyo KE, Zhou H, Stephanopoulos GN (2006) High-throughput screen for poly-3-hydroxybutyrate in *Escherichia coli* and *Synechocystis sp.* strain PCC6803. Appl Environ Microbiol 72(5):3412-3417

Van Hoek P, Van Dijken JP, Pronk JT (1998) Effect of specific growth rate on fermentative capacity of baker's yeast. Appl Environ Microbiol 64(11):4226-33

Verduyn C, Postma E, Scheffers WA, Vandijken JP (1992) Effect of benzoic-acid on metabolic fluxes in yeasts - a continuous-culture study on the regulation of respiration and alcoholic fermentation. Yeast 8(7):501-517

Zhang B, Carlson R, Srienc F (2006) Engineering the monomer composition of polyhydroxyalkanoates synthesized in *Saccharomyces cerevisiae*. Appl Environ Microbiol 72(1):536-543

Tables

Table 1: Yields and kinetic parameters obtained from batch cultivations.

	μ	r_s	Y_{sx}	Y_{sEtOH}	Y_{sGly}	Y_{sPyr}	Y_{sAce}	Y_{sSuc}
	h^{-1}	mmol/ gDW·h^{-1}	g/Cmol	Cmol / Cmol	Cmol / Cmol	Cmol / Cmol	Cmol / Cmol	Cmol / Cmol
Mean	0.34	3.79	1.84	0.2293	0.0241	0.0033	0.0064	0.0033
SD	0.01	0.52	0.26	0.01	0.00	0	0	0

The values were calculated from at least triplicate fermentations ($n \geq 3$) and are represented as mean ± SD.

μ = specific growth rate; r_s = specific substrate uptake rate; Y_{sx} = biomass yield on substrate; Y_{sEtOH} = ethanol yield on substrate; Y_{sGly} = glycerol yield on substrate; Y_{sPyr} = pyruvate yield on substrate; Y_{sAce} = acetate yield on substrate; $Y_{s\,Suc}$ = succinate yield on substrate.

Table 2: Yields and kinetic parameters obtained during chemostat cultivations.

Feeding component	Dilution rate	Y_{sx}	Y_{sEtOH}	Y_{sPHB}	Ethanol accumulation	Y_{xPHB}
	h^{-1}	Cmol/ Cmol	Cmol/C mol	Cmmol/Cmol	Cmol/L	mg/gDW
Glucose	0.05	0.51 ± 0.01	-	2.51 ± 0.07	0	4.33 ± 0.19
	0.10	0.57 ± 0	-	3.67 ± 0	0	5.59 ± 0
	0.15	0.36 ± 0.02	0.02 ± 0	2.44 ± 0	-	5.94 ± 0.64
	0.20	0.29 ± 0	0.1 ± 0	1.92 ± 0	-	5.59 ± 0.23
Ethanol	0.05	0.45 ± 0.01	0	8.50 ± 0.23	0	16.55 ± 0.02
	0.10	0.37 ± 0	-	4.94 ± 0.58	0.0964 ± 0	13.49 ± 0
	0.15	0.12 ± 0.01	-	0.46 ± 0.05	0.2364 ± 0	5.30 ± 0.31
Glucose:Ethanol (1:2)	0.05	0.48 ± 0.02	0	9.97 ± 0.07	0	18.34 ± 0.53
	0.10	0.38 ± 0	-	7.41 ± 0	0.2012	12.41 ± 0
	0.15	0.30 ± 0	-	2.57 ± 0.1	0.1637	7.50 ± 0.19
	0.20	0.22 ± 0	-	1.13 ± 0	0.2769	4.56 ± 0

The values were calculated from duplicate fermentations and are represented as mean ± SD. The formula for biomass used in this calculation is $CH_{1.8}O_{0.5}N_{0.2}$. Y_{sx} = biomass yield on substrate, Y_{sEtOH} = ethanol yield on substrate, Y_{sPHB} = PHB yield on substrate, Y_{xPHB} = PHB yield per biomass

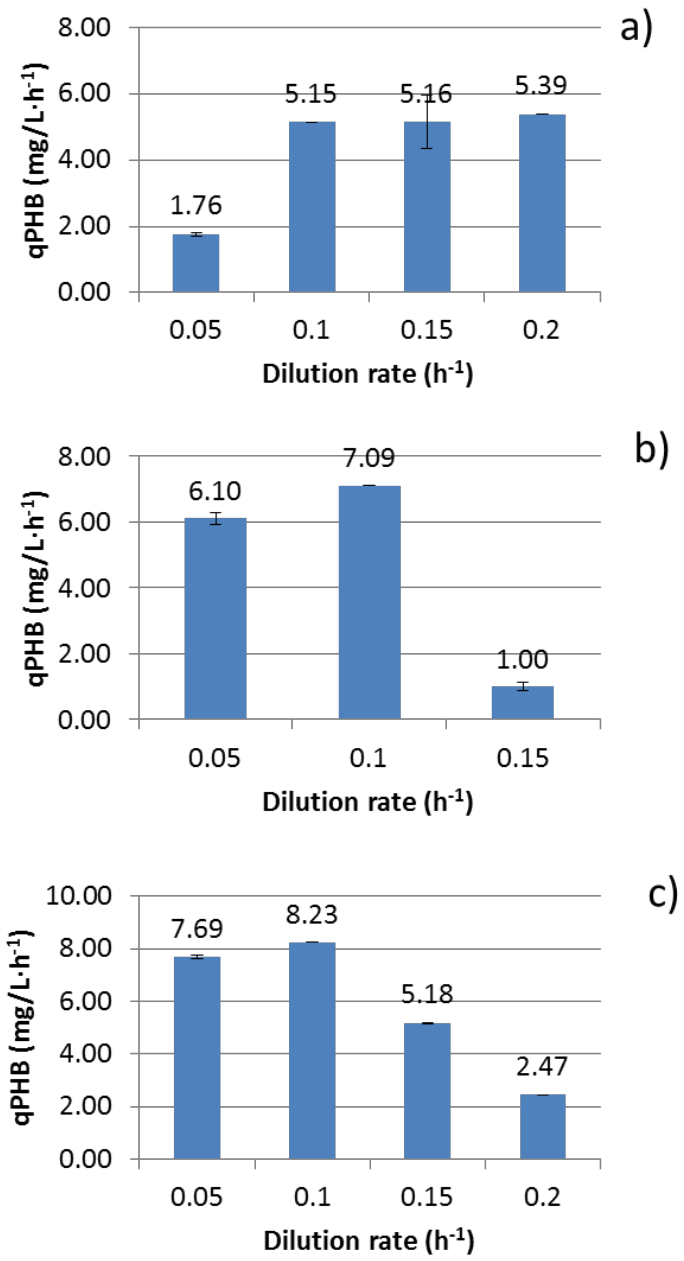

Figure 1:. PHB productivities of recombinant *S. cerevisiae* grown on different substrates at different dilution rates from the chemostat cultivation. a) Glucose, b) Ethanol, c) Mixed-substrate

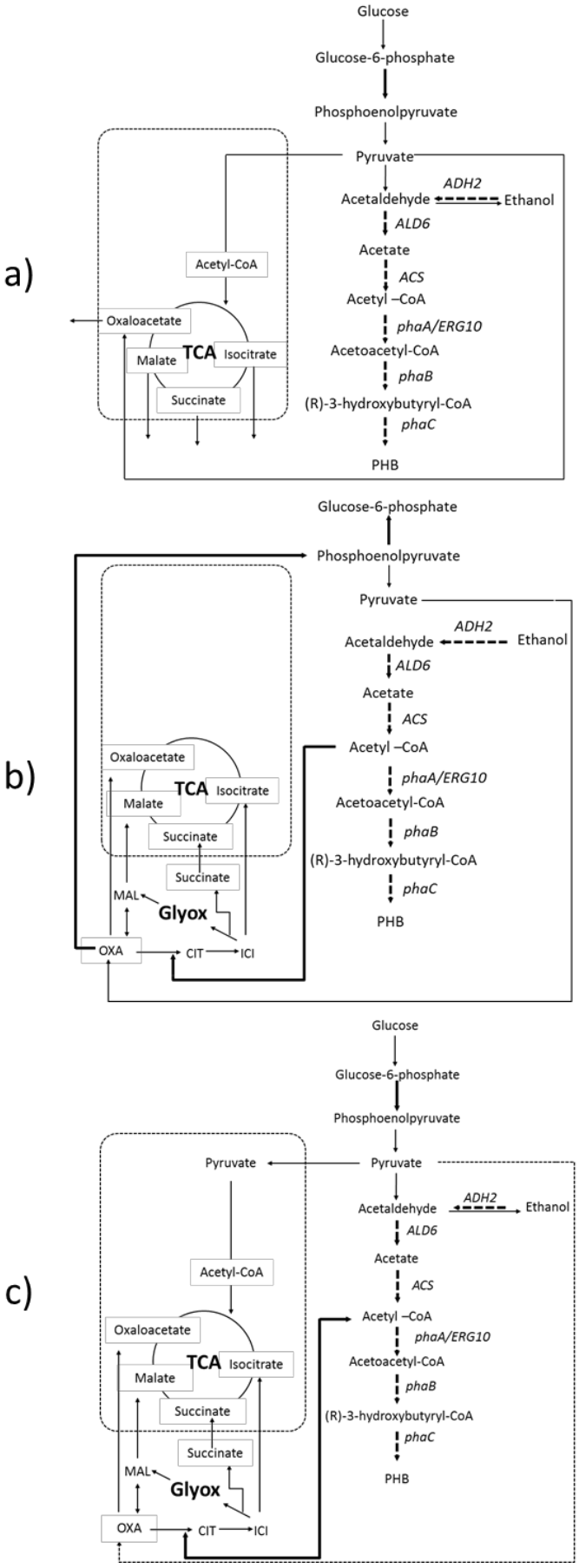

Figure 2: Central carbon metabolism of PHB producing *S. cerevisiae* grown on different substrates. a) Glucose, b) Ethanol and c) Mixed-substrate of glucose and ethanol.

ADH2 = alcohol dehydrogenase; *ALD6* = aldehyde dehydrogenase; *ACS* = acetyl-CoA synthetase (acs^{L641P}); *ERG10* = acetyl-CoA C-acetyltransferase; *PhaA* (β-ketothiolase); *PhaB* (acetoacetyl-CoA reductase); *PhaC* (polyhydroxyalkanoate synthase)

ICI = isocitrate; CIT = citrate: OXA = oxaloacetate; MAL = malate; Glyox = glyoxylate

Paper V

Improved polyhydroxybutyrate production by *Saccharomyces cerevisiae* through the use of the phosphoketolase pathway.

Kocharin K, Siewers V, Nielsen J.

Biotechnol Bioeng. 2013

[Epub ahead of print]

Improved polyhydroxybutyrate production by *Saccharomyces cerevisiae* through the use of the phosphoketolase pathway

Kanokarn Kocharin, Verena Siewers, Jens Nielsen*

Department of Chemical and Biological Engineering
Chalmers University of Technology
SE-41296 Göteborg, Sweden

Manuscript in preparation for:
Biotechnology and Bioengineering

Draft as of:
19 February 2013

*Corresponding author:
Department of Chemical and Biological Engineering
Chalmers University of Technology
Kemivägen 10
SE-412 96 Göteborg, Sweden

Telephone: +46 31 772 3804
Fax: +46 31 772 3801
email: nielsenj@chalmers.se

Abstract

The metabolic pathways of the central carbon metabolism in *Saccharomyces cerevisiae* are well studied and consequently *S. cerevisiae* has been widely evaluated as a cell factory for many industrial biological products. In this study, we investigated the effect of engineering the supply of precursor, acetyl-CoA, and cofactor, NADPH, on the biosynthesis of the bacterial biopolymer polyhydroxybutyrate (PHB), in *S. cerevisiae*. Supply of acetyl-CoA was engineered by overexpression of genes from the ethanol degradation pathway or by heterologous expression of the phophoketolase pathway from *Aspergillus nidulans*. Both strategies improved the production of PHB. Integration of *gapN* encoding $NADP^+$ dependent glyceraldehyde-3-phosphate dehydrogenase from *Streptococcus mutans* into the genome enabled an increased supply of NADPH resulting in a decrease in glycerol production and increased production of PHB. The strategy that resulted in the highest PHB production after 100 h was with a strain harboring the phosphoketolase pathway to supply acetyl-CoA without the need of increased NADPH production by *gapN* integration. The results from this study imply that during the exponential growth on glucose, the biosynthesis of PHB in *S. cerevisiae* is likely to be limited by the supply of NADPH whereas supply of acetyl-CoA as precursor plays a more important role in the improvement of PHB production during growth on ethanol.

Key Words

Polyhydroxybutyrate, acetyl-CoA, NADPH, phosphoketolase pathway

Introduction

Energy and carbon metabolism are highly interconnected, and the medium composition and the availability of oxygen during cultivation therefore impact the physiology and overall metabolism of most cells. In *Saccharomyces cerevisiae*, a widely used cell factory for production of fuels, chemicals and materials, glucose is metabolized via the Embden Meyerhof Parnas (EMP) pathway or the pentose phosphate (PP) pathway, which split at the glucose-6-phosphate branch point. The split ratios towards the PP pathway range from 2 to 44.2 moles per 100 moles of consumed glucose depending on the cellular state and culture conditions (Bruinenberg et al. 1983; Gombert et al. 2001; van Winden et al. 2005). However, almost 90% of the carbon that enters the PP pathway re-enters the lower glycolytic pathway (Gombert et al. 2001). In Crabtree negative yeasts like *Pichia stipitis,* the flux through the PP pathway is generally higher than in Crabtree positive yeasts like *S. cerevisiae* (Bruinenberg et al. 1983; Siso et al. 1996; Papini et al. 2012). Due to the relatively low catabolic fluxes through this pathway in Crabtree positive yeasts, the PP pathway is believed to be used mainly for NADPH production but not for biomass production or catabolic reactions (Blank and Sauer 2004). The major sources of cytosolic NADPH production in *S. cerevisiae* grown on glucose has been attributed to the glucose-6-phosphate dehydrogenase reaction in the PP pathway, with the cytosolic aldehyde dehydrogenase (Ald6p) as a secondary source (Grabowska and Chelstowska 2003), and the flux through the PP pathway is therefore directly related to NADPH production. The availability of NADPH influences the production of several biotechnologically relevant compounds such as α-santalene (Scalcinati et al. 2012) and polyhydroxybutyrate (PHB) (Carlson and Srienc 2006; Dawes and Senior 1973), and it is

therefore often necessary to engineer the central carbon metabolism such that there is increased supply of NADPH.

In this study, the PHB biosynthesis pathway (Figure 1) including β-ketothiolase (PhaA), NADPH-dependent acetoacetyl-CoA reductase (PhaB) and polyhydroxyalkanoate synthase (PhaC) was introduced into *S. cerevisiae*. In the PHB biosynthesis pathway, thiolase activity is mediated through the AcCoA/CoASH ratio and the acetoacetyl-CoA reductase activity is mediated by the NADPH/$NADP^+$ ratio, and these two ratios are therefore considered as the major regulators influencing PHB production in a native PHB producer, *Ralstonia eutropha* (Leaf and Srienc 1998). Earlier, a mathematical model of recombinant *S. cerevisiae* expressing the PHB pathway from *R. eutropha* was constructed by Carlson et al. in order to investigate the possible modes of PHB production in *S. cerevisiae* (Carlson et al. 2002). From analysis of the model it was suggested that the theoretical yield of PHB in *S. cerevisiae* can be improved by including a combination of ATP citrate-lyase to supply acetyl-CoA and a transhydrogenase reaction to catalyze the interconversion of NADH and $NADP^+$ to NAD^+ and NADPH (Carlson et al. 2002).

Increasing the production of cytosolic acetyl-CoA by over-expressing enzymes of the pathway from ethanol to acetyl-CoA was recently shown to improve PHB production in *S. cerevisiae* (Kocharin et al. 2012). An alternative route for providing cytosolic acetyl-CoA through expression of the phosphoketolase pathway from *Aspergillus nidulans* was recently shown to be able to shunt carbon through the PP pathway and contribute to acetyl-CoA production in *S. cerevisiae* (Papini et al. 2012). This strategy is attractive as it involves both increased production of NADPH and possible increased supply of cytosolic acetyl-CoA, and in this study we therefore investigated the effect on PHB production of heterologous expression of xylulose-5-phosphate phosphoketolase (XpkA) (EC: 4.1.2.9) and acetate kinase

(Ack) (EC: 2.7.2.1) from *A. nidulans* and an acetyl-CoA synthetase variant (Acs^{L641P}) from *Salmonella enterica* on a single episomal plasmid.

We also evaluated the combination of our earlier described strategy for increased cytosolic acetyl-CoA supply with engineering of the central carbon metabolism to increase production of NADPH. For this we introduced a non-phosphorylating, $NADP^+$ -dependent glyceraldehyde-3-phosphate dehydrogenase encoded by *gapN* from *Streptococcus mutans,* which has earlier been shown to increase ethanol yields on glucose under anaerobic conditions and at the same time reduce glycerol production (Bro et al. 2006). Finally, we also combined the two strategies for improving PHB production in *S. cerevisiae*.

Materials and Methods

Strains, media, and culture conditions

Plasmids were maintained and propagated in *E. coli* DH5 α . The preparation of competent *E. coli* cells and their transformation were performed according to standard protocols (Sambrook and Russell 2006). Luria-Bertani (LB) medium was used for routine culturing with 80 mg/L ampicillin. *S. cerevisiae* strain CEN.PK113-11C (*MAT*a *SUC2 MAL2-8*^{c} *ura3-52 his3-*Δ*1;* provided by P. Kötter, University of Frankfurt, Germany) was used as the background strain for evaluation of the PHB pathway. Engineered yeast strains were selected on synthetic dextrose (SD) medium, prepared with 6.7 g/L yeast nitrogen base without amino acids (YNB-AA) (Formedium, Hunstanton, UK) and 20 g/L glucose with complete supplement mixture (CSM) lacking uracil and/or histidine (Formedium) where appropriate.

Plasmid construction and yeast transformation.

Plasmid pIYC08 carries genes from the ethanol degradation pathway aiming for increased supply of cytosolic acetyl-CoA. Briefly, pIYC08 contains genes for alcohol dehydrogenase (*ADH2*) under control of the P_{HXT7} promoter, acetaldehyde dehydrogenase (*ALD6*) under control of the P_{PGK1} promoter while acetyl-CoA acetyltransferase (*ERG10*) and acetyl-CoA synthetase variant (acs^{L641P}) from *Salmonella enterica* are controlled by the P_{TEF1} promoter. The detailed construction of pIYC04 as a background plasmid and pIYC08 has been described by Chen and co-workers (Chen et al. 2013). The PHB biosynthesis pathway genes *phaA*, *phaB* and *phaC* were synthesized based on the genes from *R. eutropha* H16 and *gapN* encoding non-phosphorylating $NADP^+$-dependent glyceraldehyde-3-phosphate dehydrogenase was synthesized based on the gene from *S. mutans* by DNA 2.0 (Menlo Park, CA, USA). The gene *xpkA* encoding a phosphoketolase and the gene *ack* encoding acetate kinase were synthesized based on the sequence from *A. nidulans* by GenScript (Piscataway, NJ). All genes were codon optimized for optimal expression in *S. cerevisiae*. The PHB biosynthesis pathway was introduced into the *S. cerevisiae* strain CEN.PK 113-11C by using a multicopy plasmid, pKK001, based on pSP-GM2 with a P_{TEF1}-P_{PGK1} bidirectional promoter (Partow et al. 2010). The detailed construction of pKK001 has been described (Kocharin et al. 2012).

Plasmid pJC7 contains genes responsible for the utilization of the intermediate xylulose-5-phosphate from the pentose phosphate pathway to supply acetyl-CoA as a precursor for PHB production. Two of the genes, *xpkA* and *ack*, were used to construct the vector pMPa2 (Papini et al. 2012; Partow et al. 2010). The *URA3* marker of pMPa2 was changed to *HIS3* derived from pESC-HIS (Agilent Technologies, Santa Clara, USA) through restriction with *Mfe*I and *Sac*I and subsequent ligation (Gionata Scalcinati, pers. commun.). The resulting plasmid, pIGS11, was verified by PCR using the HIS-check primers (Supplementary table 1). Plasmid pIGS11 was further ligated with the PCR amplicon of the Acs^{L641P} expression cassette

derived from pIYC08 using primers JC7-ACS1/JC7-ACS2 and cloned into the *Mfe*I site (Jichen Bao, pers. commun.). The resulting plasmid was named pJC7.

Plasmid pJEF1105 containing the bacterial *neo*^{r} gene was kindly provided by Dr. Jef D. Boeke (Boeke et al. 1988). Plasmid pBluescript SK II (+) (Stratagene, La Jolla, CA) was digested with *Aat*II and ligated with the sequence of the *his3Δ1* allele, which had been amplified from genomic DNA of *S. cerevisiae* CEN.PK 113-11C using primers KK001/KK002. All primers used for strain construction are listed in Supplementary Table1. The resulting plasmid, pBluSKP-his, was used as template for PCR amplification with primers KK003/KK004 to obtain a fragment containing origin of replication, ampicillin resistance marker and the *his3Δ1* allele with restriction sites for *Kpn*2I and *Mfe*I at the respective ends. Plasmid pSP-GM2 was digested with *Kpn*2I and *Mfe*I and ligated with the PCR fragment derived from pBluSKP-his. The resulting plasmid, pSP-GM2-his, was digested with *Asc*I and *Mfe*I and ligated with the *neo*^{r} marker, which had been isolated from plasmid pJEF1105 using primers KK005/KK006, generating pCIChE-KK001. pCIChE-KK001 was further digested with *Asc*I and ligated with a second *his3Δ1* sequence amplified from the same source of genomic DNA using primers KK078/KK079. The derived plasmid, pCIChE-KK004, was used as an integration plasmid for introducing *gapN* into the chromosome. Yeast transformation was performed by using the lithium acetate/single-stranded carrier DNA/polyethylene glycol method (Gietz and Woods 2002). *S. cerevisiae* transformation with the integration cassette was performed with the following modifications. pCIChE-KK004-*GAPN* was linearized with *Ale*I and *Sal*I prior the yeast transformation. Single-stranded salmon sperm DNA (50 μg per transformation) was added together with 5-10 μg of linearized integrative plasmid, and the heat shock time at 42°C was extended from 5 to 15 min. After the heat shock, the cell suspension (ca. 0.4 mL) was mixed with 2.7 mL of

YPD medium and incubated at 30°C for 18 h with shaking. 50-100 μL of the culture were then plated on a selective YPD-G418 plate (0.1 g/L G418). All *gapN* integration strains were verified by PCR with primers KK039/KK082 and KK083/KK042. Strains used in this study are summarized in Table 1. The schematic metabolic pathway and plasmid maps are illustrated in Figure 1 and Figure 2, respectively.

Shake flask cultivation

The pre-cultures for shake flask cultivations were prepared by inoculation of 5 mL modified minimal media in a 14 mL culture tube and grown at 30ºC and 180 rpm in an orbital shaking incubator. The modified minimal medium for shake flask cultivations was prepared as follows (per liter): $(NH_4)_2SO_4$, 7.5 g; KH_2PO_4, 14.4 g, $MgSO_4 \cdot 7H_2O$, 0.5 g; 2 mL of trace metal solution and 1 mL of vitamin solution with an initial pH of 6.5. Glucose was autoclaved separately from the minimal medium and later added to media at a concentration of 20 g/L. The trace metal solution consisted of the following (per liter): EDTA (sodium salt), 15 g; $ZnSO_4 \cdot 7H_2O$, 0.45 g; $MnCl_2 \cdot 2H_2O$, 1 g; $CoCl_2 \cdot 6H_2O$, 0.3 g; $CuSO_4 \cdot 5H_2O$, 0.3 g; $Na_2MoO_4 \cdot 2H_2O$, 0.4 g; $CaCl_2 \cdot 2H_2O$, 0.45 g; $FeSO_4 \cdot 7H_2O$, 0.3 g; H_3BO_3, 0.1 g and KI, 0.1 g. The pH of the trace metal solution was adjusted to 4.0 with 2 M NaOH. The vitamin solution contained (per liter): biotin, 0.05 g; ρ-amino benzoic acid, 0.2 g; nicotinic acid, 1 g; Ca-pantothenate, 1 g; pyridoxine-HCl, 1 g; thiamine-HCl, 1 g and myo-inositol, 25 g. The pH of the vitamin solution was adjusted to pH 6.5 prior filter sterilization. Histidine and uracil stock solutions were filter sterilized and added to the medium when needed at the final concentration of 20 mg/L of each amino acid. For anaerobic cultivations, the medium was supplemented with 420 mg/L Tween 80 and 10 mg/L ergosterol, which were first dissolved in boiling pure ethanol. The supplementation of Tween80 and ergosterol is necessary for

anaerobic growth of *S. cerevisiae* (Verduyn et al. 1990). Anaerobic shake flasks were sealed with a rubber stopper equipped with a U-tube containing water to ensure anaerobic conditions. After inoculation and each sampling, the flasks were sparged with nitrogen for 5 min prior to the incubation. 75 mL of modified minimal medium in a 250 mL unbaffled flask were inoculated with an amount of pre-culture that resulted in a final optical density of 0.02 at 600 nm (OD_{600}). The culture was grown at 30ºC and 180 rpm in an orbital shaking incubator. Samples were taken to determine biomass, extracellular metabolites and PHB concentration.

Cell mass determination

Culture samples of 10 mL volume were centrifuged at 5,000 rpm and 4°C for 5 min and the pellets were washed once with distilled water and centrifuged at 14,000 g for 1 min. To lyophilize the biomass, the recovered cell pellet was immediately frozen by immersion in liquid nitrogen followed by lyophilization under vacuum (Christ Alpha 2-4 LSC, Shropshire, UK). The dry cell weight was determined and the pellet kept at 4°C for further analysis.

Metabolite analysis

Glucose and extracellular metabolites including ethanol, glycerol, and acetate were quantified in the culture supernatant using an Ultimate 3000 HPLC (Dionex, Sunnyvale, CA, USA) equipped with an Aminex HPX 87H ion exclusion column (300 mm x 7.8 mm, Bio-Rad Laboratories, Hercules, CA, USA) which was operated at 45°C and a flow rate of 0.6 mL/min of 5 mM H_2SO_4 using a refractive index detector and UV detector for analysis of sugars and organic acids, respectively.

PHB was analyzed as described previously (Karr et al. 1983; Tyo et al. 2006). 10-20 mg of dried cells were weighed and boiled in 1 mL of concentrated sulfuric acid for 60 min and

then diluted with 4 mL of 14 mM H_2SO_4. Samples were centrifuged (15 min, 16,000 × g) to remove cell debris, and the supernatant was analyzed using an Ultimate 3000 HPLC (Dionex) equipped with an Aminex HPX-87H ion exclusion column (300 × 7.8 mm; Bio-Rad Laboratories) and UV detector. Commercially available PHB (Sigma-Aldrich, St. Louis, MO, USA), processed in parallel with the samples, was used as a standard. The HPLC was operated at 60°C and a flow rate of 0.6 mL/min of 5 mM H_2SO_4.

Results

Genomic integration of *gapN*

In our earlier work on increasing acetyl-CoA supply by over-expression the ethanol degradation pathway we found that the glycerol yield on glucose had increased (Kocharin et al. 2012). Glycerol is produced as a way of handling excess NADH, and as a strategy to reduce glycerol production and improve PHB production in *S. cerevisiae* the bacterial *gapN* gene encoding non-phosphorylating $NADP^+$-dependent glyceraldehyde-3-phosphate dehydrogenase was introduced into the yeast genome. The gene was integrated at the *his3-Δ1* allele of strain CEN.PK 113-11C under control of the strong constitutive *PGK1* promoter. When *S. cerevisiae* is grown under anaerobic cultivation, apart from biomass, three major metabolites are produced from glucose: CO_2, ethanol, glycerol. Therefore, in order to investigate the effect of *gapN* expression on the growth behavior of *S. cerevisiae*, SCKK036 (harbouring *gapN*) and the parental strain, CEN.PK 113-11C, were characterized in anaerobic shake flask cultivation. The growth curves of both strains are shown in Figure 3. SCKK036 showed a growth pattern similar to the parental strain with a specific growth rate of 0.38 h^{-1} and a slightly higher ethanol yield on glucose (Table 2). The major difference between SCKK036 and the parental strain was a 45% reduction in glycerol production by the strain expressing *gapN*, which is consistent with earlier findings (Bro et al. 2006). This reduction is due to the by-pass of the two reactions from glyceraldehyde-3-phosphate to 3-phospho-D-glycerate resulting in reduced NADH production in the EMP pathway (replaced by production of NADPH).

PHB production in the strain with chromosomal *gapN* integration, SCKK033, was evaluated in aerobic shake flask cultivation and compared to SCKK005 harboring the PHB pathway without *gapN* integration. The kinetic parameters are reported in Table3. A decrease in the

specific growth rate was observed in SCKK033 compared to SCKK005. There was no significant difference in the glycerol yield on glucose. However, the ethanol yield on glucose in SCKK033 was higher than in SCKK005. Due to the fact that PHB is mainly produced during growth on ethanol, the yield of PHB on substrate was calculated to be much lower during growth on glucose compared to the ethanol consumption phase. The effect of *gapN* integration on PHB production was clearly observed as the PHB yields on glucose and on ethanol of SCKK033 were substantially higher than for SCKK005 (Table 3). The maximum cellular PHB content obtained at 100 h in SCKK033, 14.87 mg/gDW, was 3.7 times higher than in the reference strain, SCKK005.

Alternative pathway for acetyl-CoA supply

Heterologous expression of the phosphoketolase pathway from *A. nidulans* enables the utilization of xylulose-5-phosphate, an intermediate from the PP pathway, to be converted to acetyl-CoA via acetyl phosphate (acetyl-P). In order to investigate the possibility of employing the phosphoketolase pathway compared with the ethanol degradation pathway for increasing cytosolic acetyl-CoA concentration and improving PHB production, strain characterization was carried out in aerobic shake flask cultivations. The kinetic parameters are reported in Table 3. The strain that carries the phosphoketolase pathway, SCKK032, showed an improved PHB production not only compared with the reference strain, but also compared with SCKK006 that overexpressed the ethanol degradation pathway to increase cytosolic acetyl-CoA supply as reported previously (Kocharin et al. 2012). SCKK032 showed a decrease in the specific growth rate, 0.21 h^{-1}, as well as the biomass yield on glucose compared with SCKK005 as a reference strain and SCKK006. The lower biomass yield in SCKK006 and SCKK032 is associated with a higher glycerol yield on glucose. Although the PHB yield on glucose in SCKK032 was lower than SCKK006 the PHB yield on ethanol in

SCKK032 was higher than SCKK006. This resulted in a cellular PHB content in SCKK032 at 100 h of 27.86 mg/gDW.

Combined effect of cofactor enhancement and pathway engineering

The combination of integrating *gapN* into the genome and the utilization of the acetyl-CoA boost strategies to improve PHB production in *S. cerevisiae* was characterized in aerobic shake flask cultivation and physiological parameters of SCKK033, SCKK034 and SCKK035 were calculated. The values are shown in Table 3. Figure 4 shows the concentration of PHB measured at three different time points, 50, 75 and 100 h of cultivation. In general, strains engineered to have an increased supply of acetyl-CoA, SCKK006, SCKK032, SCKK034, SCKK035, showed an improved PHB production compared to the respective reference strains, SCKK005 and SCKK033. The maximum specific growth rates for all strains used in this experiment, range from 0.21-0.28 h^{-1} depending on the heterologous pathway used to manipulate cytosolic acetyl-CoA supply and *gapN* integration into the genome (Table 3). There was no difference in the specific growth rate when *gapN* was integrated into the genome of SCKK035 expressing the phosphoketolase pathway whereas *gapN* integration resulted in a decrease in the specific growth rate of a strain that utilizes the ethanol degradation pathway to supply cytosolic acetyl-CoA, SCKK034. The glucose consumption rate in strains without *gapN* integration was higher than in the strains with *gapN* integration. Among the *gapN* integration strains, SCKK034 showed the lowest ethanol yield on glucose, 0.35 g/g glc, due to the overexpression of genes from the ethanol degradation pathway in this strain. A slight decrease in the glycerol yield on glucose was observed for all strains expressing *gapN*. A positive effect of *gapN* expression on the PHB yield was clearly observed in strains that do not carry any acetyl-CoA boost plasmids. A more than 10-fold increase in PHB yield on glucose was observed in SCKK033 compared to SCKK005,

producing 0.27 ± 0.01 and 0.02 ± 0.01 g/g glc, respectively. However, only a 2 fold higher PHB yield on glucose was observed in SCKK035 compared to SCKK032 whereas no effect of *gapN* integration on Y_{sPHB} was observed in strains with overexpression of the ethanol degradation pathway, SCKK006 and SCKK034. The combination of *gapN* integration and the ethanol degradation pathway was able to improve the yield of PHB on ethanol from 6.09 ± 1.44 to 14.50 ± 2.9 mg/ g EtOH in SCKK034. The combination of *gapN* integration and expression of the phosphoketolase pathway however revealed an antagonistic effect on PHB production on ethanol. The strain without *gapN* integration but expressing the phosphoketolase pathway (SCKK032) showed the highest yield of PHB on ethanol, 56.4 mg/g EtOH, which decreased to 12.5 mg/g EtOH when the phosphoketolase pathway was combined with *gapN* integration.

Figure 5 shows the glucose consumption rate, the specific productivity of ethanol, glycerol and PHB during growth on glucose and the specific productivity of PHB during growth on ethanol. All the strains with *gapN* integration showed a decrease in glucose consumption rate compared to the non-*gapN* integration strains. Furthermore, a noticeable decrease in the glycerol flux was observed in the *gapN* integration strains especially in SCKK034 and SCKK035, which revealed an about 50% reduction in the glycerol flux compared to their respective reference strains. Integration of *gapN* has previously been investigated for improving the production of bioethanol by reducing the flux towards glycerol, however, in this study when *gapN* was integrated into the PHB strains (SCKK034, SCKK035) with the aim to enhance acetyl-CoA production, it resulted in a decrease in the ethanol flux compared to the non-integrated strains. The lowest flux towards ethanol seen for SCKK034 was probably caused by the overexpression of the ethanol degradation pathway, while the lower ethanol flux in SCKK035 might be due the redirection of carbon flux from the EMP pathway to the PP pathway and further to the phosphoketolase pathway. The highest specific

productivity of PHB during growth on glucose was obtained for the strain with *gapN* integration and without any acetyl-CoA boost plasmid (SCKK033) whereas the strain without *gapN* integration and with the reconstructed phosphoketolase pathway as the alternative route to produce acetyl-CoA and NADPH (SCKK032) gave the highest specific productivity of PHB during growth on ethanol.

Discussion

The biosynthesis of PHB in *S. cerevisiae* is initiated by the condensation of two acetyl-CoA molecules to acetoacetyl-CoA that is subsequently reduced by an NADPH-dependent acetoacetyl-CoA reductase resulting into the monomer, 3-hydroxybutyryl-CoA, which is polymerized by polyhydroxyalkanoate synthase yielding PHB. In a previous study we increased acetyl-CoA supply through overexpression of the genes of the ethanol degradation pathway and showed that this can improve the specific productivity of PHB in *S. cerevisiae* (Kocharin et al. 2012). Here we investigated an alternative pathway to increase acetyl-CoA supply with the objective to further improve PHB production. We found that by reconstruction of the phosphoketolase pathway from *A. nidulans* in combination with expression of an acetyl-CoA synthetase variant (Acs^{L641P}) from *S. enterica* enabled efficient supply of cytosolic acetyl-CoA required as a precursor for PHB production. A further advantage of using this route via the PP pathway is that excess NADPH is generated, which is needed for PHB biosynthesis. While the strain expressing the heterologous phophoketolase pathway gave the highest PHB production, it showed a decrease in both the specific growth rate and the biomass yield compared with the strain overexpressing the genes in the ethanol degradation pathway to increase the acetyl-CoA supply. This might be due to the split of carbon from the EMP to the PP pathway that likely may result in growth attenuation and

reduced biomass yield on glucose. A reduction in the biomass yield of *S. cerevisiae* expressing the phosphoketolase pathway was also observed in previous studies (Papini et al. 2012; Sonderegger et al. 2004).

In the present study, we also investigated the supply of NADPH as a major cofactor required in the reaction catalyzed by NADPH-dependent acetoacetyl-CoA reductase in the PHB biosynthesis pathway. We introduced the bacterial *gapN* gene into the yeast's genome aiming to take advantage of the NADPH formed during the catalytic activity of GapN to increase the production of NADPH and thereby improve PHB production. The effect of increased NADPH supply obtained by *gapN* integration is clearly observed in the strain harboring only the PHB production plasmid, SCKK033, as there was observed a 13 -fold increase in PHB yield on glucose and a 70-fold increase in the PHB yield on ethanol. The PHB content at 100 h was increased 3.7 times, from 4 mg/gDW to 14.87 mg/gDW. Besides influencing the redox metabolism by regenerating NADPH, integration of *gapN* may also result in altered carbon fluxes as expression of *gapN* alone results in an increased flux towards ethanol and a reduced flux towards glycerol. However, we believe that integration of *gapN* in strains carrying the PHB biosynthesis pathway helps increase the flux toward PHB production primarily by supplying more NADPH as there was no significant difference in the specific productivity of glycerol and ethanol in SCKK005 and SCKK033 (Figure 5). Therefore, we believed that *gapN* integration in this study mainly plays a role in production of NADPH required for PHB biosynthesis.

In order to investigate the combined effect of precursor and cofactor supply for improving PHB production in *S. cerevisiae*, we combined over-expression of either the ethanol degradation pathway or the reconstructed phosphoketolase pathway, to increase the supply of cytosolic acetyl-CoA, with *gapN* integration into the chromosome. It is evident that the strategy to enhance acetyl-CoA supply via the ethanol degradation pathway together with

provision of NADPH via GapN promotes the production of PHB in *S. cerevisiae* as revealed in the improved PHB production by SCKK034 compared to SCKK033 and SCKK006, respectively (Figure 3). Moreover, a reduced glycerol yield on glucose was observed as a positive side effect of *gapN* integration. This result suggests that supply of both precursor (acetyl-CoA) and cofactor (NADPH) are important to improve PHB production in *S. cerevisiae*. However, for the yeast strain carrying the reconstructed phosphoketolase pathway to generate acetyl-CoA supply there was no benefit of *gapN* expression as the resulting strain gave an amount of PHB at 75 h of cultivation comparable with the strain not having *gapN* integrated. The reason that no improvement in PHB production was observed in SCKK035 compared to SCKK032 might be due to the lack of a mitochondrial NADPH dehydrogenase in *S. cerevisiae* which otherwise couples the oxidation of cytosolic NADPH to the mitochondrial respiratory chain. Therefore, a direct oxidation of a surplus NADPH generated from GapN and the PP pathway in the respiration chain is not possible (Bruinenberg 1986; Gonzalez Siso et al. 1996). Furthermore, an increased production of NADPH by the EMP pathway may result in a reduced flux through the PP pathway as the glucose-6-phosphate dehydrogenase flux is very sensitive to the NADP/NADPH ratio (Vaseghi et al. 1999).

From the results in this study, the strain that exhibited the best performance for PHB production was SCKK032 which harbors only the PHB production plasmid and expresses the heterologous phosphoketolase pathway, which may point to that provision of acetyl-CoA is important for ensuring a high PHB production. When *S. cerevisiae* is grown on glucose, the PP pathway is the major source for NADPH production, specifically the dehydrogenase activity during the early steps in the pathway (Grabowska and Chelstowska 2003; Minard and McAlister-Henn 2005). Therefore, an increased carbon flux through the PP pathway has a direct consequence on the supply of NADPH required in various anabolic reactions and of certain anabolic precursors (Frick and Wittmann 2005). For this reason, a noticeable high

yield of PHB on ethanol was observed for the strain that can generate acetyl-CoA and NADPH simultaneously through the PP pathway, SCKK032. These results strongly support our hypothesis that the improved PHB production in *S. cerevisiae* required both sufficient precursor and cofactor supply.

Acknowledgements

We thank Chalmers Foundation, the Knut and Alice Wallenberg Foundation and the European Research Council (grant no. 247013) for funding part of this work. We also acknowledge the Thailand Science and Technology Ministry for providing a stipend to KK.

Conflict of interest

The authors declare that they have no conflict of interest.

References

Blank LM, Sauer U. 2004. TCA cycle activity in *Saccharomyces cerevisiae* is a function of the environmentally determined specific growth and glucose uptake rates. Microbiology 150(Pt 4):1085-1093.

Boeke J, Xu H, Fink G. 1988. A general method for the chromosomal amplification of genes in yeast. Science 239(4837):280-282.

Bro C, Regenberg B, Forster J, Nielsen J. 2006. In silico aided metabolic engineering of *Saccharomyces cerevisiae* for improved bioethanol production. Metab Eng 8(2):102-111.

Bruinenberg PM. 1986. The NADP(H) redox couple in yeast metabolism. Antonie Van Leeuwenhoek 52(5):411-429.

Bruinenberg PM, Vandijken JP, Scheffers WA. 1983. A theoretical-analysis of NADPH production and consumption in yeasts. J Gen Microbiol 129(Apr):953-964.

Carlson R, Fell D, Srienc F. 2002. Metabolic pathway analysis of a recombinant yeast for rational strain development. Biotechnol Bioeng 79(2):121-134.

Carlson R, Srienc F. 2006. Effects of recombinant precursor pathway variations on poly[(R)-3-hydroxybutyrate] synthesis in *Saccharomyces cerevisiae*. J Biotechnol 124(3):561-573.

Chen Y, Daviet L, Schalk M, Siewers V, Nielsen J. 2013. Establishing a platform cell factory through engineering of yeast acetyl-CoA metabolism. Met Eng 15(0):48-54.

Dawes EA, Senior PJ. 1973. The role and regulation of energy reserve polymers in micro-organisms. In: A.H. Rose and D.W. Tempest, Editor(s), Advances in Microbial Physiology, Academic Press. Volume 10, Pages 135-266.

Frick O, Wittmann C. 2005. Characterization of the metabolic shift between oxidative and fermentative growth in *Saccharomyces cerevisiae* by comparative 13C flux analysis. Microb Cell Fact 4(1):30.

Gietz RD, Woods RA. 2002. Transformation of yeast by lithium acetate/single-stranded carrier DNA/polyethylene glycol method. Methods Enzymol 350:87-96.

Gombert AK, Moreira dos Santos M, Christensen B, Nielsen J. 2001. Network identification and flux quantification in the central metabolism of *Saccharomyces cerevisiae* under Different conditions of glucose repression. J Bacteriol 183(4):1441-1451.

Gonzalez Siso MI, Freire Picos MA, Cerdan ME. 1996. Reoxidation of the NADPH produced by the pentose phosphate pathway is necessary for the utilization of glucose by *Kluyveromyces lactis rag2* mutants. FEBS Lett 387(1):7-10.

Grabowska D, Chelstowska A. 2003. The ALD6 gene product is indispensable for providing NADPH in yeast cells lacking glucose-6-phosphate dehydrogenase activity. J Biol Chem 278(16):13984-13988.

Karr DB, Waters JK, Emerich DW. 1983. Analysis of poly-beta-hydroxybutyrate in *Rhizobium japonicum* bacteroids by ion-exclusion high-pressure liquid chromatography and UV detection. Appl Environ Microbiol 46(6):1339-1344.

Kocharin K, Chen Y, Siewers V, Nielsen J. 2012. Engineering of acetyl-CoA metabolism for the improved production of polyhydroxybutyrate in *Saccharomyces cerevisiae*. AMB Express 2(1):52.

Leaf TA, Srienc F. 1998. Metabolic modeling of polyhydroxybutyrate biosynthesis. Biotechnol Bioeng 57(5):557-570.

Minard KI, McAlister-Henn L. 2005. Sources of NADPH in yeast vary with carbon source. J Biol Chem 280(48):39890-39896.

Papini M, Nookaew I, Siewers V, Nielsen J. 2012. Physiological characterization of recombinant *Saccharomyces cerevisiae* expressing the *Aspergillus nidulans* phosphoketolase pathway: validation of activity through ^{13}C-based metabolic flux analysis. Appl Microbiol Biotechnol 95(4):1001-1010.

Partow S, Siewers V, Bjorn S, Nielsen J, Maury J. 2010. Characterization of different promoters for designing a new expression vector in *Saccharomyces cerevisiae*. Yeast 27(11):955-964.

Sambrook J, Russell DW. 2006. The Inoue method for preparation and transformation of competent *E. Coli*: "Ultra-Competent" cells. Cold Spring Harb Protoc 2006(2): 3944-.

Scalcinati G, Partow S, Siewers V, Schalk M, Daviet L, Nielsen J. 2012. Combined metabolic engineering of precursor and co-factor supply to increase alpha-santalene production by *Saccharomyces cerevisiae*. Microb Cell Fact 11(1):117.

Sonderegger M, Schumperli M, Sauer U. 2004. Metabolic engineering of a phosphoketolase pathway for pentose catabolism in *Saccharomyces cerevisiae*. Appl Environ Microbiol 70(5):2892-2897.

Tyo KE, Zhou H, Stephanopoulos GN. 2006. High-throughput screen for poly-3-hydroxybutyrate in *Escherichia coli* and *Synechocystis* sp. Strain PCC6803. Appl. Environ. Microbiol. 72(5):3412-3417.

van Winden WA, van Dam JC, Ras C, Kleijn RJ, Vinke JL, van Gulik WM, Heijnen JJ. 2005. Metabolic-flux analysis of *Saccharomyces cerevisiae* CEN.PK113-7D based on mass isotopomer measurements of ^{13}C-labeled primary metabolites. FEMS Yeast Res 5(6-7):559-568.

Vaseghi S, Baumeister A, Rizzi M, Reuss M. 1999. In vivo dynamics of the pentose phosphate pathway in *Saccharomyces cerevisiae*. Metab Eng 1(2):128-140.

Verduyn C, Postma E, Scheffers WA, van Dijken JP. 1990. Physiology of *Saccharomyces cerevisiae* in anaerobic glucose-limited chemostat cultures. J Gen Microbiol 136(3):395-403.

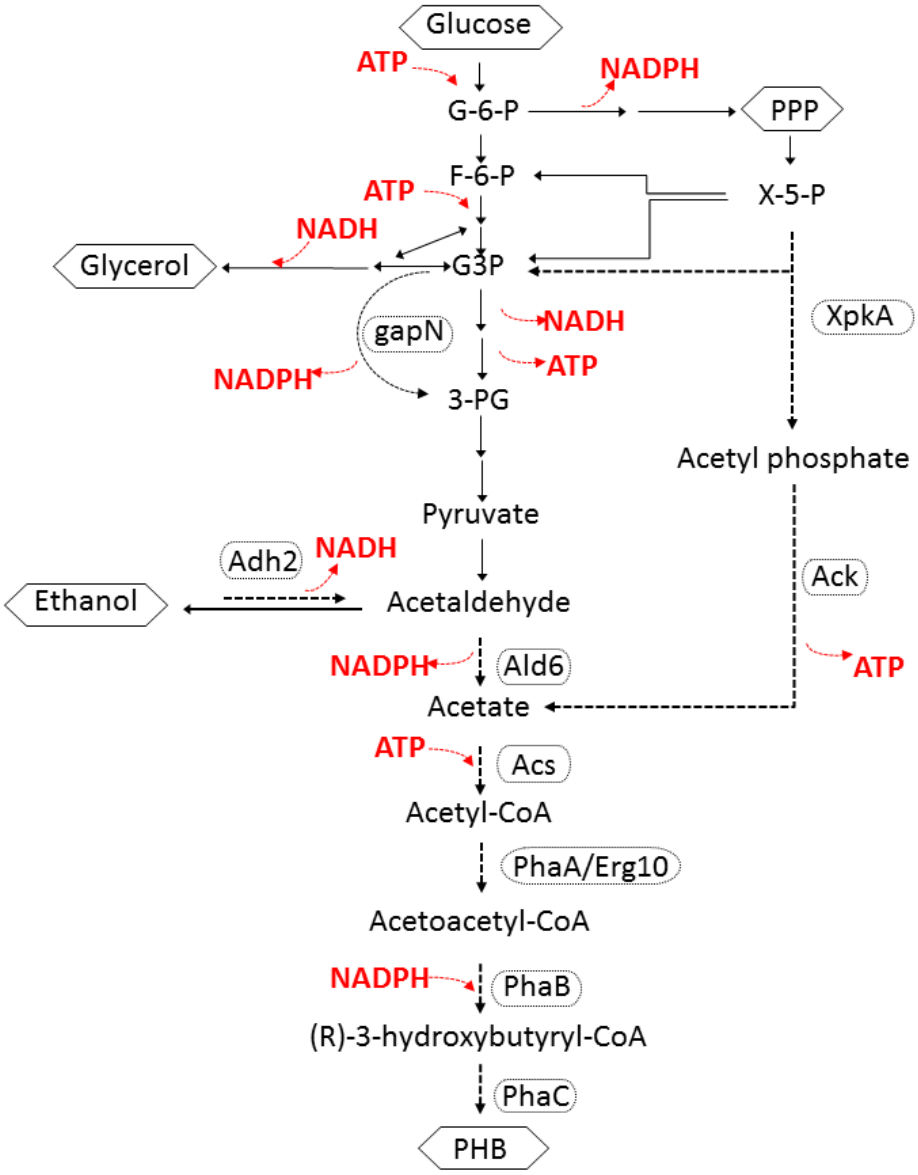

Figure 1: Schematic pathway representing metabolic engineering strategies for improving PHB production in *S. cerevisiae*. PPP = Pentose phosphate pathway, G-6-P = Glucose-6-phosphate, F-6-P = Fructose-6-phosphate, G3P = Glyceraldehyde-3-phosphate, 3-PG = 3-Phosphoglycerate, PHB = Polyhydroxybutyrate. Dashed arrows represent engineered pathway steps.

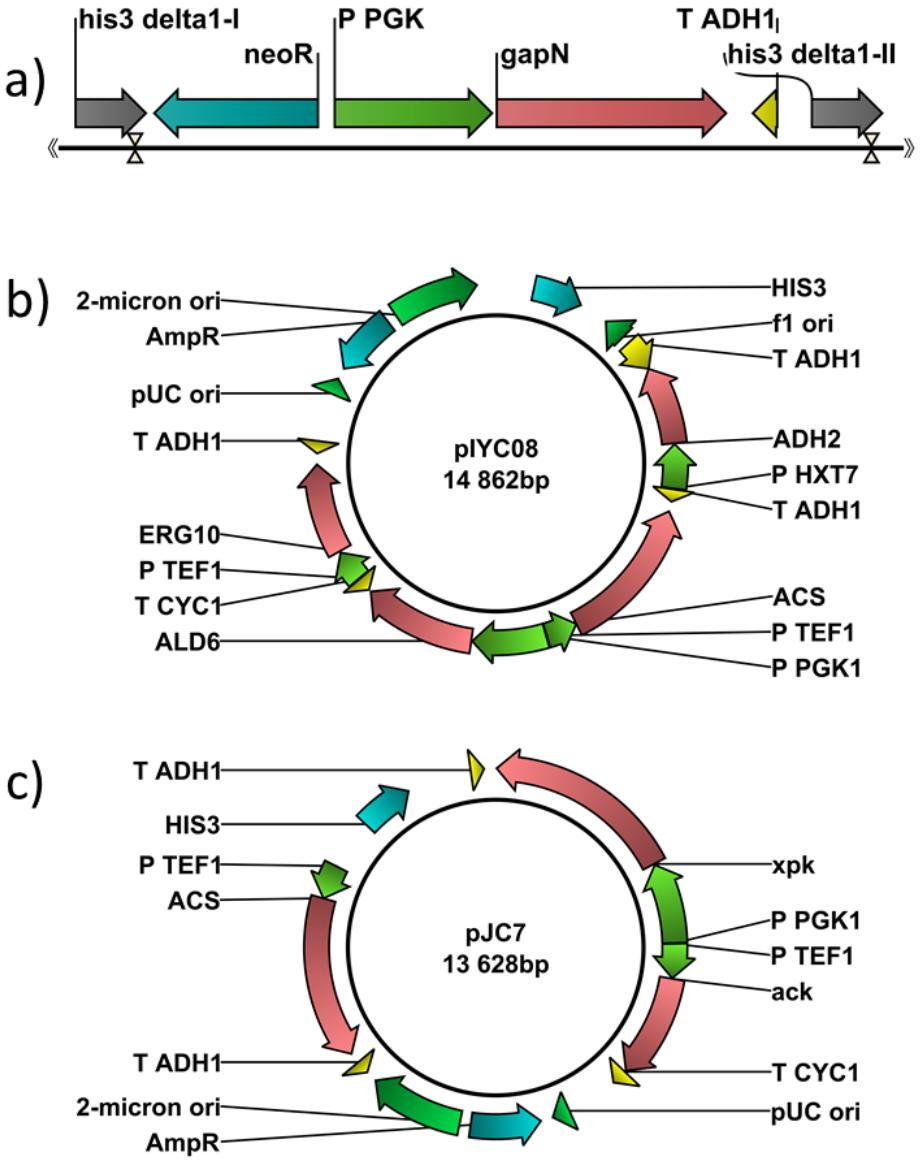

Figure 2: Plasmid maps a) Integration cassette derived from pCIChE-KK004-GAPN containing the *his3-Δ1* allele at both ends of the cassette, b) Plasmid pJC7 containing genes for xylulose-5-phosphate phosphoketolase (*xpkA)*, acetate kinase (*ack)* and acetyl-CoA synthetase (Acs^{L641P}), c) Plasmid pIYC08 containing genes for alcohol dehydrogenase (*ADH2*), aldehyde dehydrogenase (*ALD6*), acetyl-CoA synthetase (Acs^{L641P}) variant and acetyl-CoA acetyltransferase (*ERG10*)

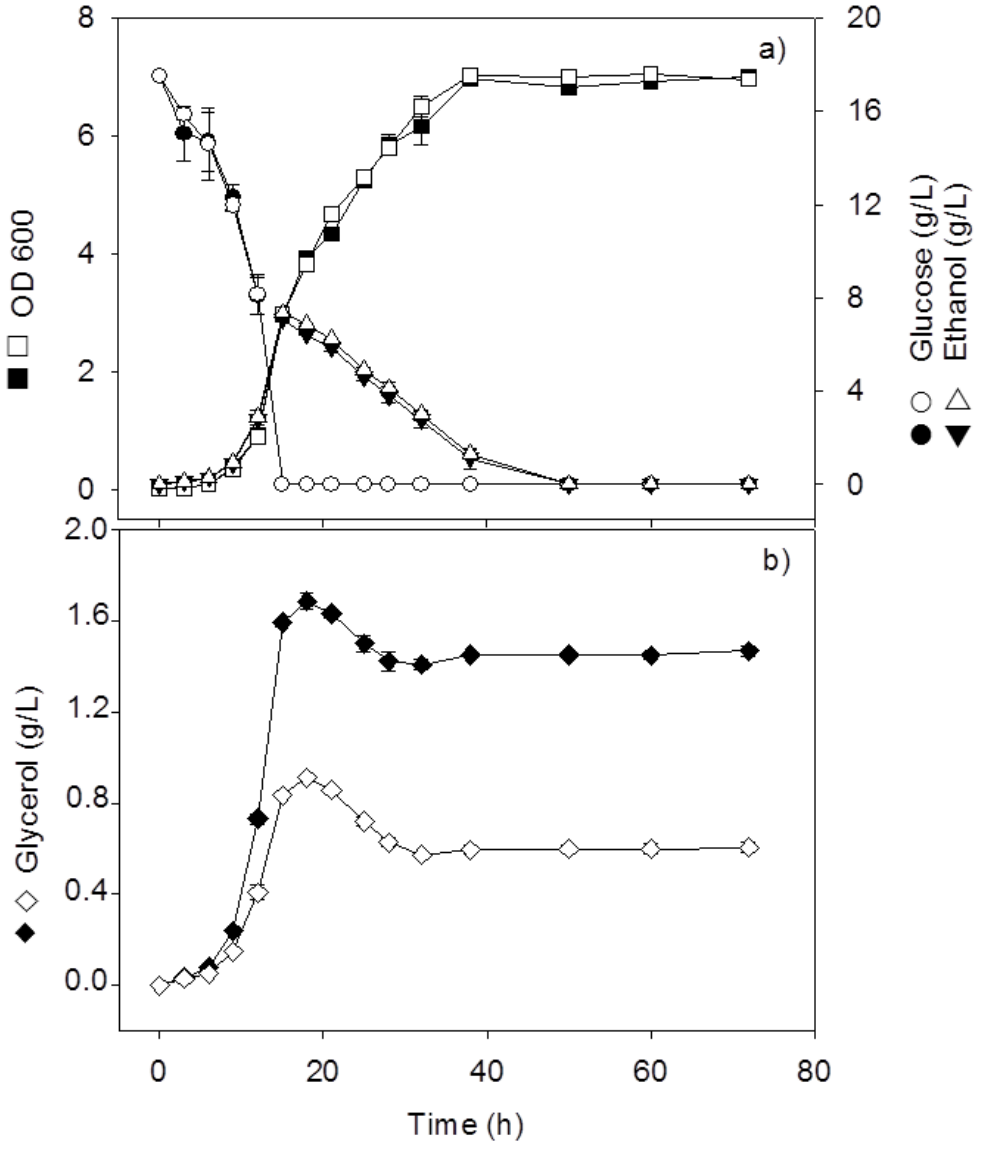

Figure 3: Fermentation profile of *S. cerevisiae* CEN.PK 113-11C and SCKK036 during growth in anaerobic shake flask cultivation. Bold and open symbols represent the reference strain (CEN.PK 113-11C) and the reference strain with *gapN* integration (SCKK036), respectively.

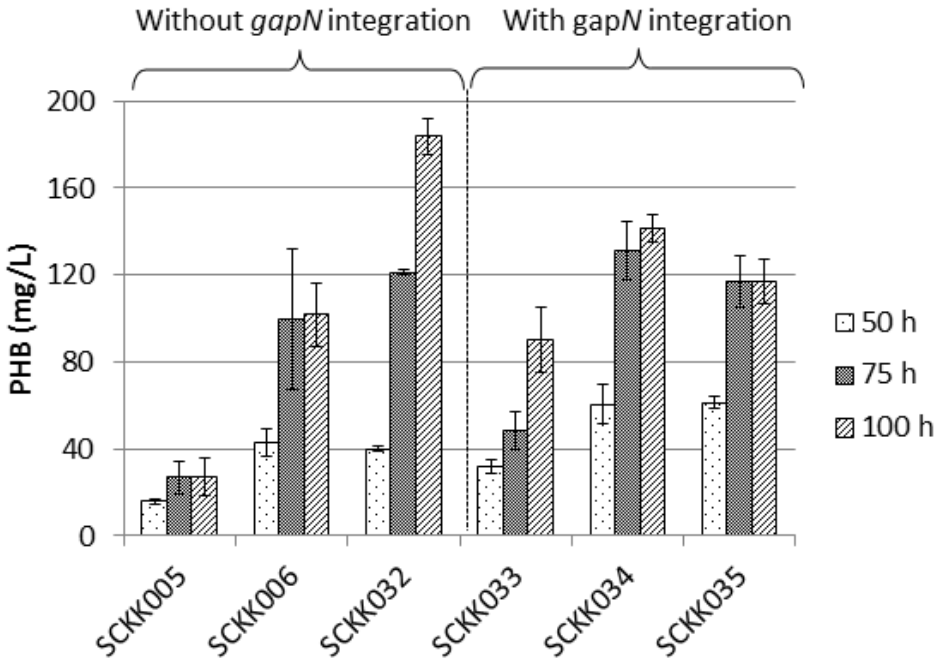

Figure 4 Polyhydroxybutyrate production in *S. cerevisiae* employing different strategies to improve PHB production. SCKK005 and SCKK033 harbor only the PHB plasmid (pKK01). SCKK032 and SCKK035 carry pJC7 (phosphoketolase pathway) whereas SCKK006 and SCKK034 carry pIYC08 (ethanol degradation pathway). Samples for PHB measurement were taken at 50 h (the glucose phase), 75 h (the ethanol phase) and 100 h (the end of fermentation where all the glucose and ethanol were depleted).

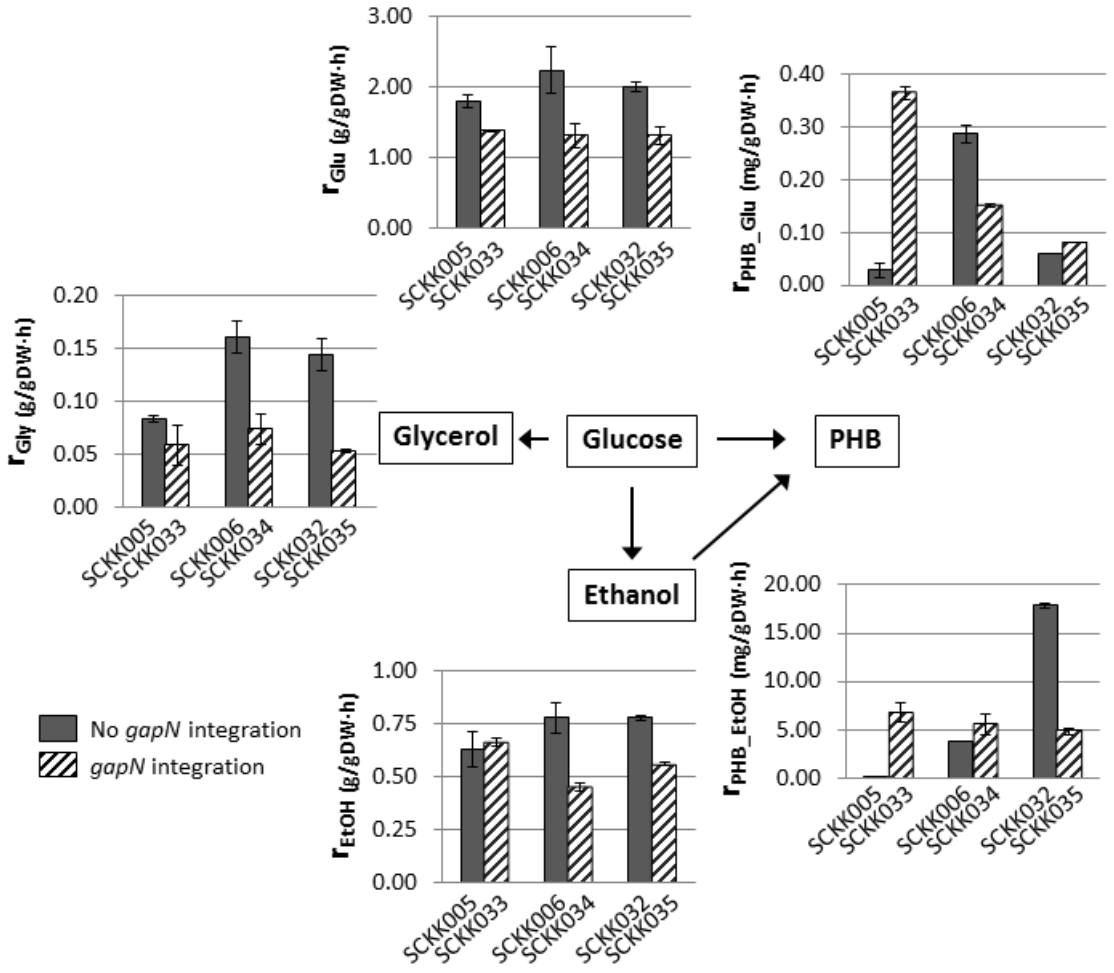

Figure 5 Specific productivity of ethanol, glycerol and PHB obtained from shake flask cultivations. The specific product formation rates were calculated by using the equation: $r_p = \mu_{max} Y_{sp}/Y_{sx}$

r_{EtOH} = specific productivity of ethanol, r_{Gly} = specific productivity of glycerol, r_{PHB_Glu} = specific productivity of PHB in the glucose consumption phase, r_{PHB_EtOH} = specific productivity of PHB in the ethanol consumption phase

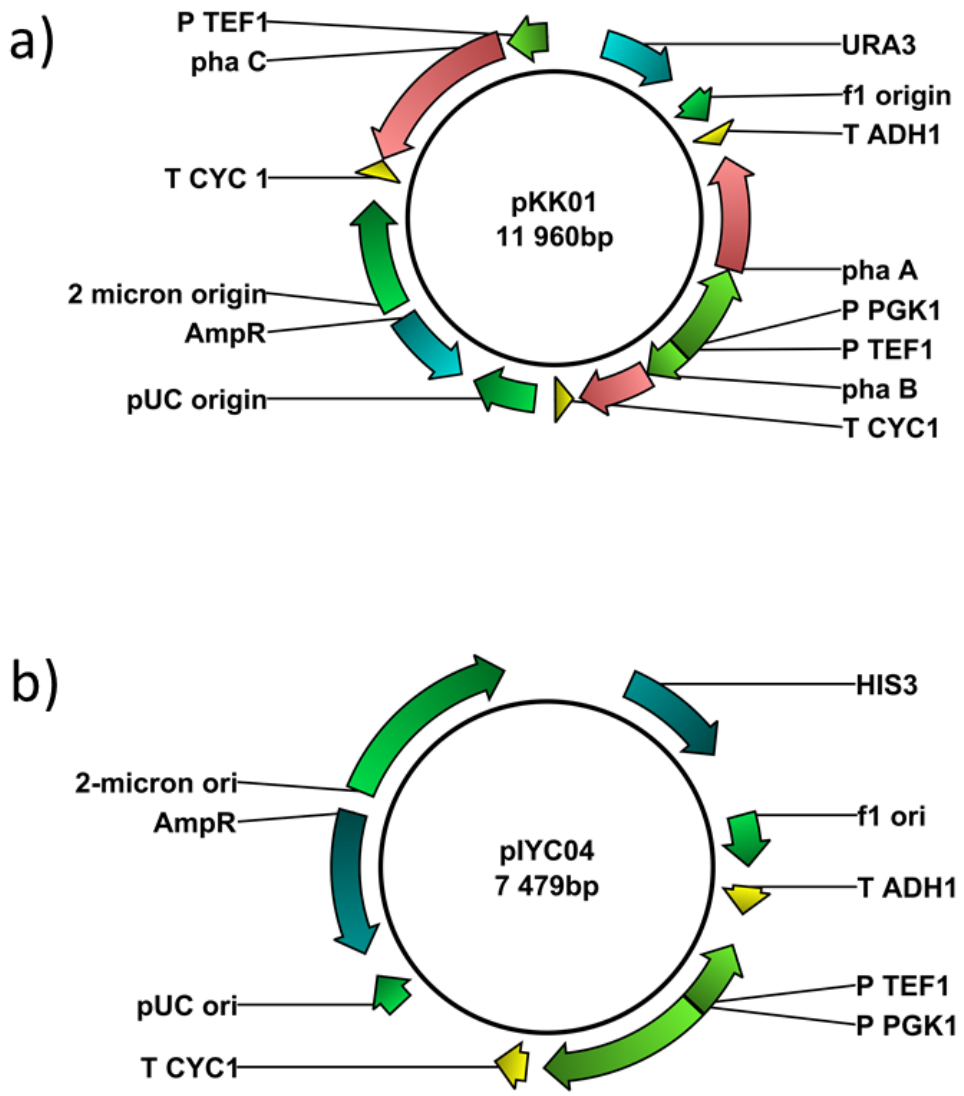

Figure S1. **Plasmid maps** a) PHB plasmid containing *phaA*, *phaB* and *phaC*, pKK01 b) Empty control plasmid, pIYC04

Table 1 Yeast strains used in this study.

Strain	Genotype or relevant feature(s)	Plasmid	Source
CEN.PK 113-11C	*MATa SUC2 MAL2-8^c ura3-52 his3-Δ1*	-	P. Kötter[a]-
SCKK005	*MATa SUC2 MAL2-8^c ura3-52 his3-Δ1*	pIYC04/pKK01	(Kocharin et al. 2012)
SCKK006	*MATa SUC2 MAL2-8^c ura3-52 his3-Δ1*	pIYC08/pKK01	(Kocharin et al. 2012)
SCKK032	*MATa SUC2 MAL2-8^c ura3-52 his3-Δ1*	pJC7/pKK01	This study
SCKK033	*MATa SUC2 MAL2-8^c ura3-52 his3-Δ1::gapN*[b]	pIYC04/pKK01	This study
SCKK034	*MATa SUC2 MAL2-8^c ura3-52 his3-Δ1::gapN*	pIYC08/pKK01	This study
SCKK035	*MATa SUC2 MAL2-8^c ura3-52 his3-Δ1::gapN*	pJC7/pKK01	This study
SCKK036	*MATa SUC2 MAL2-8^c ura3-52 his3-Δ1::gapN*		This study

[a] Institute of Microbiology, J.W. Goethe Universität, Frankfurt, Germany

[b] *gapN* here represents the integration cassette including *neo*^{r} and *gapN* under control of the *PGK1* promoter and *ADH1* terminator.

Table 2: Yields and specific growth rates of the parental strain CEN.PK 113-11C and the recombinant strain SCKK036 with *gapN* integration.

Strain	CEN.PK 113-11C	SCKK036
μ_{max} (h^{-1})	0.39 ± 0.00	0.38 ± 0.01
Y_{SEtOH} (g/ g glc)	0.50 ± 0.02	0.53 ± 0.03
Y_{SGly} (g/g glc)*	0.10 ± 0.01	0.05 ± 0.01

The values reported were calculated for the exponential growth phase during anaerobic shake flask cultivation in minimal media with 20 g/L glucose as sole carbon source. These values were calculated from at least triplicate shake flasks ($n \geq 3$) and are represented as mean ± SD.

* The values are significant difference at *p*-value ≤ 0.05

Table 3: Physiological parameters obtained during growth on minimal media with 20 g/L glucose in shake flask cultivations

Strain	Strains without *gapN* integration			Strains with *gapN* integration		
	SCKK005	SCKK006	SCKK032	SCKK033	SCKK034	SCKK035
μ_{max} (h^{-1})	0.27 ± 0.02	0.28 ± 0	0.21 ± 0.01	0.22 ± 0	0.23 ± 0.02	0.22 ± 0.02
r_s (g/gDW/h)	1.80 ± 0.09	2.24 ± 0.33	2.00 ± 0	1.37 ± 0	1.31 ± 0.18	1.30 ± 0.12
Y_{SX} (g/g glc)	0.15 ± 0.01	0.13 ± 0.02	0.11 ± 0	0.16 ± 0	0.18 ± 0.02	0.17 ± 0.02
Y_{SEtOH} (g/ g glc)	0.35 ± 0.05	0.35 ± 0.07	0.39 ± 0.01	0.48 ± 0.01	0.35 ±0.01	0.43 ± 0
Y_{SGly} (g/g glc)	0.05 ± 0	0.07 ± 0	0.07 ± 0	0.04 ± 0.01	0.05 ± 0.01	0.04 ± 0
Y_{SPHB} (mg/ g glc)	0.02 ± 0.01	0.13 ± 0.02	0.03 ± 0	0.27 ± 0.01	0.12 ± 0	0.06 ± 0
$Y_{EtOH \cdot PHB}$ (mg/ g EtOH)	0.22 ± 0.04	6.09 ± 1.44	56.40 ± 0.77	16.11 ± 2.38	14.50 ± 2.90	12.48 ± 0.81
PHB content at 100 h (mg/gDW)	4.02 ± 0.16	15.89 ± 0	27.86 ± 0	14.87 ± 0.4	27.52 ± 4.82	21.41 ± 0.69

These values were calculated from at least triplicate shake flasks ($n \geq 3$) and are represented as mean ± SD. The values for SCKK005 and SCKK006 are taken from a previous study (Kocharin et al. 2012).

All strains listed in Table 3 harbor the PHB plasmid (pKK01). SCKK005 and SCKK032 carry pKK001 and pIYC04. SCKK032 and SCKK035 express the phosphoketolase pathway, SCKK006 and SCKK034 overexpress the ethanol degradation pathway.

μ_{max} = maximum specific growth rate on glucose, r_s = specific glucose consumption, Y_{SX} = biomass yield on substrate (glucose), Y_{SEtOH} = ethanol yield on substrate (glucose), Y_{SGly} = glycerol yield on substrate (glucose) Y_{SPHB} = PHB yield on substrate (glucose), $Y_{EtOH \cdot PHB}$ = PHB yield on ethanol

Table S1 Oligonucleotides used in this study.

Primer name	Sequence
JC7-ACS1	CTATCTCAATTGGCACACACCATAGCTTC
JC7-ACS2	TCTAAACAATTGAATTGGAGCGACCTCATGC
HIS-check FW1	CAATGTTGTGGAAGCGG
HIS-check FW2	GATTTGCGCCTTTGGATGA
HIS-check REW1	CAAGAAAATGCGGGATCA
HIS-check REW2	AAAAAGTCAAACTGCGCC
KK001 His3 (f) AatII	TCGACGTCACAGAGCAGAAAGCCCTA
KK002 His3 (r) AatII	CAGACGTCCTTTGGTGGAGGGAACAT
KK003 pBluSk (f) AatII	ACGACGTCAGATAGGGTTGAGTGTTGT
KK004 pBluSk (r) AatII	TCGACGTCTTTTCGGGGAAATGTGCG
KK005 neoR (f) MfeI	CACAATTGGTCCCGTCAAGTCAGCGTAA
KK006 neoR (r) AscI	TGGCGCGCCTATATCATCATGAACAATAA
KK078-his3d1 II-(F)	CGGCGCGCCATCCATGGAATCTAGAAGGGC GACACGGAAATGTTGAA
KK079-his3d1 II (R)	TGGCGCGCCTGACGGGACGGCGGATCTATT
KK080-PGK-GapN (F)	AGCCATGGGGAGTCCGAGAAAATCTGGAAG AG
KK081-GapN-Adh (R)	CTTCTAGAGCCTCTTCGCTATTACGCCAGCT
KK039 his3d1_integration DN (f)	GGCATTAGTCAGGGAAGTCATAACACAGTC

KK082-GapN-Checking (F)	TCATCTGTAACATCATTGGCAACGC
KK083-GapN-Checking (R)	GCGATTTTGGAGCCAGCTAAGTTG
KK042 his3d1_integration UP (r)	GGAATACCACTTGCCACCTATCACCAC

Restriction sites are underlined.